The Recruitment of Stromal Cells to the Site of Tumor Formation

by

Matthew P. Saelzler

B.A. Biology
University of Chicago, 2000

SUBMITTED TO THE DEPARTMENT OF BIOLOGY IN PARTIAL FULFILLMENT
OF THE REQUIREMENTS FOR THE DEGREE OF

DOCTOR OF PHILOSOPHY IN BIOLOGY
AT THE
MASSACHUSETTS INSTITUTE OF TECHNOLOGY

December 2009

Signature of Author:_____
Department of Biology
December 15th, 2009

Certified by:_____
Robert A. Weinberg
Professor of Biology
Thesis Supervisor

Accepted by:_____
Stephen P. Bell
Professor of Biology
Chairperson, Graduate Committee

The Recruitment of Stromal Cells to the Site of Tumor Formation

by

Matthew P. Saelzler

Submitted to the Department of Biology on December 15th, 2009
in Partial Fulfillment of the Requirements for the
Degree of Doctor of Philosophy

Abstract

Myofibroblasts are an alpha-smooth muscle actin (α-SMA)-expressing cell type found within human mammary carcinomas, but not in the normal mammary gland. Myofibroblasts can enhance tumor formation by promoting angiogenesis and invasion, and we therefore sought to better understand how myofibroblasts are incorporated into breast carcinomas. By identifying secreted factors that recruit myofibroblasts as well as the physical niche where they originated, we aimed to identify possible therapeutic targets to inhibit their incorporation. Using a newly developed mammary carcinoma model, termed BPLER, we identified CXCL1, VEGF, CCL5, and IL-6 as factors that may be important for the recruitment of myofibroblasts. We tested the ability of CXCL1, $VEGF_{164}$, or CCL5 to affect tumor formation and induce the incorporation of α-SMA-positive cells. We show that the expression in MCF-7-Ras modified human breast cancer cells of $VEGF_{164}$, but not CXCL1 or CCL5, results in the promotion of primary tumor growth and the increased incorporation of α-SMA-positive cells. Furthermore, we demonstrate that these α-SMA-positive cells do not correlate with cells expressing CD34, a marker of endothelial cells, suggesting that these cells are not α-SMA-positive smooth muscle cells. Thus, we propose that VEGF is a critical factor that recruits myofibroblasts to the site of breast cancer formation.

In another line of experiments, we examined the source of the α-SMA-positive cell population recruited to another mammary tumor model, termed BPHER-3. In order to investigate whether these cells are derived from the bone marrow, we utilized chimeric mice that express green fluorescent protein (GFP) in their bone marrow and blood cells in order to look for incorporation of GFP-labeled cells within the stroma of a subcutaneously grown tumor. We demonstrated that green bone marrow-derived cells are robustly recruited to the site of BPHER-3 tumor formation; however strikingly, almost 100% of the α-SMA positive cells analyzed were GFP negative. Our results demonstrate that the α-SMA-positive cell population recruited to BPHER-3 tumors is not bone marrow-derived, but is instead recruited from the adjacent tissue microenvironment.

Thesis Advisor: Robert A. Weinberg
Title: Professor of Biology, MIT; Member, Whitehead Institute for Biomedical Research

Biographical Note
Matthew P. Saelzler

Whitehead Institute for Biomedical Research
9 Cambridge Center, Room 309
Cambridge, MA 02142
(617)-258-5165
mps@mit.edu

Education:

Massachusetts Institute of Technology — **Cambridge, MA**
Ph.D. Candidate in the Department of Biology.
Degree expected September 2009.

University of Chicago — **Chicago, IL**
Bachelor of Arts, Biology June 2000
with Honors

Research Experience:

Massachusetts Institute of Technology — **Cambridge, MA**
Ph.D. Thesis, Laboratory of Dr. Robert A. Weinberg
"The Recruitment of Stromal Cells to the Site of Tumor Formation" (2002-2009)

University of Chicago — **Chicago, IL**
Technician, Laboratory of Mark K. Abe (2000-2002)

University of Chicago — **Chicago, IL**
Undergraduate Research Assistant (1999-2000)

Publications:

McAllister SS, Gifford AM, Greiner AL, Kelleher SP, Saelzler MP, Ince TA, Reinhardt F, Harris LN, Hylander BL, Repasky EA, Weinberg RA. (2008) Systemic endocrine instigation of indolent tumor growth requires osteopontin. *Cell* 133(6):994-1005.

Saelzler MP, Spackman CC, Liu Y, Martinez LC, Harris JP, Abe MK. ERK8 down-regulates transactivation of the glucocorticoid receptor through Hic-5. (2006) *J Biol Chem.* 281(24):16821-32.

Abe MK, Saelzler MP, Espinosa R 3rd, Kahle KT, Hershenson MB, Le Beau MM, Rosner MR. ERK8, a new member of the mitogen-activated protein kinase family. (2002) *J Biol Chem.* 277(19):16733-43.

Abe MK, Kahle KT, Saelzler MP, Orth K, Dixon JE, Rosner MR. ERK7 is an autoactivated member of the MAPK family. (2001) *J Biol Chem.* 276(24):21272-9.

Awards:

Harvey Lodish Service Award for Outstanding Contribution to the Whitehead Partnership for Science Education Program (2007)

Department of Defense Breast Cancer Research Pre-Doctoral Traineeship Award (2005-2008)

Teaching Experience:

Massachusetts Institute of Technology **Cambirdge, MA**

7.27 Principles of Human Disease (Spring 2006)	Teaching Assistant
7.012 Introductory Biology (Fall 2003)	Teaching Assistant

Related Experience:

Whitehead Partner: The Whitehead Seminar Series for High School Teachers
(2005-2008)

Whitehead Spring Lecture Series for High School Students
(2005-2007, 2009)

Invited Talks:

Era of Hope Department of Defense Breast Cacner Research Program Meeting Baltimore, Maryland June 2008

Conference Presentations:

Era of Hope Department of Defense Breast Cancer Research Program Meeting, Poster Baltimore, Maryland June 2008

---

for my father
for my mother
for Tina

Acknowledgements

I would like to thank Bob for the opportunity to do research in his lab. I would especially like to thank him for his patience, understanding, and support through difficult times.

I would like to thank my committee members, Dr. Jacqueline Lees and Dr. David Housman, for their time, scientific input, and support over the course of my graduate career.

I would like to thank Dr. Michael Hemann and Dr. Randolph Watnick for their time as members of my Thesis Defense Committee

I would like to thank my friend Tina Yuan. I was only able to make it to this point because of her strength, caring, and love. She has carried me through the most difficult time in my life. I do not know how I would have gotten through this without her. I cannot say or do enough to convey what she has done for me. I would also like to thank her for editing my thesis.

I would like to thank my parents for everything they have done for me. They have provided me with so many opportunities and the support to achieve what I could not have done alone.

I would like to thank my Mother, Linda Saelzler, for always being there for me. I am inspired by her strength, kindness, and understanding. My mother's love and support has gotten me through the last year and a half.

I would like to thank my father, Paul Saelzler, who passed away while I was in graduate school. He has always been a fierce supporter and protector of me and all his children.

I would like to thank by brother and sister who have always supported me. I love them both.

I would like to thank Sandra McAllister. She has been a good friend, mentor, and collaborator. I thank her for her patience and support over all the years of my graduate career. I am especially grateful for her caring and support through some very rough periods.

These people have provided me with support, friendship, and many laughs: Scott Valastyan, Lynne Waldman, and Ericka Anderson. I especially thank them for listening to me and helping me when I needed them. Additionally, I would like to thank Scott for his editing skills on parts of this document, and Lynne for editing the introduction.

I would also like to thank other members of the Weinberg Lab who have either listened to me or helped me over the years including: Rick Lee, Tamer Onder, Priya Rai, and Christine Chaffer.

I would like to thank Christine Hickey and Sumiko Williams for their support and help.

I would also like to thank Ferenc Reinhardt. He has saved me countless hours through his mouse work in these experiments.

Table of Contents

BIOGRAPHICAL NOTE **3**

ACKNOWLEDGEMENTS **6**

TABLE OF CONTENTS **8**

CHAPTER 1: INTRODUCTION **10**

BREAST CANCER 11
Cancer is Caused by Alterations in the DNA of Normal Cells 11
The Progression of Ductal Carcinomas from Normal Breast Tissue 12
Tumor Progression is Facilitated by Changes that Occur Outside of the Cancer Cells 13
THE CELLULAR COMPONENT OF THE STROMA AND ITS IMPACT ON TUMOR PROGRESSION 16
Stromal Cells Can Facilitate Tumor Initiation 17
Stromal Cells are Essential for Angiogenesis 18
Stromal Cells Affect Tumor Cell Invasion and Metastasis 21
THE PROTEIN COMPONENT OF THE STROMA AND ITS IMPORTANCE FOR CANCER AND STROMAL CELL INTERACTION 22
The Gene Expression Profiles of Stromal Cells are Affected by Extracellular Proteins 23
The Secretion Growth Factors, Chemokines and Cytokines and Their Effects on Stromal Cells and Tumors Cells 25
The Secretion of Extracellular Matrix Proteins and Their Effect on Tumor Progression 27
The Secretion of Proteases and Their Effects on Tumor Progression 29
MYOFIBROBLASTS ARE PRESENT AT SITES OF WOUND HEALING, FIBROSIS AND BREAST CARCINOMA 31
MYOFIBROBLASTS PLAY SEVERAL ROLES IN TUMOR PROGRESSION 33
CAFs Involvement in Facilitating Tumor Initiation 33
CAFs Involvement in the Promotion of Angiogenesis 34
CAFs Involvement in Invasion and Metastasis 35
QUESTIONS ADDRESSED 36
REFERENCES 38

CHAPTER 2: THE ROLE OF VEGF, CXCL1, AND CCL5 IN THE RECRUITMENT OF α-SMA-EXPRESSING STROMAL CELLS TO THE SITE OF TUMOR FORMATION . 42

INTRODUCTION 43
Identification of Secreted Factors Potentially Important in the Recruitment of Myofibroblasts 50
Determining the Effect of CXCL1, CCL5, and VEGF on In-Vivo Tumor Growth 55
Examining the Recruitment of α-SMA-Positive Cells and CD34-Positive Cells to the Factor Expressing MCF-7-Ras Tumors Grown in NOD-SCID Mice 58
DISCUSSION 62
MATERIALS AND METHODS 64
SUPPLEMENTARY MATERIAL 72
REFERENCES 74

CHAPTER 3: THE RECRUITMENT OF BONE MARROW-DERIVED CELLS TO THE SITE OF TUMOR FORMATION 77

INTRODUCTION 78
RESULTS 83

The Recruitment of Bone Marrow-Derived Cells to BPHER-3 Tumors at Different Time Points During Tumor Growth 83
The Recruitment of Bone Marrow Derived Cells to MDA-MB-231 and BPHER-3 Tumors 88
The Source of α-SMA-Positive Cells in the BPHER-3 Tumors 91
DISCUSSION 97
MATERIALS AND METHODS 99
REFERENCES 103

CHAPTER 4: CONCLUSIONS AND FUTURE DIRECTIONS 105

FACTORS INVOLVED IN THE RECRUITMENT OF MYOFIBROBLASTS TO THE SITE OF BREAST CANCER FORMATION 107
The Effects of VEGF, CXCL1, and CCL5 expression in Breast Carcinoma Formation 107
Mechanisms of VEGF-A Action 109
Direct Mechanisms of VEGF-A Action 113
Indirect Mechanisms of VEGF-A Action 118
THE RECRUITMENT OF BONE MARROW-DERIVED CELLS TO THE SITE OF TUMOR FORMATION 120
REFERENCES 125

APPENDIX 1: PERTURBATIONS OF CELLS IN THE BLOOD BY SUBCUTANEOUSLY GROWING HUMAN BREAST CANCER XENOGRAFTS 129

INTRODUCTION 130
RESULTS 133
Creation of Tumor Bearing and Control Mice for Blood Analysis 133
Description of Blood Analysis 133
Analysis of Blood in Tumor-Bearing Mice 137
DISCUSSION 140
SUPPLEMENTARY MATERIAL 145
REFERENCES 148

Chapter 1: Introduction

Breast Cancer

Breast cancer represents more than a quarter of cancers diagnosed in American women. It is one of the most common forms of cancer, second only to skin, and one of the leading causes of cancer-related deaths in US women, second only to lung cancer (American Cancer Society). During the period of 2001 through 2005 the incidence rate of female breast cancer was 126.1 per 100,000 women and the mortality rate was 25 per 100,000 women (Ries LAG et al. 2008).

Importantly, breast cancer is not a single disease, but instead represents a group of neoplasms that all arise in the breast. Among the different breast cancer neoplasms, carcinomas are the most common. Carcinomas are defined as a type of cancer that arises from epithelial cells. Ductal carcinoma in-situ (DCIS) and invasive ductal carcinoma (IDC) are the most common forms of non-invasive and invasive breast cancer, respectively. In fact, IDC represents approximately 70% of all breast cancers (MayoClinic.com). In order to improve the treatment of breast cancer, it is necessary to understand the causes of cancer, the progression of the disease and the factors that facilitate its progression.

Cancer is Caused by Alterations in the DNA of Normal Cells

Cancer is caused by both genetic and epigenetic alterations of cells that transform them into cancer cells. Moreover, it is clear that multiple alterations are required to convert a normal cell into a cancer cell. Accordingly, the formation of a tumor is a multi-step evolutionary process, with each successive modification providing one cell in the

population with some selective advantage (Hanahan and Weinberg, 2000). Properties that confer a selective advantage on cells in a tumor include unregulated growth and proliferation, evasion of apoptosis, increased replicative potential, the induction of angiogenesis, and eventually invasion and metastasis (Hanahan and Weinberg, 2000). Ultimately, a subset of cells is created, the cancer cells, which have accumulated all of the necessary genetic alterations that provide this set of cells with the properties necessary to form a robustly growing tumor.

The Progression of Ductal Carcinomas from Normal Breast Tissue

In order to understand the progression of ductal breast carcinomas from hyperplasia to a robustly growing and invasive tumor, it is essential to know the normal context in which it arises. The normal mammary gland contains ducts that serve as passageways for milk. A duct consists of a layer of epithelial cells, which line the lumen of the duct, and they are surrounded by a layer of myoepithelial cells and a basement membrane (Bissell MJ and Radisky D. 2001). The basement membrane is composed of various types of extracellular matrix (ECM) proteins (Bissell MJ and Radisky D. 2001). ECM proteins serve as a scaffold for various cellular structures. The ductal structure described above is surrounded by an environment that is referred to as the stroma, which is discussed in detail below.

The initial stages of tumor progression including hyperplasia, dysplasia and carcinoma in-situ all occur in the confines of the duct. As the tumor evolves the basement membrane can be broken down and the carcinoma cells are able to invade into

the surrounding tissue; this is called invasive ductal carcinoma (IDC) (Kalluri and Zeisberg, 2006). Following invasion into the surrounding tissue, the cancer cells can travel to other sites in the body and form secondary tumors, the process called metastasis. Metastasis requires several steps beginning with intravasation of cancer cells in the primary tumor into a blood vessel. Metastatic cells travel through the blood stream to a secondary site in the body and extravasate into the new tissue. Finally, the extravasated cells proliferate at the new site forming a secondary tumor.

Tumor Progression is Facilitated by Changes that Occur Outside of the Cancer Cells

Research was initially focused on identifying the genetic abnormalities within the cancer cell and how they endow a cell with the capacity to complete the multiple steps of tumorigenesis from hyperplasia to metastasis. This research has lead to the identification of many genes that are responsible for some aspect of tumor progression. However, cancer progression not only involves changes that occur within the cancer cell, but also changes that occur in the environment surrounding the cancer cells. The environment surrounding the cancer cells, like the environment surrounding the ducts in the normal breast, is referred to as the stroma. It is important to recognize the changes in the stroma surrounding the cancer cells, because they are essential for many aspects of tumor progression.

The normal mammary stroma and the tumor stroma include two components, an extracellular protein component and a cellular component (Figure 1). In the normal breast, the stroma comprises the majority of the tissue volume (Rønnov-Jessen L et al.

1996). Interestingly, in a disease marked by the unregulated proliferation of cancer cells, the tumor stroma can in some cases comprise a majority of the tumor mass (Rønnov-Jessen L et al. 1996). However, the tumor stroma is distinct from the normal stroma in both the extracellular protein component and cellular component. Furthermore, the changes in the stroma impact tumor initiation, angiogenesis, invasion and metastasis, as illustrated below.

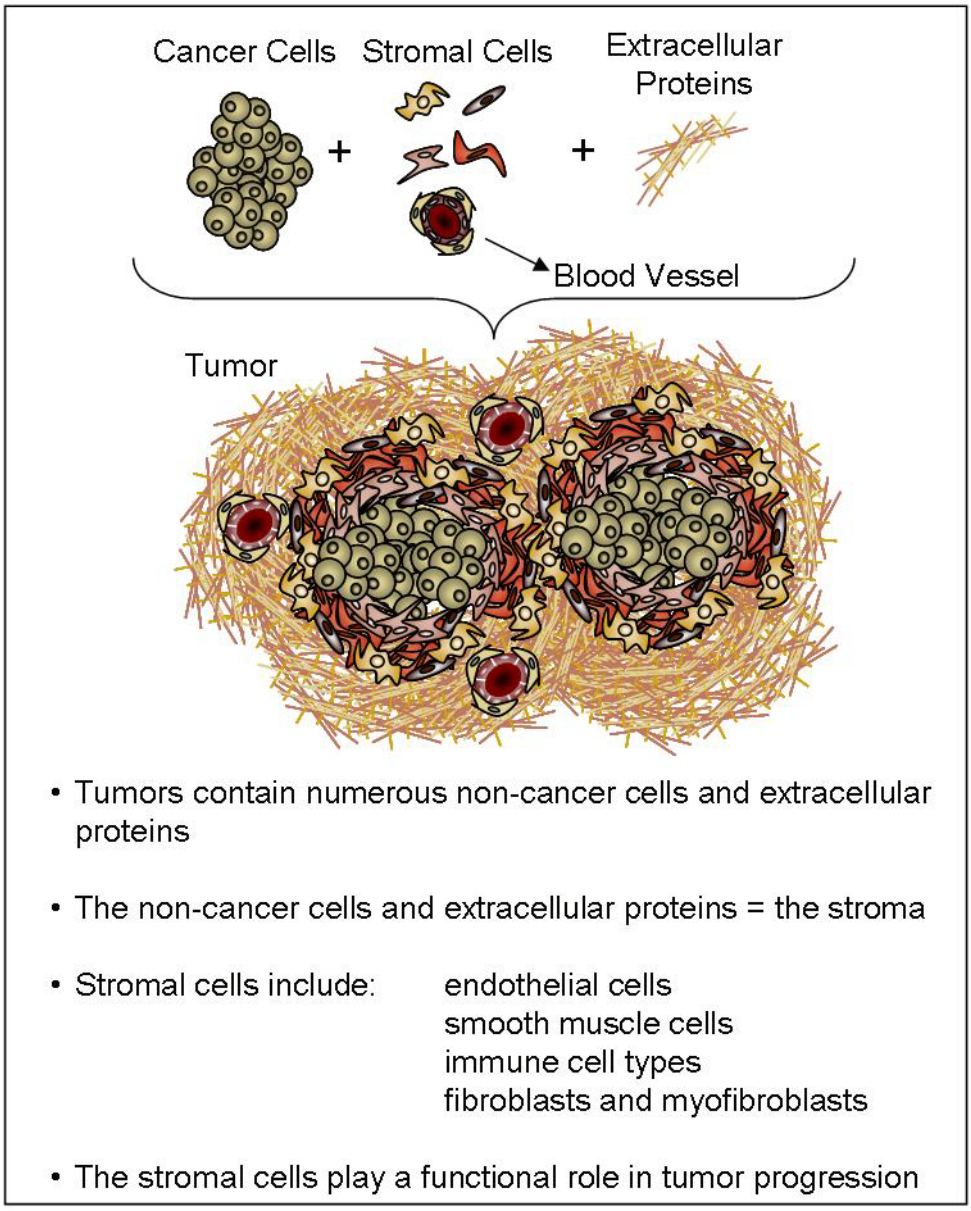

Figure 1: Breast Carcinomas Contain a Stromal Component That Consists of Cells and Extracellular Proteins: Tumors arise through the overproliferation of cancer cells (top left), but tumors also contain many non-cancer cell components, including stromal cells (top middle) and extracellular proteins (top right). Stromal Cells consist of a heterogeneous population of cells that can include several cell types. Extracellular Proteins include extracellular matrix (ECM) proteins, growth factors, chemokines, cytokines, and proteases.

The Cellular Component of the Stroma and Its Impact on Tumor Progression

The stromal cells present in a carcinoma can include fibroblasts, myofibroblasts, endothelial cells, smooth muscle cells and several immune cell types. There are several distinctions in the cellular component of the stroma compared to the normal tissue that can occur during tumor progression. First, the organization of the cell types in the tumor stroma can be different relative to the normal tissue. For example, blood vessels within a tumor can be structurally different from their normal counterparts. In tumors, blood vessels have been described as leaky and tortuous (Bergers G and Benjamin LE 2003). Additionally, unlike normal vessels, the blood vessels in tumors are not always fully covered by smooth muscle cells (Bergers G and Benjamin LE 2003). Secondly, the diversity of stromal cell types present can be perturbed during tumor progression. One of the more distinctive changes seen in the stroma of breast carcinomas, and the focus of my studies, is the presence of a cell type called the myofibroblast, which is absent in the normal mammary tissue (Skalli O et al. 1986, Barth PJ et al. 2002, Chauhan H et al. 2003, Yazhou C et al. 2004). Finally, the gene expression profile of the stromal cells present in breast carcinomas can be distinct from the profile of stromal cells present in the normal breast tissue (Allinen M et al 2004).

The cells present in the stroma of tumors are not just an altered form of their normal counterparts, but play essential roles in tumor progression that have both positive and negative influences on tumor progression. In this thesis, I focus on the functional aspects of stromal cells that facilitate the multiple steps of tumor progression, including tumor initiation, angiogenesis, invasion, metastasis and drug resistance. Furthermore, the

impact specifically of myofibroblasts on tumor progression will be discussed in a subsequent section.

Stromal Cells Can Facilitate Tumor Initiation

Although cancer originates because of changes in the DNA of cancer cells, the stromal cells can facilitate tumor initiation in the normal precursors of the cancer cell. It has been demonstrated that alterations in stromal fibroblasts can cause neoplastic phenotypes in normal neighboring epithelial cells. The cytokine, transforming growth factor-β (TGF-β) affects several distinct cell types, including stromal fibroblasts, by binding to a TGF-β receptor expressed by these cells and has been implicated in several aspects of tumorigenesis. Bhowmick et al. demonstrated that when the transforming growth factor-β type II receptor (TGF-β-IIR) is knocked-out in stromal fibroblasts of mice, it leads to neoplasia in the prostate and invasive cancers in the forestomach (Bhowmick NA et al. 2004). These data demonstrate that alterations in the stroma can lead to changes that facilitate the initiation of tumorigenesis.

Stromal cells were also shown in a mouse model of invasive squamous cell carcinoma to aid in initial tumor formation (Coussens LM et al., 2000). In this model, squamous carcinomas are initiated by the transgenic expression of an oncogene, the human papillomavirus type 16 (HPV16) early region, under a keratin 14 promoter. The tumors in the K14-HPV16 mice are infiltrated by mast cells, neutrophils and macrophages, all of which express matrix metalloproteinase-9 (MMP-9) (Coussens LM et al., 2000). MMPs, as will be discussed later, are thought to play multiple roles in

tumor progression through their ability to degrade ECM proteins (Lynch and Matrisian, 2002). In the study by Coussens et al., the occurrence of squamous cell carcinomas is reduced when K14-HPV16 mice are crossed to mice lacking MMP-9. Furthermore, the wild type tumor phenotype can be recapitulated by providing the MMP-9 deficient animals with wild type bone marrow through a bone marrow transplantation procedure. These data suggest that the expression of MMP-9 by these stromal cell types is important for initial tumor formation and that these stromal cells are of bone marrow origin. These experiments taken together reveal the impact that stromal cells can have on tumor formation at very early stages.

Stromal Cells are Essential for Angiogenesis

Following the initiation of a tumor, cancer cells, like normal cells, rely on a blood supply to survive. A tumor needs to induce angiogenesis, which is the growth of new blood vessels, if it is to grow and progress past a certain size (Hanahan D and Folkman J 1996). Angiogenesis is probably the most well known example of cancer cells needing additional cell types to aid in their growth. Blood vessels, which consist of endothelial cells surrounded by a layer of smooth muscle cells, are essential to the survival of normal tissue and tumor tissue because they provide oxygen and essential nutrients to the cells in these tissues. While tumor cells themselves can directly induce angiogenesis, other cell types recruited to the tumor stroma, like mast cells, macrophages and neutrophils, have been implicated in various animal models to play a role in the induction of angiogenesis during tumor formation (Coussens LM et al. 1999, Lin EY et al 2006, Nozawa H et al.

2006). Thus, stromal cells are involved in two aspects of tumor angiogenesis: first, the stromal endothelial and smooth muscle cells are essential in the formation of tumor blood vessels; secondly, other stromal cell types can aid in the induction of angiogenesis.

Angiogenesis not only effects primary tumor growth but also affects the establishment and subsequent growth of metastasis. In Id-deficient mutant mice, which show defective angiogenesis during tumor growth, the primary tumor growth of Lewis lung carcinoma (LLC) cells is decreased and metastasis to the lung is greatly inhibited (Lyden D et al. 1999). Moreover, metastasis of the LLC cells to the lungs following tail vein injection is also inhibited in these mice. These data suggest that in the Id-deficient mutant mice there are problems with the ability of the tumors cells to get to the lung and/or the colonization of the lung by the tumor cells. It is thought that angiogenesis not only provides nutrients to the growing tumor and its secondary metastasis, but also serves to create conduits for the tumor cells to move to other sites in the body.

Angiogenesis has been associated with disease progression in cancer patients and represents a prime therapeutic target. An increase in the number of blood vessels in the tumor mass has been associated with poor prognosis in breast and prostate cancer (Hanahan D and Folkman J 1996). Based on clinical data and the essential role angiogenesis plays during tumor progression, one avenue of clinical therapies has been focused on inhibiting the process of angiogenesis. Vascular endothelial growth factor (VEGF) is the most well known inducer of angiogenesis. It acts as both a growth factor and chemoattractant for endothelial cells, as discussed later (Cross MJ et al., 2003). One

way to inhibit the actions of VEGF is through the development of antibodies that bind VEGF and inhibit its activity.

Therapies that target the stromal cells recruited to a tumor are useful for two reasons; first, stromal cells influence the course of disease progression; secondly, they can contribute to the resistance of tumors to particular drugs. In a study by Shojaei F et al., it was demonstrated that the growth of some xenograft tumors is greatly inhibited by a monoclonal antibody that neutralizes VEGF (anti-VEGF) and these tumors were therefore dubbed sensitive tumors (Shojaei F et al. 2007). On the other hand, there were other tumor xenografts that were more resistant to anti-VEGF's inhibitory effects and these were designated as refractory tumors. The authors went on to demonstrate that the sensitive tumors are rendered less sensitive when the tumor cells are mixed with CD11b+Gr-1+ myeloid cells that were previously isolated from refractory tumors or the bone marrow of mice bearing refractory tumors. Furthermore, the growth of the refractory tumors is inhibited to a greater extent when the anti-VEGF treatment is combined with an anti-Gr-1 treatment, an antibody that recognizes Gr-1. These data reveal that the recruitment of myeloid cells can play a role in tumors that are insensitive to anti-VEGF treatment (Shojaei F et al. 2007). The study of angiogenesis during tumor formation provides a prime example of the potential therapeutic benefits of exploring the biology of stromal cells in cancer.

Stromal Cells Affect Tumor Cell Invasion and Metastasis

In addition to initial tumor formation and angiogenesis, stromal cells affect both tumor cell invasion and metastasis. For example, mammary stromal fibroblasts lacking the TGF-β-IIR enhanced tumor formation and invasion when co-mingled with mouse breast cancer cells, relative to wild-type fibroblasts (Cheng N et al. 2005). The knock-out of the TGF-β-IIR in fibroblasts led to an increase in secretion of hepatocyte growth factor (HGF, also known as scatter factor (SF)) by these cells. A neutralizing antibody to HGF was demonstrated in vitro to inhibit the increase in proliferation and migration of mouse mammary carcinoma cells in response to the knock-out fibroblasts (Cheng N et al. 2005). This data suggests that fibroblasts present in the tumor stroma can promote tumor cell invasion though the secretion of specific factors recognized by the cancer cells.

Stromal cell types of the myeloid lineage within tumors have been implicated in facilitating both tumor invasion and metastasis (Lin EY et al. 2001, Kitamura T et al 2007, Yang L et al. 2008). The myeloid lineage of cells consists of the myeloid progenitors and the cells they give rise to, including macrophages, neutrophils, mast cells, and dendritic cells among other cell types (Janeway CA et al. 2001). In clinical data, the presence of macrophages in a majority of cancer studies is correlated with poor prognosis (Pollard 2004). Furthermore, macrophage infiltration has been correlated with both a decrease in the relapse-free survival and in the overall survival of breast cancer patients (Leek RD et al. 1996).

As demonstrated above, stromal cells play functional roles that can facilitate the multiple steps of tumorigenesis and targeting their recruitment can be therapeutically

beneficial. Specifically, the growth of tumors was inhibited by targeting the factor, VEGF, which can induce angiogenesis. Thus, it is important to understand the mechanisms behind the recruitment of stromal cells to the sites of tumors formation. Additionally, it is important to understand the mechanisms underlying the functional roles of stromal cells during tumorigenesis.

The Protein Component of the Stroma and Its Importance for Cancer and Stromal Cell Interaction

One of the main means by which cell types communicate and affect the biology of surrounding cells is through the release of proteins into the extracellular environment. As mentioned above, the stroma of the normal breast tissue and the tumor stroma contain an extracellular protein component. The protein component of the stroma can consist of several types of extracellular proteins including ECM proteins, growth factors, cytokines, chemokines, and proteases. Importantly, the composition, abundance, and distribution of extracellular proteins in the stroma of mammary carcinomas are distinct from those found in the normal mammary stroma (Rønnov-Jessen L et al. 1996).

The extracellular protein component of the stroma is essential for tumor progression, because the stromal cells incorporated into the growing tumor mass are determined by the extracellular proteins secreted by the cancer cells. Subsequently, the extracellular proteins secreted by the stromal cells affect the biology of the cancer cells and also serve to recruit other stromal cell types. Each of the multiple steps of tumor formation is affected by this communication and therefore greatly influences the progression of the disease. This communication is the mechanism that underlies the

functional impact that stromal cells and cancer cells have on each other. Thus, it is important to elucidate some of the specific differences in the extracellular protein environment present in breast cancer relative to normal breast tissue. Additionally, it is critical to understand the biological consequences of this communication and how this communication produces an effect on tumor progression.

The Gene Expression Profiles of Stromal Cells are Affected by Extracellular Proteins

It has already been established that the extracellular protein environment within a tumor is distinct relative to the normal tissue. These changes in the extracellular environment can lead to changes in the gene expression profiles of the tumor stromal cells relative to the normal tissue. As mentioned previously, the expression profiles of stromal cells in breast carcinomas were shown to be different from the stromal cells in a normal mammary gland (Allinen M et al 2004). Specifically, Allinen et al. isolated different cell populations from the normal breast and those from mammary carcinomas. The populations of cells that they examined were epithelium, myoepithelium and myofibroblasts, leukocytes, and endothelium. After isolating each of the cell types they performed gene expression arrays on the different populations. In each of the cell populations the gene expression profile of the cells isolated from mammary carcinomas was different from that isolated from a normal mammary gland (Allinen M et al 2004).

Interestingly, the gene expression profiles of stromal cells in tumors have been correlated with disease outcome. In a study by Bacac et al., they examined a set of upregulated genes in the stromal cells of a mouse model of invasive prostate cancer

(Bacac M et al. 2006). The authors demonstrate that the human homologs of this upregulated gene set were positively correlated with decreased disease-free recurrence periods in patients with prostate cancer. While not true for other types of cancer, this upregulated gene set was also positively correlated with a shorter metastasis-free survival and a decreased overall survival in human patients with breast cancer (Bacac M et al. 2006). In another recently published paper, an expression signature derived from the stromal cells of invasive breast cancer was reported to have predictive power in patients (Finak G et al. 2008). Thus, an understanding of the changes in stromal cell gene expression induced during tumorigenesis could lead to a difference in how cancer patients are treated.

Changes that occur in the stromal gene expression profile during tumorigenesis could be the result of two factors; first, changes in the gene expression of a particular stromal cell type in response to the altered extracellular protein environment. Secondly, it could be the result of a change in the composition of stromal cell types present relative to the normal tissue stroma. It is most likely that the stromal gene expression pattern in tumors is a combination of both these factors. In light of the clinical data presented above, it is important to understand how growth factors, chemokines, cytokines, ECM proteins, and proteases produce these changes in the stromal cells and how these factors facilitate tumor progression.

The Secretion Growth Factors, Chemokines and Cytokines and Their Effects on Stromal Cells and Tumors Cells

The release of growth factors, chemokines, and cytokines by cancer cells affect certain stromal cell types because particular subsets of stromal cells express the appropriate receptor. Furthermore, the secretion one ligand by a cancer cell has the ability to influence multiple cell types (Figure 2A). For example, tumor cells can induce angiogenesis by secreting one of the members of the VEGF family of proteins called VEGF-A. VEGF-A in the extracellular environment is recognized by two transmembrane receptors VEGF-receptor-1 (VEGFR1) and VEGF-receptor-2 (VEGFR2) (Cross MJ et al., 2003). VEGF-A induces angiogenesis because endothelial cells express both VEGFR-1 and VEGFR-2 and therefore respond to VEGF-A (Cross MJ et al., 2003). VEGFR-1 is also expressed by other cell types including hematopoietic stem cells, monocytes and macrophages (Cross MJ et al., 2003). Similarly, VEGFR-2 expression is not limited to endothelial cells. The expression of a particular receptor by several different cell types is not limited to VEGFR-1 and VEGFR-2, but is also true for many other types of receptors. The overlapping expression of receptors on multiple cells types is the reason the secretion of one factor by a cancer cell can influence multiple cell types.

The binding of a ligand to its receptor produces changes in gene expression on the receptor expressing cell that can lead to several functional consequences (Figure 2B). For example, the binding of VEGF-A to the VEGFR-2 receptor on endothelial cells can lead to several biological outputs including migration, proliferation, and cell survival (Cross MJ et al., 2003). Each of these responses seems appropriate based on the fact that

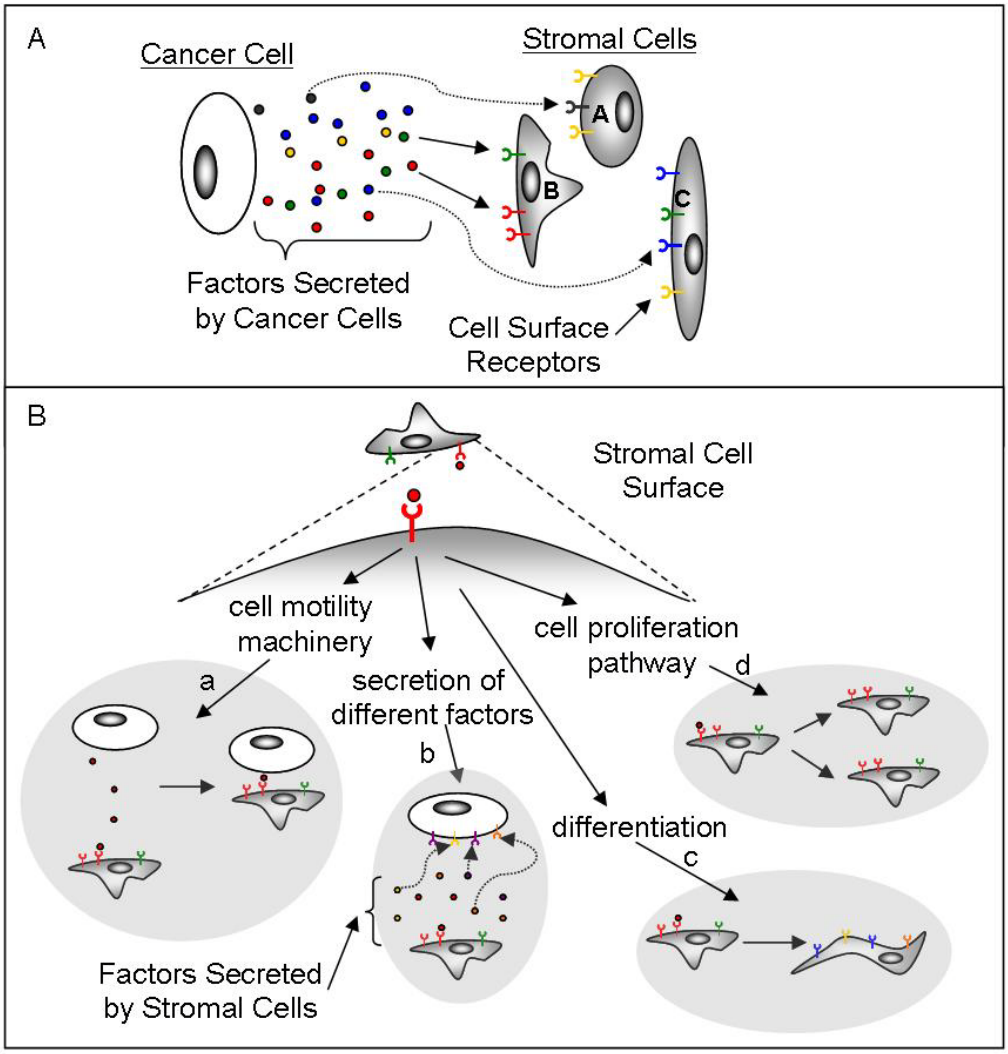

Figure 2: Cancer Cells and Stromal Cells Communicate and Influence Each Other Through the Secretion of Growth Factors, Cytokines and Chemokines. (A) Cancer cells can secrete a variety of growth factors, chemokines, and cytokines which are represented in the picture by different colored circles. These different factors bind to specific receptors. The ligand and its cognate receptor are given the same color in the picture. The different factors secreted by the cancer cells act on different stromal cell populations and is dependant on the receptors expressed by the stromal cells. (B) The binding of these secreted molecules to receptors expressed on the surface of the stromal cell membrane leads to changes on the inside of the cell through signaling pathways that results in several different biological outcomes. These outcomes can include the (a) movement of the stromal cell to the cancer cell, (b) the secretion of different factors by the stromal cell, (c) the differentiation or transdifferentiation of the stromal cell and (d) the proliferation of the stromal cell.

VEGF-A induces the growth of new blood vessels. Thus, a cancer cell can recruit certain tumor-promoting stromal cells to the site of tumor formation because some of the factors they release induce the migration of these cells upon binding to the receptor. These factors are said to act as chemoattractants. Furthermore, once a stromal cell type is present, the cancer cells can increase the numbers of these stromal cells through the release of extracellular proteins that promote their proliferation or survival. The stromal cells recruited into the tumor microenvironment can then secrete growth factors, chemokines, and cytokines that reciprocally affect the tumor cells' proliferation, survival, invasion and metastasis.

In addition to the effects mentioned above, the binding of ligands to their cognate receptors can also induce changes in the gene expression profiles of stromal cells that lead to the differentiation or trans-differentiation of a recruited stromal cell. For example, TGF-β is thought to cause the trans-differentiation of fibroblasts into myofibroblasts (Desmoulière A et al. 1993). The myofibroblasts created could then impact tumor progression in multiple ways, as presented below.

The Secretion of Extracellular Matrix Proteins and Their Effect on Tumor Progression

ECM proteins are also present in the tumor microenvironment and affect tumor progression. The ECM protein environment present in the tumor is distinct from the normal tissue. Carcinomas of the breast can display a desmoplastic stroma, often referred to as the desmoplastic response in contrast to normal breast tissue. The desmoplastic

stroma is typified by the increased deposition of ECM proteins including collagen and fibronectin (Rønnov-Jessen L et al. 1996).

The changes in the ECM can begin to occur prior to invasion and direct contact of the carcinoma cells with the stroma. In a study examining 18 patients with DCIS, in-situ hybridization demonstrated the increased expression of collagen, fibronectin, and ED-A+ fibronectin by stromal cells surrounding the duct (Brown LF et al. 1999). Furthermore, in a mouse model of prostate cancer, Bacac M et al. demonstrated an increase in the expression of particular extracellular matrix proteins, including pro-collagen type III, pro-collagen type IV, and biglycan in the stroma of invasive tumors, relative to the stroma of prostate intraepithelial neoplasia (Bacac M et al. 2006). While one might have initially suspected the distinction in extracellular proteins to be simply caused by the altered cancer cells, the stromal cells are clearly contributing to the changes seen in the extracellular protein environment. Furthermore, the study by Bacac M et al. demonstrates that the stromal gene expression profile continues to change over the course of tumor progression.

The ECM proteins secreted into the tumor microenvironment are recognized by their own set of cell surface receptors found on both stromal cells and tumor cells. As mentioned earlier, ECM proteins provide a scaffold for the growth of cells and cellular structures. ECM protein receptors can also transduce signals that lead to cell growth, survival, and migration (Kass L et al. 2007). Thus, ECM proteins are thought to play a role in several aspects of tumorigenesis including invasion (Kass L et al. 2007). Finally,

the remodeling of ECM proteins by factors such as proteases contributes to disease progression as discussed below.

The Secretion of Proteases and Their Effects on Tumor Progression

In addition to the secretion of ECM proteins, growth factors, chemokines and cytokines by the recruited stromal cells, they can secrete proteases that also affect tumor progression. Proteases are proteins with an enzymatic function that allow them to cleave specific protein substrates. Interestingly, it has been demonstrated in a mouse model of prostate cancer that one of the most over-represented set of genes in the stroma of invasive tumors, compared to the stroma of prostate intraepithelial neoplasia, falls into the category termed endopeptidase activity (Bacac M et al. 2006). Some of the genes in this set are capable of re-modeling the extracellular environment through their ability to degrade specific proteins.

Matrix-remodeling proteins include matrix metalloproteinases (MMPs). MMPs represent a family of proteases that cleave specific target proteins and, as their name implies, they degrade ECM proteins (Lynch and Matrisian, 2002). MMPs show a distinctive pattern of expression during breast cancer progression. A matrix metalloproteinase, stromelysin-3 (Str-3), was shown to be expressed by the stromal cells in breast carcinomas but absent in the normal mammary gland (Basset P et al. 1990, Wolf C et al.1993). Additionally, the expression of other MMPs in breast cancer including: MMP-2, MMP-9, MMP-11, MMP-12, and MMP-14; while showing different patterns of expression, were all expressed by stromal cells (Heppner KJ, 1996). Similar to Str-3,

Heppner et al. demonstrate that these other MMPs expressed by the stromal cells were seldom seen in normal breast tissue.

The changes in MMP expression detected during tumorigenesis affect the biology of the cancer cells in at least two ways. First, MMPs released by stromal cells can affect cancer pathogenesis through their ability to degrade ECM proteins that might serve as barriers to infiltrating cancer cells, thus promoting tumor cell invasion. (Lynch and Matrisian, 2002). Secondly, MMPs may also play a role in tumor formation through their ability to increase the availability of growth factors and cytokines in the extracellular space that can then bind to their cognate receptors (Lynch and Matrisian, 2002). For example, it has been shown that inhibition of MMP-9 reduces angiogenesis and tumor formation in a mouse model of pancreatic cancer (Bergers G et al., 2000). The authors were able to demonstrate that MMP-9 regulates the availability of VEGF, a potent inducer of angiogenesis.

The crosstalk between tumor cells and stromal cells through the release of extracellular proteins can control many aspects of tumorigenesis. Thus, the communication between cancer cells and stromal cells is a prime target therapeutically because of its impact on tumor progression. However, the particular subsets of stromal cells present in the tumor stroma are most likely recruited in response to different sets of factors. Thus, it is important to understand how particular stromal cell populations effect tumor progression and the factors that induce their recruitment.

Myofibroblasts are Present at Sites of Wound Healing, Fibrosis and Breast Carcinoma

In my studies, I have focused on the recruitment of a stromal cell type called the myofibroblast. Myofibroblasts were originally identified as altered fibroblasts present at the sites of wound healing. Myofibroblasts have also been described at sites of fibrosis, which is characterized by the superfluous deposition of ECM proteins (Gabbiani G 2003, Hinz B et al. 2007, De Wever O et al. 2008). In addition to their role in tumor formation, myofibroblasts are actively involved in wound repair, in part through the secretion of extracellular matrix molecules, growth factors, and cytokines important in the resolution of the wound. Furthermore, myofibroblasts display contractile abilities and play a role in the contraction of wounds (Powell DW et al. 1999, De Wever O et al. 2008, Gabbiani G 2003). Thus, myofibroblasts aid in the wound healing process in several ways. In contrast to wound healing, where myofibroblasts play a positive role in the repair process, they appear to be conspirators in the formation of tissue fibrosis and tumor formation (Hinz B et al. 2007). Furthermore, unlike wound healing, where myofibroblasts are no longer present following resolution of the wound, they are thought to be continuously present in areas of fibrosis and during the growth of carcinomas (Gabbiani G 2003, De Wever O et al. 2008).

As mentioned previously, probably one of the most distinctive changes in the stroma of mammary carcinomas is the presence of numerous myofibroblasts. Myofibroblasts in cancer are sometimes referred to as activated-fibroblasts and are most often distinguished from fibroblasts by their expression of alpha-smooth muscle actin (α-

SMA). In the normal mammary gland α-SMA expression is limited to myoepithelial cells and the smooth muscle cells that line blood vessels (Skalli O et al. 1986, Lazard D et al. 1993). In contrast to the normal mammary gland, α-SMA can be expressed by approximately 80% of the cells present in the stroma of breast carcinomas (Sappino AP et al. 1988). Furthermore, in many mammary carcinomas, including invasive ductal carcinomas, α-SMA is expressed by myofibroblasts that populate the tumor stroma. Indeed, myofibroblasts are particularly interesting because they are absent in the normal mammary gland but present in mammary carcinomas (Skalli O et al. 1986, Barth PJ et al. 2002, Chauhan H et al. 2003, Yazhou C et al. 2004).

Recently, clinical studies have investigated whether the presence of myofibroblasts correlates with disease progression. In colorectal cancer the presence of myofibroblasts, as assessed by immunohistochemistry using an antibody recognizing α-SMA, was negatively correlated with overall survival and disease-free survival (Tsujino T et al. 2007). In another study looking at 58 patients with invasive ductal carcinomas, tumors were scored as either being positive for myofibroblasts or negative (when the percent of α-SMA expressing fibroblasts were <10%) for myofibroblasts. After examining each group for the percentage of patients with positive lymph node metastasis, the subset of patients scored as being positive for myofibroblasts (n=33) had a higher percentage of lymph node-positive patients, 72.7%, than the subset scored as negative for myofibroblasts (n=25), 44% (Yazhou C et al. 2004). These studies suggest that the presence of myofibroblasts during tumor formation results in a poor prognosis for the

patient. However, they do not illuminate the specific contributions of myofibroblasts to the progression of a tumor.

Myofibroblasts Play Several Roles in Tumor Progression

A number of studies examine the role of myofibroblasts and fibroblasts in tumor progression as a population referred to as cancer associated fibroblasts (CAFs). CAFs isolated from carcinomas are most likely to be a mixture of myofibroblasts and fibroblasts. Myofibroblasts and fibroblasts facilitate several aspects of tumor progression including initiation, angiogenesis and invasion.

CAFs Involvement in Facilitating Tumor Initiation

CAFs have been shown to facilitate tumor initiation. In a prostate cancer model, Olumi et al. use initiated prostate cells that are genetically abnormal and express the oncogene SV40-T antigen but do not form tumors when injected into mice (Olumi AF et al. 1999). However, they demonstrated that CAFs were capable of fostering tumor formation when they were co-mixed with these initiated prostate cells, whereas normal fibroblasts had no effect on tumor formation. In addition to demonstrating a role for CAFs in the early stages of tumorigenesis, these data also suggest that CAFs are functionally distinct from normal fibroblasts.

CAFs Involvement in the Promotion of Angiogenesis

CAFs can aid in the process of angiogenesis by providing potent pro-angiogenic molecules. As stated above, angiogenesis is essential for tumor progression and can be initiated by VEGF. Some have demonstrated that in response to hypoxic conditions both normal and cancer-associated mammary fibroblasts upregulate expression of VEGF mRNA (Hlatky L et al. 1994). Additionally, when murine mammary carcinoma cells were grown subcutaneously in transgenic mice that express green fluorescent protein (GFP) under the control of a VEGF promoter, GFP expression was detected in the tumor mass (Fukumura D et al., 1998). Histological analysis revealed that GFP expression was detected in cells whose morphology was consistent with that of fibroblasts. Thus, these data suggest that CAFs may induce angiogenesis during tumor growth through their ability to secrete VEGF.

Work form our own lab has demonstrated that CAFs in breast cancer can enhance tumor formation through their ability to induce angiogenesis (Orimo A et al. 2005). In this study, fibroblasts were isolated from 6 invasive ductal carcinomas of the breast (CAF1-6), normal breast tissue from the same patient (counterpart fibroblasts 1-6), and normal breast tissue from a patient without cancer. In four out of the six cases, cancer-associated fibroblasts enhanced the tumor formation of MCF-7 Ras breast cancer cells relative the actions of both normal and counterpart fibroblasts. Examination of tumors derived from MCF-7 Ras cells co-mingled with CAF1 demonstrated an increase in angiogenesis relative to both the normal and counterpart fibroblasts (Orimo A et al. 2005). It was also discovered that several of the CAF populations displayed increased

expression of the chemokine stromal-derived factor-1 (SDF-1), and that inhibition of SDF-1 was sufficient to prevent the enhanced tumor formation and angiogenesis.

CAFs Involvement in Invasion and Metastasis

CAFs are thought to play a role in promoting tumor invasion and metastasis through several mechanisms, which include their ability to secrete specific growth factors and matrix-remodeling proteins (Kalluri and Zeisberg, 2006). In a transwell assay, conditioned media from myofibroblasts, created by treating fibroblasts with conditioned media from squamous carcinoma cells (SCCs), were able to promote the migration of SCCs in an HGF-dependant manner (Lewis MP et al. 2004). Additionally, myofibroblasts isolated from colon adenocarcinomas, relative to fibroblasts isolated from the adjacent normal tissue, show an increased ability to promote in vitro invasion of colon cancer cells into collagen gels (De Wever O et al. 2004). In the same study, fibroblasts differentiated into myofibroblasts through treatment with TGF-β are also capable of promoting the invasion of colon cancer cells relative to untreated fibroblasts. The ability of myofibroblasts to promote invasion in this study was attributed to their ability to secrete both HGF and Tenascin-C (De Wever O et al. 2004). Thus, fibroblasts and myofibroblasts are not only present at the site of tumor formation, but they are also capable of influencing multiple steps in tumorigenesis.

Questions Addressed

In my studies, I wanted to identify the factors responsible for the recruitment of myofibroblasts to the site of breast cancer formation. I focused on this cell type for two reasons: first, it is present in carcinomas of the breast, but absent in the normal mammary gland; second, it plays a functional role in tumor progression. These two factors/considerations make myofibroblasts an important therapeutic target, because blocking their recruitment should inhibit them from affecting tumor formation without affecting the normal physiology of the breast. Thus, it is important to identify the factors responsible for recruiting these cells to the site of tumor formation.

When this work began, a novel experimental model of breast cancer development, termed BPLER, was developed in our lab and was demonstrated to form tumors with areas that contain numerous myofibroblasts; the histopathology of these tumors resembled that of adenocarcinomas found in the clinic. In my work, I wanted to identify and investigate factors secreted by the BPLER tumor cells that are responsible for the presence of numerous myofibroblasts seen in the desmoplastic areas of the BPLER tumors.

In a second line of experiments, I was interested in whether the cell types that give rise to myofibroblasts are derived from the bone marrow. I was interested in the source of myofibroblasts because they are present in carcinomas and not in the normal mammary gland, which suggests that they are derived from another cell type. Myofibroblasts could be derived from a preexisting cell type in the adjacent tissue or they could also be derived from a systemic source like the bone marrow/blood. The source of

the cells recruited into the tumor stroma has important therapeutic implications, because if a cell type is recruited from the bone marrow, it would be advantageous to intercept it in the blood stream, thereby blocking its recruitment.

In my work, I was interested in whether one of our genetically engineered tumor models is capable of recruiting cell types from the bone marrow. Myofibroblasts, in addition to smooth muscle cells, express α-SMA. As mentioned earlier, Sappino AP et al. assessed that α-SMA can be expressed by approximately 80% of the cells present in the stroma of breast carcinomas (Sappino AP et al. 1988). Thus, I wanted to specifically investigate whether any of the α-SMA-positive stromal cells present in our tumor model are derived from the bone marrow.

References

Allinen M, Beroukhim R, Cai L, Brennan C, Lahti-Domenici J, Huang H, Porter D, Hu M, Chin L, Richardson A, Schnitt S, Sellers WR, Polyak K. (2004) Molecular characterization of the tumor microenvironment in breast cancer. *Cancer Cell*, **6**(1), 17-32.

American Cancer Society. Breast Cancer Facts & Figures 2007-2008. Atlanta: American Cancer Society, Inc.

Bacac M, Provero P, Mayran N, Stehle JC, Fusco C, Stamenkovic I. (2006) A mouse stromal response to tumor invasion predicts prostate and breast cancer patient survival. *PLoS ONE*, Dec 20, **1**:e32.

Barth PJ, Ebrahimsade S, Ramaswamy A, Moll R. (2002) CD34+ fibrocytes in invasive ductal carcinoma, ductal carcinoma in situ, and benign breast lesions. *Virchows Arch*, **440**(3), 298-303.

Basset P, Bellocq JP, Wolf C, Stoll I, Hutin P, Limacher JM, Podhajcer OL, Chenard MP, Rio MC, Chambon P. (1990) A novel metalloproteinase gene specifically expressed in stromal cells of breast carcinomas. *Nature*, **348**(6303), 699-704.

Bergers G, Benjamin LE. Tumorigenesis and the angiogenic switch. (2003) *Nat Rev Cancer*, **3**(6), 401-10.

Bergers G, Brekken R, McMahon G, Vu TH, Itoh T, Tamaki K, Tanzawa K, Thorpe P, Itohara S, Werb Z, Hanahan D. (2000) Matrix metalloproteinase-9 triggers the angiogenic switch during carcinogenesis. *Nat Cell Biol*, **2**(10), 737-44.

Bhowmick NA, Chytil A, Plieth D, Gorska AE, Dumont N, Shappell S, Washington MK, Neilson EG, Moses HL. (2004) TGF-beta signaling in fibroblasts modulates the oncogenic potential of adjacent epithelia. *Science*, **303**(5659), 848-51.

Bissell MJ, Radisky D. Putting tumours in context. (2001) *Nat Rev Cancer*, **1**(1), 46-54.

Brown LF, Guidi AJ, Schnitt SJ, Van De Water L, Iruela-Arispe ML, Yeo TK, Tognazzi K, Dvorak HF. (1999) Vascular stroma formation in carcinoma in situ, invasive carcinoma, and metastatic carcinoma of the breast. *Clin Cancer Res*, **5**(5), 1041-56.

Chauhan H, Abraham A, Phillips JR, Pringle JH, Walker RA, Jones JL. (2003) There is more than one kind of myofibroblast: analysis of CD34 expression in benign, in situ, and invasive breast lesions. *J Clin Pathol*, **56**(4), 271-6.

Cheng N, Bhowmick NA, Chytil A, Gorksa AE, Brown KA, Muraoka R, Arteaga CL, Neilson EG, Hayward SW, Moses HL. (2005) Loss of TGF-beta type II receptor in fibroblasts promotes mammary carcinoma growth and invasion through upregulation of TGF-alpha-, MSP- and HGF-mediated signaling networks. *Oncogene*, **24**(32), 5053-68.

Coussens LM, Raymond WW, Bergers G, Laig-Webster M, Behrendtsen O, Werb Z, Caughey GH, Hanahan D. (1999) Inflammatory mast cells up-regulate angiogenesis during squamous epithelial carcinogenesis. *Genes Dev*, **13**(11), 1382-97.

Coussens LM, Tinkle CL, Hanahan D, Werb Z. (2000) MMP-9 supplied by bone marrow-derived cells contributes to skin carcinogenesis. *Cell*, **103**(3), 481-90.

Cross MJ, Dixelius J, Matsumoto T, Claesson-Welsh L. (2003) VEGF-receptor signal transduction. *Trends Biochem Sci*, **28**(9), 488-94.

De Wever O, Demetter P, Mareel M, Bracke M. (2008) Stromal myofibroblasts are drivers of invasive cancer growth. *Int J Cancer*, **123**(10), 2229-38.

De Wever O, Nguyen QD, Van Hoorde L, Bracke M, Bruyneel E, Gespach C, Mareel M. (2004) Tenascin-C and SF/HGF produced by myofibroblasts in vitro provide convergent pro-invasive signals to human colon cancer cells through RhoA and Rac. *FASEB J*, **18**(9), 1016-8.

Desmoulière A, Geinoz A, Gabbiani F, Gabbiani G. (1993) Transforming growth factor-beta 1 induces alpha-smooth muscle actin expression in granulation tissue myofibroblasts and in quiescent and growing cultured fibroblasts. *J Cell Biol*, **122**(1), 103-11.

Elenbaas B, Weinberg RA. (2001) Heterotypic signaling between epithelial tumor cells and fibroblasts in carcinoma formation. *Exp Cell Res*, **264**(1), 169-84.

Finak G, Bertos N, Pepin F, Sadekova S, Souleimanova M, Zhao H, Chen H, Omeroglu G, Meterissian S, Omeroglu A, Hallett M, Park M. (2008) Stromal gene expression predicts clinical outcome in breast cancer. *Nat Med*, **14**(5), 518-27.

Fukumura D, Xavier R, Sugiura T, Chen Y, Park EC, Lu N, Selig M, Nielsen G, Taksir T, Jain RK, Seed B. (1998) Tumor induction of VEGF promoter activity in stromal cells. *Cell*, **94**(6), 715-25.

Gabbiani G. (2003) The myofibroblast in wound healing and fibrocontractive diseases. *J Pathol*, **200**(4), 500-3.

Hanahan D, Folkman J. (1996) Patterns and emerging mechanisms of the angiogenic switch during tumorigenesis. *Cell*, **86**(3), 353-64.

Hanahan D, Weinberg RA. (2000) The hallmarks of cancer. *Cell*, **100**(1), 57-70.

Heppner KJ, Matrisian LM, Jensen RA, Rodgers WH. (1996) Expression of most matrix metalloproteinase family members in breast cancer represents a tumor-induced host response. *Am J Pathol*, **149**(1), 273-82.

Hinz B, Phan SH, Thannickal VJ, Galli A, Bochaton-Piallat ML, Gabbiani G. (2007) The myofibroblast: one function, multiple origins. *Am J Pathol*, **170**(6), 1807-16.

Hlatky L, Tsionou C, Hahnfeldt P, Coleman CN. (1994) Mammary fibroblasts may influence breast tumor angiogenesis via hypoxia-induced vascular endothelial growth factor up-regulation and protein expression. *Cancer Res*, **54**(23), 6083-6.

Janeway CA, Travers P, Walport M, Shlomchik M. (2001) Immunobiology. New York and London, Garland Science.

Kalluri R, Zeisberg M. (2006) Fibroblasts in cancer. *Nat Rev Cancer*. **6**(5), 392-401.

Kass L, Erler JT, Dembo M, Weaver VM. (2007) Mammary epithelial cell: influence of extracellular matrix composition and organization during development and tumorigenesis. *Int J Biochem Cell Biol*, **39**(11), 1987-94.

Kitamura T, Kometani K, Hashida H, Matsunaga A, Miyoshi H, Hosogi H, Aoki M, Oshima M, Hattori M, Takabayashi A, Minato N, Taketo MM. (2007) SMAD4-deficient intestinal tumors recruit CCR1+ myeloid cells that promote invasion. *Nat Genet*, **39**(4), 467-75.

Lazard D, Sastre X, Frid MG, Glukhova MA, Thiery JP, Koteliansky VE. Expression of smooth muscle-specific proteins in myoepithelium and stromal myofibroblasts of normal and malignant human breast tissue. (1993) *Proc Natl Acad Sci U S A*, **90**(3), 999-1003.

Leek RD, Lewis CE, Whitehouse R, Greenall M, Clarke J, Harris AL. (1996) Association of macrophage infiltration with angiogenesis and prognosis in invasive breast carcinoma. *Cancer Res*, **56**(20), 4625-9.

Lewis MP, Lygoe KA, Nystrom ML, Anderson WP, Speight PM, Marshall JF, Thomas GJ. (2004) Tumour-derived TGF-beta1 modulates myofibroblast differentiation and promotes HGF/SF-dependent invasion of squamous carcinoma cells. *Br J Cancer*, **90**(4):822-32.

Lin EY, Li JF, Gnatovskiy L, Deng Y, Zhu L, Grzesik DA, Qian H, Xue XN, Pollard JW. (2006) Macrophages regulate the angiogenic switch in a mouse model of breast cancer. *Cancer Res*, **66**(23), 11238-46.

Lin EY, Nguyen AV, Russell RG, Pollard JW. (2001) Colony-stimulating factor 1 promotes progression of mammary tumors to malignancy. *J Exp Med*, **193**(6), 727-40.

Lyden D, Young AZ, Zagzag D, Yan W, Gerald W, O'Reilly R, Bader BL, Hynes RO, Zhuang Y, Manova K, Benezra R. (1999) Id1 and Id3 are required for neurogenesis, angiogenesis and vascularization of tumour xenografts. *Nature*, **401**(6754), 670-7.

Lynch CC, Matrisian LM. Matrix metalloproteinases in tumor-host cell communication. (2002) *Differentiation*, **70**(9-10), 561-73.

MayoClinic.com.http://www.mayoclinic.com/health/breast-cancer/HQ00348/METHOD=print.

Nagy JA, Dvorak AM, Dvorak HF. (2007) VEGF-A and the induction of pathological angiogenesis. *Annu Rev Pathol*, **2**, 251-75.

Nozawa H, Chiu C, Hanahan D. Infiltrating neutrophils mediate the initial angiogenic switch in a mouse model of multistage carcinogenesis. (2006) *Proc Natl Acad Sci U S A*, **103**(33), 12493-8.

Olumi AF, Grossfeld GD, Hayward SW, Carroll PR, Tlsty TD, Cunha GR. (1999) Carcinoma-associated fibroblasts direct tumor progression of initiated human prostatic epithelium. *Cancer Res*, **59**(19), 5002-11.

Orimo A, Gupta PB, Sgroi DC, Arenzana-Seisdedos F, Delaunay T, Naeem R, Carey VJ, Richardson AL, Weinberg RA. (2005) Stromal fibroblasts present in invasive human breast carcinomas promote tumor growth and angiogenesis through elevated SDF-1/CXCL12 secretion. *Cell*, **121**(3), 335-48.

Pollard JW. Tumour-educated macrophages promote tumour progression and metastasis. (2004) *Nat Rev Cancer*, **4**(1), 71-8.

Powell DW, Mifflin RC, Valentich JD, Crowe SE, Saada JI, West AB. Myofibroblasts. I. Paracrine cells important in health and disease. (1999) *Am J Physiol*, **277**(1 Pt 1):C1-9.

Ries LAG, Melbert D, Krapcho M, Stinchcomb DG, Howlader N, Horner MJ, Mariotto A, Miller BA, Feuer EJ, Altekruse SF, Lewis DR, Clegg L, Eisner MP, Reichman

M, Edwards BK (eds). (2008) SEER Cancer Statistics Review, 1975-2005, National Cancer Institute. Bethesda, MD, http://seer.cancer.gov/csr/1975_2005/, based on November 2007 SEER data submission, posted to the SEER web site.

Rønnov-Jessen L, Petersen OW, Bissell MJ. (1996) Cellular changes involved in conversion of normal to malignant breast: importance of the stromal reaction. *Physiol Rev*, **76**(1), 69-125.

Sappino AP, Skalli O, Jackson B, Schürch W, Gabbiani G. (1988) Smooth-muscle differentiation in stromal cells of malignant and non-malignant breast tissues. *Int J Cancer*, **41**(5), 707-12.

Skalli O, Ropraz P, Trzeciak A, Benzonana G, Gillessen D, Gabbiani G. (1986) A monoclonal antibody against alpha-smooth muscle actin: a new probe for smooth muscle differentiation. *J Cell Biol*, **103**(6 Pt 2):2787-96.

Shojaei F, Wu X, Malik AK, Zhong C, Baldwin ME, Schanz S, Fuh G, Gerber HP, Ferrara N. (2007) Tumor refractoriness to anti-VEGF treatment is mediated by CD11b+Gr1+ myeloid cells. *Nat Biotechnol*, **25**(8), 911-20.

Tsujino T, Seshimo I, Yamamoto H, Ngan CY, Ezumi K, Takemasa I, Ikeda M, Sekimoto M, Matsuura N, Monden M. (2007) Stromal myofibroblasts predict disease recurrence for colorectal cancer. *Clin Cancer Res*, **13**(7):2082-90.

Wolf C, Rouyer N, Lutz Y, Adida C, Loriot M, Bellocq JP, Chambon P, Basset P. (1993) Stromelysin 3 belongs to a subgroup of proteinases expressed in breast carcinoma fibroblastic cells and possibly implicated in tumor progression. *Proc Natl Acad Sci U S A*, **90**(5), 1843-7.

Yang L, Huang J, Ren X, Gorska AE, Chytil A, Aakre M, Carbone DP, Matrisian LM, Richmond A, Lin PC, Moses HL. (2008) Abrogation of TGF beta signaling in mammary carcinomas recruits Gr-1+CD11b+ myeloid cells that promote metastasis. *Cancer Cell*, **13**(1):23-35.

Yazhou C, Wenlv S, Weidong Z, Licun W. (2004) Clinicopathological significance of stromal myofibroblasts in invasive ductal carcinoma of the breast. *Tumour Biol*, **25**(5-6), 290-5.

Zhang YW, Vande Woude GF (2003) GF.HGF/SF-met signaling in the control of branching morphogenesis and invasion. *J Cell Biochem*, **88**(2), 408-17.

Chapter 2: The Role of VEGF, CXCL1, and CCL5 in the Recruitment of α-SMA-Expressing Stromal Cells to the Site of Tumor Formation

Matthew P. Saelzler[1,2], Ferenc Reinhardt[1], Sandra S. McAllister[1], Mark Bray[3], Tan A. Ince[1,4], and Robert A. Weinberg[1,2]

(1) Whitehead Institute for Biomedical Research, Cambridge, MA 02142
(2) Department of Biology, Massachusetts Institute of Technology, Cambridge, MA 02139
(3) Broad Institute of MIT and Harvard, Cambridge, MA 02142
(4) Department of Pathology, Division of Women's and Perinatal Pathology, Brigham and Women's Hospital, Harvard Medical School, Boston, MA 02115

Ferenc Reinhardt performed all the mouse procedures up to and including the injection of tumor cells into the mice. The preliminary observations about the recruitment of α-SMA-positive cells to the MCF-7 Ras, MDA-MB-231, and BPLER tumors was performed by Sandra McAllister. Mark Bray from the broad institute designed the pipeline for the Cell Profiler analysis. All other experiments carried out by the thesis author, Matthew Saelzler.

Introduction

Myofibroblasts are detectable in both ductal carcinoma in situ (DCIS) and aggressive breast carcinomas. However, they are not detected in the normal mammary gland (Skalli O et al. 1986, Lazard D et al. 1993, Barth PJ et al. 2002, Chauhan H et al. 2003, Yazhou C et al. 2004). This critical observation supports the hypothesis that myofibroblasts play a functional role in tumor progression and suggests the potential clinical utility of identifying the factors involved in the recruitment of myofibroblasts to the site of tumor formation so that this recruitment process may be pharmacologically blocked.

Myofibroblasts are not only detected at sites of tumor formation, but are also detected at other pathological/inflammatory states, such as wound healing and fibrosis. The cell type(s) that give rise to myofibroblasts under various circumstances is still being elucidated and most likely depends on the tissue and pathological situation being studied. For example, the liver- specific hepatic stellate cell is thought to be a precursor to myofibroblasts found in liver fibrosis, but is likely distinct from the myofibroblast precursor in breast tumors (Hinz B et al. 2007). Furthermore, it is possible that myofibroblasts present within a single tissue may be derived from several alternative sources. One such source is resident tissue fibroblasts, which are one of the most well studied precursors. Myofibroblasts are often distinguished from fibroblasts by their expression of α-smooth muscle actin (α-SMA). Interestingly, α-SMA is also expressed by blood vessel-associated smooth muscle cells, which represent yet another potential source of myofibroblasts (Rønnov-Jessen L et al. 1995). It has also been postulated that

endothelial cells and epithelial cells, through the process of endothelial-mesenchymal transition (EndMT) and epithelial-mesenchymal transition (EMT), respectively, are also potential sources of myofibroblasts (Hinz B et al. 2007, Zeisberg EM et al. 2007, Kalluri R and Zeisberg M 2006). Lastly, the presence of bone marrow/blood-derived myofibroblasts has also been demonstrated in models of fibrosis and cancer (Hinz B et al. 2007, Ishii G et al. 2003, Sangai T et al. 2005, Direkze NC et al. 2004, Guo X et al. 2008). Taken together these data suggest that myofibroblasts present at the site of tumor formation may be derived from several sources, including neighboring cell types in the local tissue microenvironment or from systemic sources such as the bone marrow and blood.

Secreted proteins are likely necessary to recruit and/or differentiate these myofibroblast precursors as well as to support the growth and proliferation of myofibroblasts. Candidate factors include growth factors, cytokines, extracellular matrix proteins (ECM), and proteases. One of the most well studied factors is transforming growth factor-β (TGF-β). TGF-β, which induces the presence of myofibroblasts in granulation tissue when injected subcutaneously into rat, increases the expression of α-SMA in human fibroblasts in vitro (Desmoulière A et al. 1993). Fibroblasts isolated from the breast and then kept quiescent were shown to induce α-SMA expression under TGF-β stimulation, but not under stimulation by platelet-derived growth factor (PDGF), interleukin-1 (IL-1), insulin-like growth factor-1 (IGF-1), acidic fibroblast growth factor (aFGF), basic fibroblast growth factor (bFGF), epidermal growth factor (EGF), or interferon-γ (IFN-γ) (Rønnov-Jessen L and Petersen OW, 1993). Furthermore, TGF-β

has been implicated in differentiating fibrocytes, a cell type in peripheral blood, into myofibroblast-like cells and plays a role in inducing both the EMT and EndMT (Abe R et al. 2001, Schmidt M et al. 2003, Zeisberg EM et al. 2007, Kalluri R and Zeisberg M 2006).

In addition to the factors that directly act on myofibroblast precursors, it is also possible that factors secreted by cancer cells recruit myofibroblasts through an indirect mechanism, such as through the stimulation of intermediate cell types. One such mechanism may be initiated by granulocyte-macrophage colony-stimulating factor (GM-CSF) secretion. GM-CSF is a potent inducer of macrophages, which are thought to induce the appearance of myofibroblasts in other pathological situations through the expression of TGF-β (Serini G and Gabbiani G, 1999).

Despite its inability to induce α-SMA expression in mammary fibroblasts, PDGF can induce the proliferation and migration of fibroblasts and is another critical factor that is likely to influence myofibroblast recruitment (Dong J et al. 2004, Tejada ML et al. 2006). Conditioned media from both a fibrosarcoma and lung carcinoma cell line was able to induce *in vitro* proliferation and migration of 3T3 fibroblasts. Fractionation of the conditioned media identified PDGF-A as the factor responsible for these biological activities, although PDGF-C could also be playing a role. Furthermore, PDGF-B, when added exogenously, induced similar effects. (Dong J et al. 2004, Tejada ML et al. 2006). In a separate study it was demonstrated that c-*ras* transfected MCF-7 mammary carcinoma cells have a higher tumor incidence when injected into mice, and more importantly, the tumors that grew out showed an increase in the incorporation of

myofibroblasts (Shao ZM et al. 2000). These increases were inhibited upon expression of a dominant-negative form of PDGF-A. Furthermore, more recent data suggests that PDGF-C is involved in the *in-vivo* recruitment of cancer-associated fibroblasts (CAFs) in a melanoma model (Anderberg C et al. 2009). In the study by Anderberg C et al, some of these CAFs identified also expressed α-SMA, but this was not quantitated. These data taken together suggest a model where PDGF plays a role in the recruitment and accumulation of fibroblasts to the site of tumor formation, while other factors, including TGF-β, are responsible for their differentiation into myofibroblasts.

Lastly, ECM proteins and proteases may also contribute to the presence of myofibroblasts at the site of tumor formation. Fibronectin secreted from mouse colon cancer cells can induce fibroblast migration, and a disintegrin and metalloproteinase with thrombospondin motifs (ADAMTS) was recently implicated in the recruitment of myofibroblasts in a lung cancer model (Morimoto M and Irimura T 2001, Rocks N et al. 2008). In this study by Rocks N et al., tumors derived from BZR cancer cells overexpressing ADAMTS display an increase in the recruitment of α-SMA-positive cells. Additionally, conditioned media from the ADAMTS-expressing cells promoted the in vitro migration of fibroblasts, which was inhibited by neutralizing antibodies against either TGF-β or interleukin-1β. These data suggest that in addition to the recruitment and differentiation of myofibroblast precursors, the local environment may be remodeled to support the influx and growth of myofibroblasts.

Several factors have been implicated in the recruitment of myofibroblasts to the site of tumor formation; however our understanding remains incomplete. Not only are

there several potential precursors of myofibroblasts, they are all likely to respond to unique combinations of secreted factors, and their recruitment can either be direct or indirect. We therefore sought to identify factors specifically involved in the recruitment of myofibroblasts to breast carcinoma cells.

In order to determine the factors important for the recruitment of myofibroblasts in breast carcinoma, it is important to have a model that 1) recapitulates what is histologically seen in human tumors and 2) forms tumors with areas of myofibroblast-rich stroma. These criteria were met by a cell line developed in our lab termed BPLER. This cell line was derived from a reduction mammoplasty utilizing a chemically defined medium tailored for the growth of breast epithelial cells. Using a protocol previously developed in the lab, the newly isolated breast epithelial (BP) cells were transformed through the expression of hTERT (L), the SV40 early region (E) and H-Ras V12 (R) (Ince TA et al. 2007). In parallel, HMLER cells were derived by isolating mammary epithelial cells using the common HMEC media, which were then transformed using the same genes as in the BPLER cells. While these two epithelial cell lines are isolated from the breast and transformed with the same genes, they show very different phenotypes when injected into immune-compromised mice. The HMLER cells form poorly differentiated carcinomas and do not metastasize. In contrast, the BPLER cells form tumors that histologically resemble adenocarcinomas found in the clinic and that metastasize in mice to the lungs. More importantly for our studies, unlike the HMLER cells which contain little desmoplastic stroma, the BPLER tumors contain areas with a desmoplastic stroma. The desmoplastic areas of the BPLER tumors consist of many α-

SMA-positive myofibroblasts (Figure 1). We have also employed two widely used xenograft models, MCF-7 Ras and MDA-MB-231, for comparison to the BPLER tumor xenografts. The MCF-7-Ras and MDA-MB-231 cells are breast carcinoma cell lines originally derived from a pleural effusion in patients with invasive ductal carcinoma.

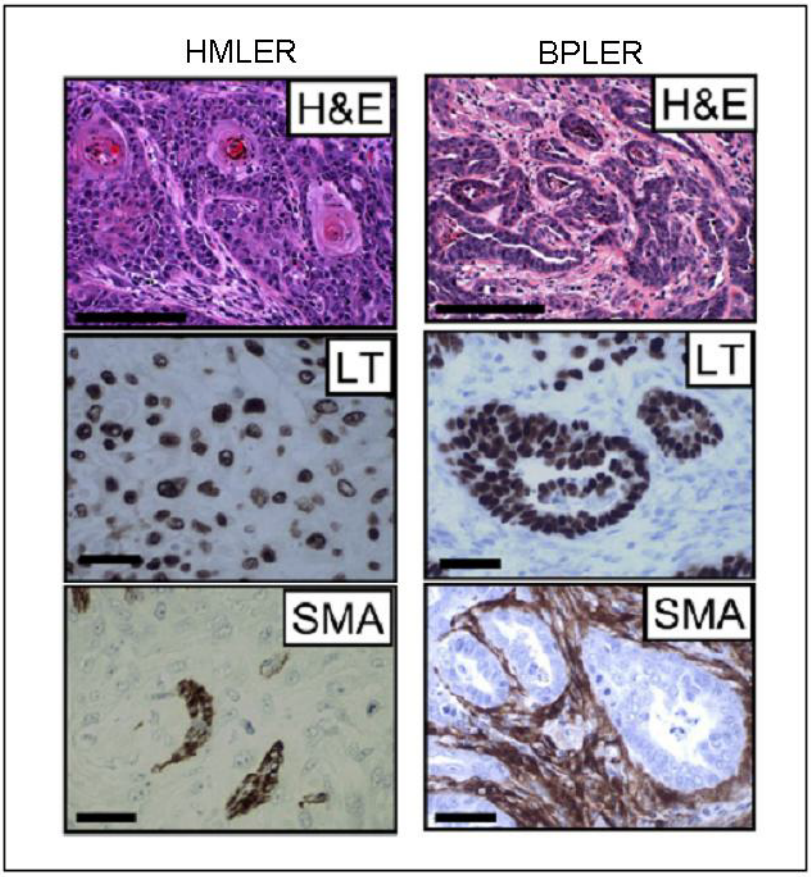

Figure 1: HMLER and BPLER Cells Elicit Different Stromal Reactions During Tumor Formation in Mice. Hematoxylin and Eosin (H&E) stained tumor sections (top), tumor sections stained for Large T (middle) marking the tumor cells, and sections stained for α-SMA (bottom) from HMLER (left) and BPLER (right) tumor-bearing mice reveal the differences in the stroma surrounding the tumor cells. (Adapted from Ince et al. 2007)

As mentioned above, the BPLER tumors form with areas of myofibroblast-rich desmoplastic stroma. In order to identify factors important for the recruitment of myofibroblasts, we compared paracrine factors released by the BPLER cells relative to MDA-MB-231, MCF-7 Ras and HMLER cells. In this study we identified four factors including CXCL1, vascular endothelial growth factor (VEGF), CCL5, and IL-6 that were differentially expressed in the various tumor models. We tested the ability of VEGF, CCL5, and CXCL1 to affect the recruitment of α-SMA-positive stromal cells to MCF-7 Ras tumors, and our results suggest that VEGF, but not the other two factors, increases primary tumor formation and the recruitment of α-SMA-positive cells.

Results

Identification of Secreted Factors Potentially Important in the Recruitment of Myofibroblasts

Preliminary observations suggested that, when compared to tumors formed by MCF-7 Ras and MDA-MB-231 cells, the BPLER tumors recruit more α-SMA-positive cells and the α-SMA-positive cells are distributed more widely and uniformly through the tumor mass (Figure 2). In order to identify factors that may be important for the recruitment of myofibroblasts to the BPLER xenograft tumors, we wanted to compare the paracrine factors secreted by the BPLER cells to those secreted by MCF-7-Ras, MDA-MB-231, and HMLER cells. This was accomplished by comparing the secreted proteins present in the conditioned media of *in vitro* cultures from these cells. The factors present in the conditioned media were detected using an antibody array purchased from RayBiotech Inc., which allows for the simultaneous detection of 79 proteins. The proteins detected by the array are shown in Figure 3A and include growth factors, chemokines, and cytokines. The secreted protein profiles for each of the cell lines are displayed in Figure 3B. Using this approach, we identified four cytokines that appeared to be expressed at higher levels in the BPLER cells and expressed at lower levels in the other cell lines; these cytokines were CXCL1/GRO-α, RANTES/CCL5, VEGF and IL-6. The relative expression of these factors was then confirmed by an enzyme-linked immunosorbent assay (ELISA) (Figure 3C-F). For the ELISA measurements, the various cell lines were plated at different densities depending on their proliferation rate and the number of cells, at the end of the experiment, was counted following the collection of the

conditioned medium. The ELISA measurements confirm that CXCL1/GRO-α, RANTES/CCL5, VEGF, and IL-6 are indeed expressed at higher levels *in vitro* in the BPLER cells when compared to MDA-MB-231, MCF-7 Ras and HMLER cells.

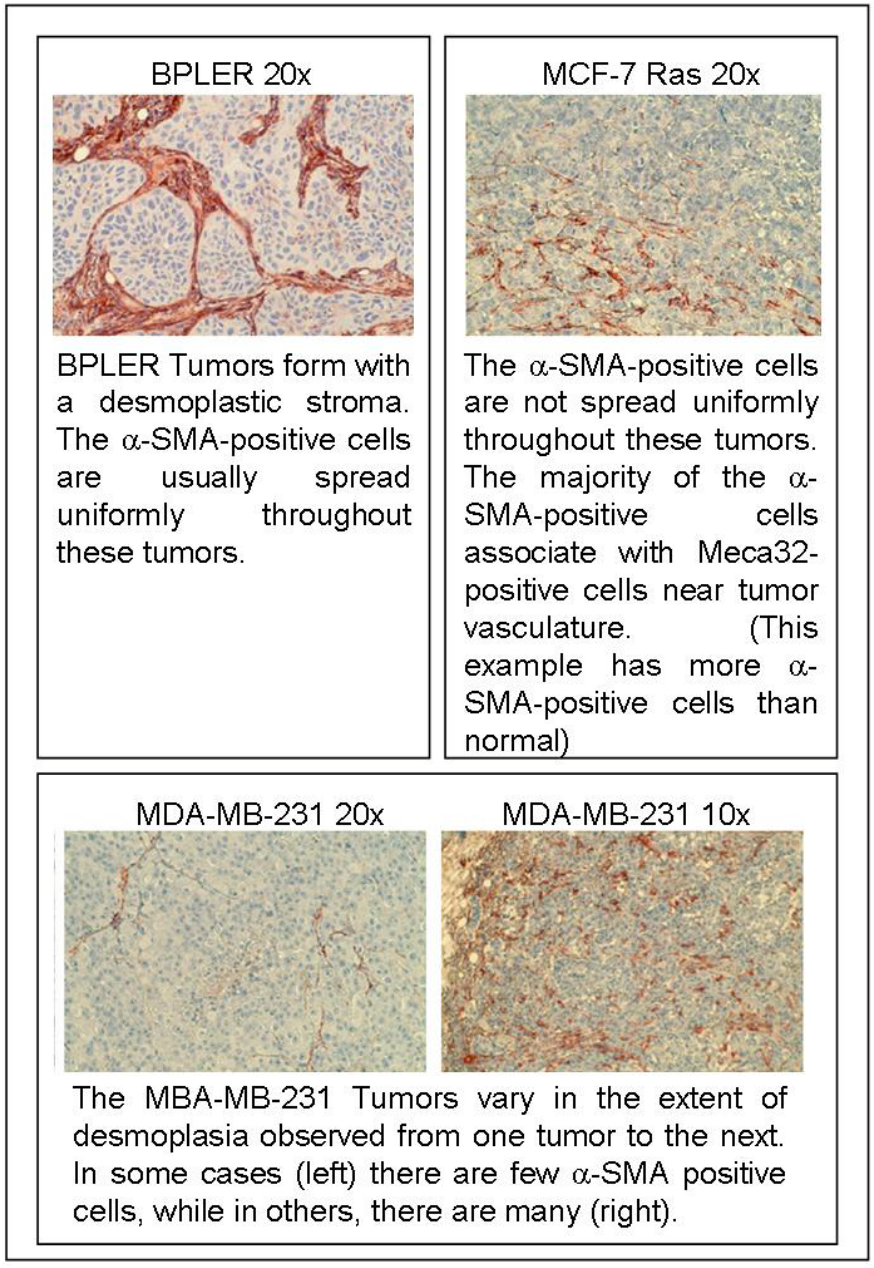

Figure 2: Histopathological Differences of α-SMA-Positive Stromal Cells in Various Human Breast Carcinoma Xenografts. BPLER (top left) tumors tend to recruit more α-SMA-positive stromal cells than the MDA-MB-231 (bottom) and MCF-7 Ras (top right) human carcinoma models. Tumor sections stained with an anti-α-SMA antibody (red) and counterstained with hematoxylin to label nuclei (blue).

Figure 3:

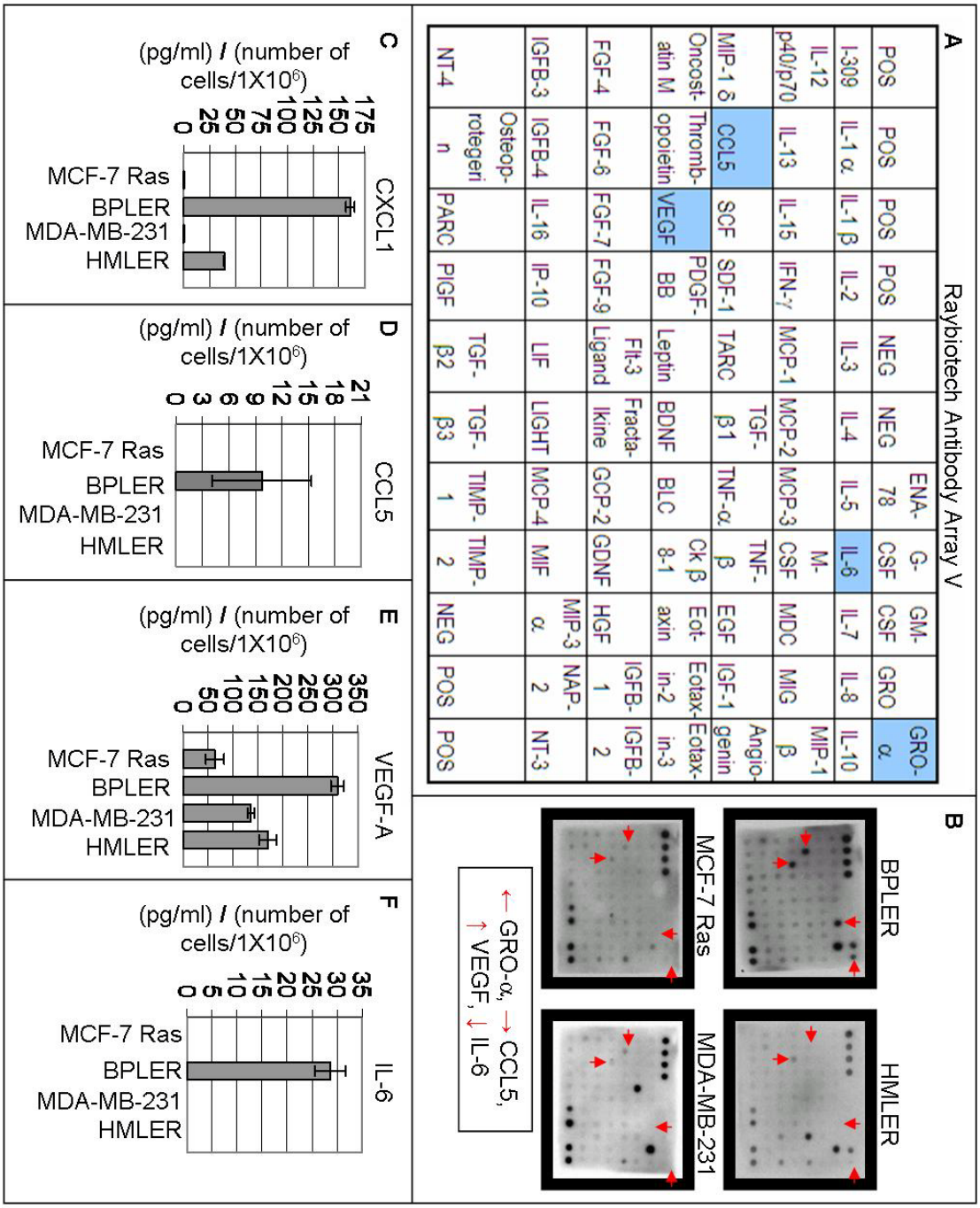
A
Raybiotech Antibody Array V
POS POS POS NEG NEG ENA-78 G-CSF GM-CSF GRO POS
I-309 IL-1 α IL-1 β IL-2 IL-3 IL-4 IL-5 IL-6 IL-7 IL-8 IL-10
IL-12 p40/p70 IL-13 IL-15 IFN-γ MCP-1 MCP-2 MCP-3 M-CSF MDC MIG MIP-1 β
MIP-1 δ Oncost-atin M CCL5 Thromb-opoietin SCF VEGF SDF-1 PDGF-BB TARC Leptin TGF-β1 BDNF TNF-α BLC TNF-β Ck β 8-1 EGF Eot-axin IGF-1 Eotax-in-2 Angio-genin Eotax-in-3
FGF-4 FGF-6 FGF-7 FGF-9 Flt-3 Ligand Fracta-lkine GCP-2 GDNF HGF MIP-3 α IGFB-1 NAP-2 IGFB-2
IGFB-3 IGFB-4 IL-16 IP-10 LIF LIGHT MCP-4 MIF TIMP-1 TIMP-2 NEG POS NT-3
NT-4 Osteop-rotegerin PARC PIGF TGF-β2 TGF-β3
B
BPLER
MCF-7 Ras
MDA-MB-231
HMLER
← GRO-α, → CCL5,
↑ VEGF, ↓ IL-6
C
(pg/ml) / (number of cells/1X10⁶)
CXCL1
MCF-7 Ras
BPLER
MDA-MB-231
HMLER
D
(pg/ml) / (number of cells/1X10⁶)
CCL5
MCF-7 Ras
BPLER
MDA-MB-231
HMLER
E
(pg/ml) / (number of cells/1X10⁶)
VEGF-A
MCF-7 Ras
BPLER
MDA-MB-231
HMLER
F
(pg/ml) / (number of cells/1X10⁶)
IL-6
MCF-7 Ras
BPLER
MDA-MB-231
HMLER

Figure 3 (continued):

Figure 3: Analysis of Conditioned Media from Several Cancer Cell Lines Reveals That VEGF-A, CCL5, CXCL1 and IL-6 are Expressed at Higher Levels in BPLER Cells Relative to the Other Breast Cancer Cell Lines. (A) The proteins recognized by the Raybiotech Antibody Array V and their location on the array. The proteins identified by the array as being expressed at higher levels in the BPLER cells are in the blue colored boxes. **(B)** Analysis of conditioned media from BPLER, MCF-7 Ras, MDA-MB-231 and HMLER cells using the Raybiotech Antibody Array V. The arrows point to proteins that appear to be expressed at higher levels in the BPLER-1 cells when compared to the three other cell lines. ELISA analysis for the relative expression of GRO-α/CXCL1 **(C)**, CCL5 **(D)**, VEGF-A **(E)** and IL-6 **(F)** in MCF-7 Ras, BPLER, MDA-MB-231, BPHER-3, and HMLER cells.

Determining the Effect of CXCL1, CCL5, and VEGF on In-Vivo Tumor Growth

As noted above, preliminary observations suggested that BPLER tumors recruited more α-SMA-positive cells than the MCF7-Ras cells. Therefore, we wanted to determine if CXCL1, CCL5, or VEGF played a role in recruitment of α-SMA-positive stromal cells in the MCF-7 Ras tumor model. We infected MCF-7-Ras cells with retroviral constructs to stably overexpress each of the three genes. For initial experiments, we used the mouse CXCL1 (mCXCL1, also mouse Gro-1), the mouse $VEGF_{164}$ ($mVEGF_{164}$), and the human CCL5 (hCCL5) genes. Three different expression vectors were used: mCXCL1 and $mVEGF_{164}$ were expressed from the pBabe-zeo vector (pBzeo); hCCL5 was expressed from the pLZ-IRES-GFP (pLZR) vector; and a truncated mutant of human CCL5, CCL5 (9-68) (ΔhCCL5), which has been described as an antagonist of CCL5 (Gong JH et al. 1996), was expressed in the pWZL-Blast vector. We also generated three control cell lines, each expressing one of the empty vectors. We confirmed the expression of each of the factors by ELISA (Figure 4A). mCXCL1 and mVEGF were only detected in the MCF-7-Ras cells containing the mCXCL1 gene or the $mVEGF_{164}$ gene, respectively, and hCCL5 was detected in the MCF-7-Ras cells containing either the hCCL5 gene or the ΔhCCL5 gene.

We next determined if the expression of these various factors had any effect on the *in vitro* proliferation of these cell lines. As shown in Figure 4B, there are no major differences observed in their proliferation. We then wanted to see whether the expression of these factors would influence tumor formation. Each of the factor-expressing cell lines were injected subcutaneously into NOD-SCID mice and tumor formation was assessed.

The $mVEGF_{164}$-expressing MCF-7-Ras cells, but not those expressing mCXCL1, hCCL5, or ΔhCCL5, displayed enhanced tumor growth, as assessed by final tumor weight (Figure 4C).

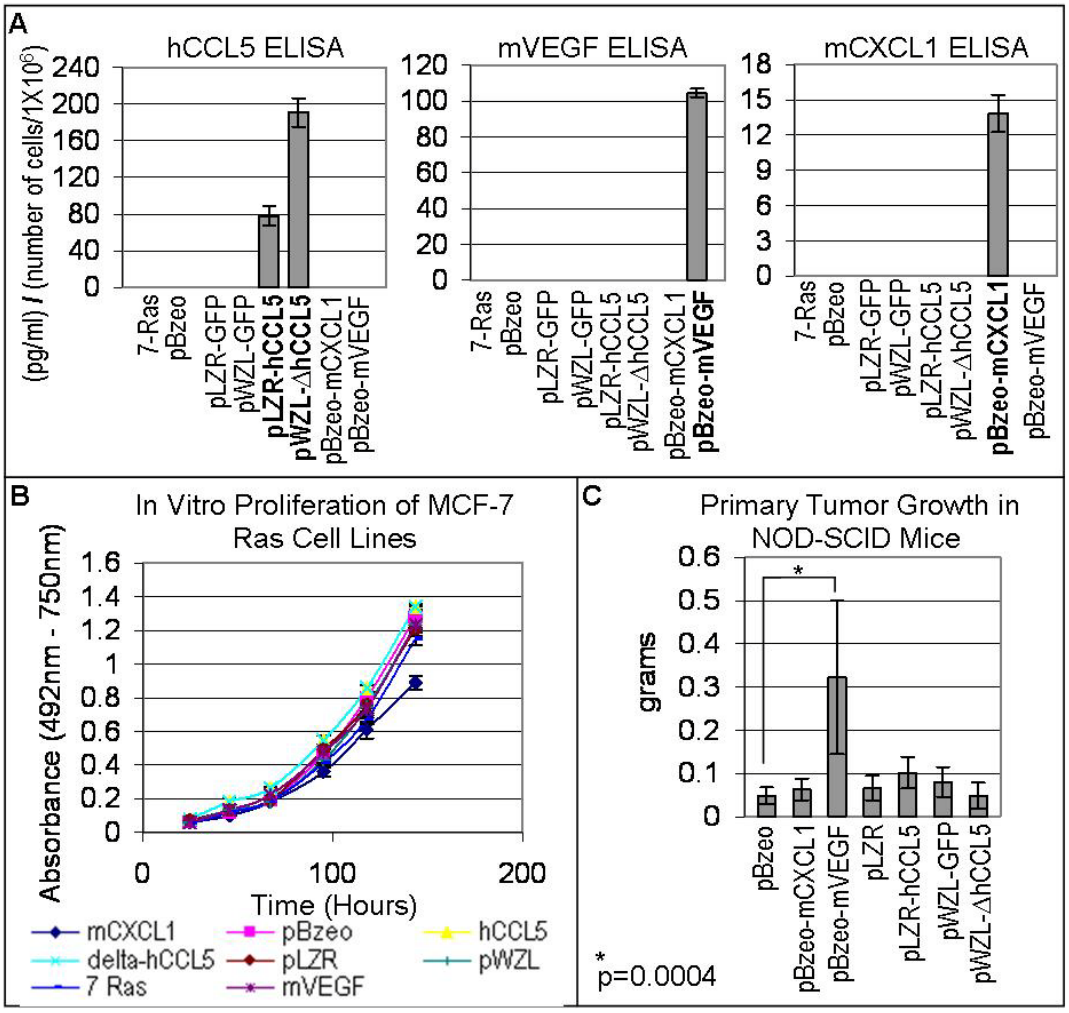

Figure 4: mVEGF$_{164}$-, but not mCXCL1- nor hCCL5-, Expressing MCF-7 Ras Cells Display Increased Tumor Growth in NOD-SCID Mice (A) ELISA analysis for human CCL5 (left), mouse VEGF (middle), mouse CXCL1 (right) expression in the MCF-7 Ras cells ectopically expressing either mouse VEGF$_{164}$ (pBzeo-mVEGF), mouse CXCL1 (pBzeo-mCXCL1), human CCL5 (pLZR-hCCL5), human ΔhCCL5 (pWZL-ΔhCCL5) or the control empty vectors pBabe-zeo (pBzeo), pWZL-GFP, or pLZR-GFP. Additionally, ELISA analysis was performed on MCF-7 Ras cells containing none of the vectors (7 Ras) **(B)** The In vitro growth of the MCF-7 Ras cell lines was analyzed for 7 days using the CellTiter 96® AQueous One Solution Cell Proliferation Assay. The proliferation assay was performed in triplicate and a representative experiment is shown. **(C)** MCF-7 Ras cell lines were injected subcutaneously into NOD-SCID mice to assess in vivo tumor growth. The bar graph displays the average tumor weight at the end of the experiment, and the mVEGF$_{164}$-expressing tumors are significantly larger than the pBzeo-expressing MCF-7 Ras tumors. The p value for the difference in tumor weight between mVEGF$_{164}$- and pBzeo-expressing tumors is also displayed on the chart, $p=4x10^{-4}$.

Examining the Recruitment of α-SMA-Positive Cells and CD34-Positive Cells to the Factor Expressing MCF-7-Ras Tumors Grown in NOD-SCID Mice

Given that the $mVEGF_{164}$-expressing tumors displayed an increase in tumor growth, we wanted to test the hypothesis that $mVEGF_{164}$, more than the other factors, increases the recruitment of α-SMA-positive myofibroblasts and enhances tumor growth. The expression of α-SMA in breast carcinomas is not confined to myofibroblasts, but is also expressed by smooth muscle cells, which associate with endothelial cells to form blood vessels, and myoepithelial cells (Skalli O et al. 1986, Lazard D et al. 1993). Therefore, it was important to distinguish between the recruitment of both α-SMA-positive stromal cells and α-SMA-positive smooth muscle cells.

To do so, tumor sections from each of the factor-overexpressing carcinomas were co-stained with antibodies against α-SMA and CD34, a marker of endothelial cells, and analyzed using immunofluorescence. In order to quantitate the recruitment of these cell types, we used the Cell Profiler image analysis program. Using this program, a module was designed to measure the total area stained for CD34 and the total area stained for α-SMA within a given image. The cell profiler program also produces a photomicrograph that outlines the areas it has identified as blue (DAPI staining), green (CD34 staining), or red (α-SMA staining). An example of the photomicrographs produced by the program is displayed in Supplementary Figure 1.

$mVEGF_{164}$-expressing MCF-7-Ras (MCF-7-Ras-$mVEGF_{164}$) tumors, but not the other chemokine over-expressing tumors, displayed an increase in the recruitment of α-SMA-positive cells and CD34-positive cells as assessed by the average area per tumor

section stained for α-SMA and CD34, respectively (Figure 5A and B). There was a 1.5 fold increase in the average area per tumor section stained for α-SMA compared to the pBzeo control tumors. The $mVEGF_{164}$ tumors also displayed a 5.5 fold increase in the average area per tumor section stained for CD34, relative the control pBzeo tumors. In a second analysis, MCF-7-Ras-$mVEGF_{164}$ tumors were compared to another control cell line, the MCF-7-Ras cells expressing the pWZL-GFP vector. In this experiment the $mVEGF_{164}$-expressing tumors displayed a 1.2 fold and 4.3 fold increase in the average area per tumor section stained for α-SMA and CD34, respectively, confirming the results of the first analysis (Supplementary Figure 2A). Furthermore, a cursory examination of the MCF-7-Ras-$mVEGF_{164}$ tumor sections revealed that some of them had what appeared to be extensive areas of necrosis. The large necrotic looking areas in some of the $mVEGF_{164}$ tumors might be a result of their increased size.

Figure5:

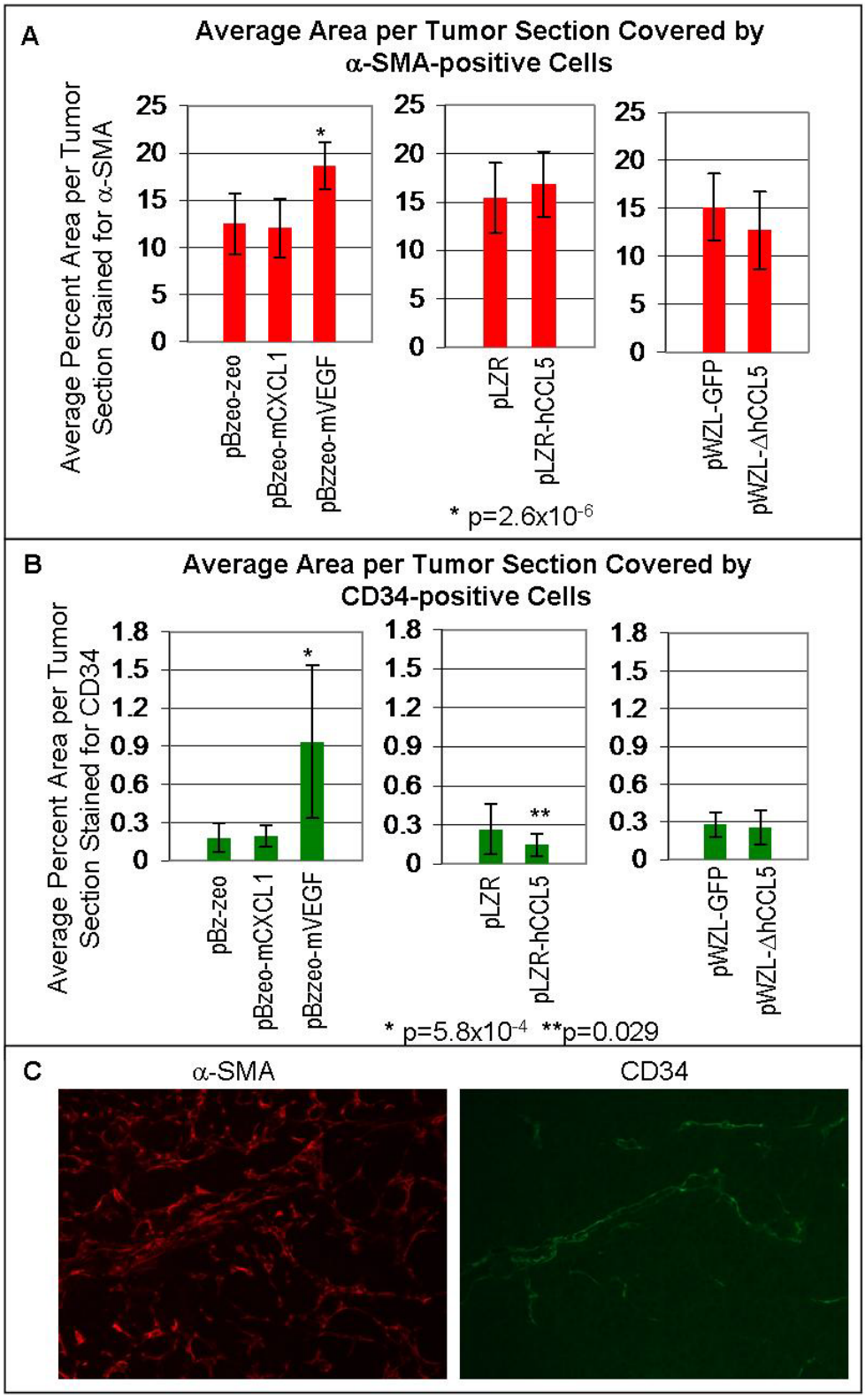
A
Average Area per Tumor Section Covered by α-SMA-positive Cells
Average Percent Area per Tumor Section Stained for α-SMA
25
20
15
10
5
0
*
pBzeo-zeo
pBzeo-mCXCL1
pBzzeo-mVEGF
pLZR
pLZR-hCCL5
pWZL-GFP
pWZL-ΔhCCL5
* p=2.6x10-6
B
Average Area per Tumor Section Covered by CD34-positive Cells
Average Percent Area per Tumor Section Stained for CD34
1.8
1.5
1.2
0.9
0.6
0.3
0
*
**
pBz-zeo
pBzeo-mCXCL1
pBzzeo-mVEGF
pLZR
pLZR-hCCL5
pWZL-GFP
pWZL-ΔhCCL5
* p=5.8x10-4 **p=0.029
C
α-SMA
CD34

Figure 5 (continued):

Figure 5: $mVEGF_{164}$-, but not mCXCL1- nor hCCL5-, Expressing MCF-7 Ras Cells Display Increased Incorporation of α-SMA-Positive cells and CD34-Positive cells. Tumors sections from NOD-SCID mice bearing MCF-7 Ras-derived carcinomas expressing either $mVEGF_{164}$ (pBzeo-mVEGF), mCXCL1 (pBzeo-mCXCL1), hCCL5 (pLZR-hCCL5), or ΔhCCL5 (pWZL-ΔhCCL5) were stained using immnuofluorescence for both α-SMA (red) and CD34 (green), nuclei were counterstained with DAPI (blue). The area of a photomicrograph covered by α-SMA staining or CD34 staining was measured by using the program Cell Profiler. For the graphs shown in (A) and (B), the average percent area per tumor section stained for both the α-SMA stain and CD34 stain was calculated as follows: The area covered by either of the stains in a photomicrograph was calculated by taking the area stained divided by the total area and then multiplying it by 100. Next, for each tumor section on a slide, a number of photomicrographs were taken depending on the size of the tumor, and the percent area stained for each of the photomicrographs was added together and divided by the number of photomicrographs to give the average percent area stained for that tumor section. The average percent area stained for each of the tumor sections within an experimental group were then added together and divided by the number of tumor sections in the group. Graphs showing average percent area covered by α-SMA staining ,**(A)** or CD34 staining, **(B)** for $mVEGF_{164}$- and mCXCL1-expressing tumors relative to control pBzeo-expressing tumors (left), for hCCL5-expressing tumors relative to control pLZR-GFP-expressing tumors (middle), and for ΔhCCL5-expressing tumors relative to pWZL-GFP-expressing tumors (right). The p values for statistically significant changes are displayed below the graphs. **(C)** Representative pictures of α-SMA positive staining and CD34 positive staining of tumor sections from $mVEGF_{164}$-expressing MCF-7 Ras tumor bearing mice.

These results suggest that $mVEGF_{164}$ enhances the recruitment of CD34-positive cells and α-SMA-positive cells. The dramatic increase in CD34-positive cells confirms that the $mVEGF_{164}$ expressed in our cells is indeed functional, given the well characterized role of VEGF in inducing angiogenesis. We next examined whether the increase in α-SMA-positive cells was due to an increase in α-SMA-positive cells associated with CD34-positive cells. We compared the total area stained by α-SMA and CD34 in individual tumor sections and found no correlation between α-SMA-positivity and CD34-positivity (R^2=0.18). Furthermore, by looking at the localization of α-SMA-positive cells within a tumor section, there are numerous α-SMA-positive cells that are clearly not proximal to CD34-positive cells (Figure 5C). This suggests that the increase in α-SMA-positive cells is not solely from an increase in smooth muscle cells, but also from another α-SMA-positive cell type which we hypothesize is myofibroblasts.

Discussion

By comparing the factors secreted by BPLER cells relative to other breast carcinoma cells lines, we identified CXCL1, CCL5, VEGF and IL-6 as potential candidates responsible for the recruitment of myofibroblasts to the site of BPLER tumor formation. The expression of $mVEGF_{164}$, but not mCXCL1 nor hCCL5 in MCF-7-Ras cells resulted in increased tumor growth and α-SMA-positive cell recruitment. Our data suggest that these α-SMA-positive cells are not only vessel-associated smooth muscle cells, but also contain myofibroblasts.

While other studies have implicated other factors including PDGF and TGF-β in the recruitment of myofibroblasts to breast carcinomas, our results suggest a role for VEGF in recruiting myofibroblasts to the sites of breast cancer formation. There are many approved drugs that target VEGF signaling such as Avastin, which neutralizes the VEGF ligand, and Sutent, which blocks a VEGF receptor (Folkman J, 2007). It will be interesting to see how these drugs affect the recruitment of myofibroblasts, in addition to their anti-angiogenic effects, and if this can be applied to the clinic.

Acknowledgements: We would like to thank Tina Yuan for her editing and critical comments on this chapter. We would like to thank Scott Valastyan for his editing and critical comments on the figures presented in this chapter. We would like to thank Tony Karnoub for both the hCCL5 virus and the ΔhCCL5 construct. We would also like to thank Sandra McAllister, Scott Valastyan, and Lynne Waldman for helpful discussions on this work. We would especially like to thank Tina Yuan for her helpful discussions on this work

Materials and Methods

Cell Lines and Tissue Culture: The BPLER, BPHER-3, and HMLER cells were obtained from within the lab and were created as previously explained (Elenbaas B et al. 2001, Ince TA et al. et al. 2007). The HMLER cells used in this study were not the ones used in the study by Ince TA et al. (Ince TA et al. et al. 2007). The BPLER and BPHER-3 cells were cultured as previously described except that the final concentration of glutamine was 1mM instead of 2mM (Ince TA et al. et al. 2007). In general, the HMLER-HR cells were cultured in a 1:1 mix of Dulbecco's Modified Eagle's (DME) Medium and F12 Medium. The DME/F12 mix was supplemented with 5% calf serum, 10 ng/mL of EGF, 1-2 ug/mL of hydrocortisone, 10 ug/ul of insulin, penicillin and streptomycin. The HMLER cells were cultured in a 1:1 mix of MEGM or MEMB (LONZA, Walkersville MD) and DME/F12 Media supplemented as described above but without the calf serum. MCF-7 Ras and MDA-MB-231 cells were cultured under standard conditions.

Tumor Xenografts: Nude mice were bought from Taconic (Hudson, NY). The NOD-SCID mice were bred in the lab. For subcutaneous injection, all cancer cell lines were resuspended in BD Matrigel™ Matrix (BD Biosciences, Bedford MA) diluted in tissue culture media. For BPLER xenografts approximately $1x10^6$ cells were injected. For the NOD-SCID mouse experiment and the NUDE experiment looking at the MCF-7 Ras cell line variants, approximately $5x10^5$ cells were injected subcutaneously.

Measurement of Chemokines by Antibody Array: For the arrays, media conditioned by HMLER-1, BPLER-1, MDA-MB-231 or MCF-7 Ras cells was placed on the Human Cytokine Array V from Raybiotech (RayBiotech, Norcross GA). The arrays were then washed and processed according to the manufacturer's protocol.

Preparation of Conditioned Media for Measurement by ELISA: Conditioned media for each of the cell lines was produced in the same way, but was not necessarily done on the same day. On the first day the cells were plated into 10cm culture dishes in triplicate. The number of cells plated per 10cm dish was approximately: $1x10^6$ BPLER-1 cells, $5x10^5$ HMLER cells, $1.5x10^6$ or 1 $x10^6$ MCF7-Ras cells, $2x10^6$ or 1 $x10^6$ MDA-MB-231 cells. The media was changed on the second day. On the third day the media was changed again and was then collected 24 hours later. Next, the conditioned media was passed through a 0.45 um filter in order to remove any floating cells or debris. The media was then aliquoted placed at -20°C. After collecting the conditioned media the number of cells on each of the plates was determined using a coulter counter.

Conditioned media was also produced to confirm the overexpression of human CCL5, human ΔCCL5, mouse GRO-1 and mouse VEGF in the MCF-7 Ras cell line variants. The MCF-7 Ras cell lines were plated at $1x10^6$ cells per 10cm tissue culture dish in triplicate. The cells were allowed to grow for 2 days and then media was conditioned overnight. The media was collected and the cells were counted similar to the other experiment, except that the conditioned media was passed through the 0.45 um filter after the samples were thawed and right before being measured by ELISA.

Creation of the MCF-7 Ras Chemokine Expressing Cell Lines: The following vectors were used: pBabe-zeo, pWZL-blast-GFP, pLZR-GFP, pBabe-zeo-mGRO-1, pBabe-zeo-mVEGF, pWZL-blast-ΔhCCL5, pLZR-hCCL5-GFP. The pLZR-hCCL5-GFP construct produces a bi-cistronic message containing the sequence for human CCL5 and GFP. In general, the transfections and infections using the pBabe and pWZL vectors were carried out similar to what has been previously described (Stewart SA et al 2003). Cells infected with virus produced by using pBabe-zeo were selected in media containing at least 33.3 ug/mL of zeocin. Cells infected with virus produced by using pWZL-blast were selected in media containing at least 2 ug/mL of blastacidin. Control non-infected cells were also treated with either blastacidin or zeocin. Viral supernatant containing the control pLZR-GFP gene and the pLZR-hCCL5-GFP gene was obtained from T. Karnoub in lab (Karnoub AE et al. 2007). Infected cells were selected using fluorescence-activated cell sorting (FACS) by gating for GFP expression. The cells were then cultured for a period of time before undergoing a second round of FACS for GFP expression.

ELISA: The human IL-6, human CCL5, human VEGF, human CXCL1 and mouse VEGF ELISAs were purchased from R&D Systems, Minneapolis MN. The mouse GRO ELISA was purchased from Immuno-Biological Laboratories, Japan. The conditioned media was removed from the -20°C freezer and thawed. For the experiment comparing different cell lines, conditioned media was diluted 1:4 in DME medium for the human CXCL1 ELISA and1:1 in DME medium for the CCL5, IL-6 and VEGF ELISAs. For measuring the levels of overexpression in the MCF-Ras cell line variants, conditioned media was not diluted for measurement of mouse CXCL1 by ELISA. For the other measurements, the conditioned media was diluted 1:19 in DME medium. After dilution, the samples were added to the ELISA plates and the ELISAs were run following the manufacturer's protocol. At the end of the experiment the absorbance was read at 450nm and 595nm. The absorbance at 595nm was subtracted from the absorbance at 450nm to take into account any general absorbance not due to the color reagent. The numbers plotted on the graph is the amount of protein (pg/mL) per million cells in the diluted media.

Proliferation Assays: The MCF-7 Ras cell line variants were plated in triplicate into 96 well plates. The cell lines were plated at a density of 1000 cells per well. The proliferation assays were performed using the CellTiter 96® AQ_{ueous} One Solution Cell Proliferation Assay (Promega, Madison WI) and following the manufacturer's protocol. The final absorbance was obtained by subtracting the absorbance at 750nm from the

absorbance at 492 nm. The proliferation was measured over the course of seven days. The media was changed every other day. On the day proliferation was measured, the media was removed and replaced with fresh media before starting the Assay.

Immunohistochemistry and Immunofluorescence: Tumor and tissues were dissected from the mice and placed into PBS and then fixed in 4-10% formalin overnight at a minimum. The tissues were then kept in 70% ethanol until they could be processed further. Next, the tissues were embedded into paraffin wax. The embedded tumors were sectioned and placed on glass slides. For staining, the tumors sections on the slides were deparaffinized by incubating them in xylenes for at least 12 minutes. The sections were then rehydrated through serial dips in 100% ethanol, 95% ethanol, 70% ethanol and then placed in phospho-buffered saline (PBS). For antigen retrieval, the slides were placed into 0.01M citrate buffer (pH 6.0) and heated in the microwave at 50% power for a minimum of 6 minutes. Then, the slides were left to cool in the citrate buffer for 1 hour. After antigen retrieval, the slides were rinsed in PBS and then placed in a blocking buffer for a minimum of 30 minutes. Before blocking slides for immunohistochemistry, some of the sections were incubated in methanol containing approximately 2% hydrogen peroxide for 15 minutes in order to quench any endogenous peroxidases. Following the methanol treatment, the slides were rinsed with PBS-T before putting them into the blocking buffer. The slides were blocked in PBS containing 0.1% TWEEN-20 (PBS-T) and 5% inactivated fetal calf serum (IFS). The primary antibodies were made up in PBS-T containing 2% IFS. In general the antibody dilutions used were: mouse monoclonal

anti-α-SMA antibody (Vector Laboratories, Burlingame CA) 1:50 and a rat monoclonal anti-CD34 (MEC 14.7) antibody (Novus Biologicals, Littleton CO) 1:100. The sections were placed in primary antibody overnight. The next day the primary antibody was removed and the slides were washed with PBS. Following the washes, the slides were placed in secondary antibody for approximately 1 hour. The secondary antibodies were diluted in PBS containing 1%IFS.

For immunohistochemistry, the Vectastain Elite ABC kits (Vector Laboratories, Burlingame CA) were used to detect the primary antibody. After incubation with the secondary antibody, the slides were washed with PBS. The slides were then placed in the ABC reagent for 30 minutes. Next, the slides were rinsed several times in PBS. The Nova Red Kit (Vector Laboratories, Burlingame CA) was used to detect positive cells. Following the Nova Red treatment, the slides were placed into water before 5 being stained with Hematoxylin. Next the slides were rinsed in water, dipped twice in 2% Glacial Acetic Acid, rinsed with water, dipped once in 0.1% NH_3OH and then rinsed again with water. The sections were then dehydrated by serial rinses in 70%, 95% and then 100% Ethanol. Before being mounted, the slides were incubated in xylenes. Following the xylenes treatment, the slides were mounted with a glass slide using either Permount (Fisher Scientific, Fair Lawn NJ) or VectaMount (Vector Laboratories, Burlingame CA).

For immunofluorescence, fluorescent conjugated secondary antibodies were used to detect the primary antibody. A donkey anti-mouse Alexa Fluor® 594 and a donkey anti-rat Alexa Fluor® 488 (Invitrogen: Molecular Probes, Eugene OR) were used to

detect the α-SMA antibody and CD34 antibody, respectively. The secondary antibodies were used at a 1:200 dilution. Following the secondary antibody incubation the slides were rinsed several times with PBS. A DAPI Nucleic Acid Stain (Invitrogen: Molecular Probes, Eugene OR) was used to detect the cell nuclei. The stock solution of DAPI was made according to the manufacturer's protocol. The stock solution was diluted in PBS at 1:10,000 and the slides were stained with DAPI for 10 minutes. Following the nucleic acid stain, the slides were rinsed twice with water and a cover slip was mounted on the slide with SlowFade® Gold antifade reagent (Invitrogen: Molecular Probes, Eugene OR). The slides were then placed at 4^{o}C in the dark until pictures could be taken with a fluorescent microscope.

Cell Profiler Analysis: Pictures of the immunofluorescently stained tumors were taken on a fluorescent microscope using the 20x objective. Approximately, one to ten pictures were taken of a single tumor section, depending on the size of the tumor. For each area, a picture was taken of the α-SMA-positive stain, the CD34-postive stain, and the DAPI stain. After all the pictures were taken, the images were loaded into the Cell Profiler Program for analysis. The Cell Profiler program calculated the area covered by each of the stains within a single image. Because, some of the $mVEGF_{164}$-expressing tumors may have been cut in half to fit them into the tissue cassette, the average percent area per tumor section stained for both the CD34 stain and α-SMA stain was calculated as follows: The area covered by either of the stains in a photomicrograph was calculated by taking the area stained divided by the total area and then multiplying it by 100. Next, for

each tumor section on a slide, a number of photomicrographs were taken depending on the size of the tumor, and the percent area stained for each of the photomicrographs was added together and divided by the number of photomicrographs to give the average percent area stained for that tumor section. The average percent area stained for each of the tumor sections within an experimental group were then added together and divided by the number of tumor sections in the group.

Statistical Analysis: T-tests were performed using excel. A one-tailed T-test with unequal variance was performed to calculate the p-values for all comparisons.

Supplementary Material

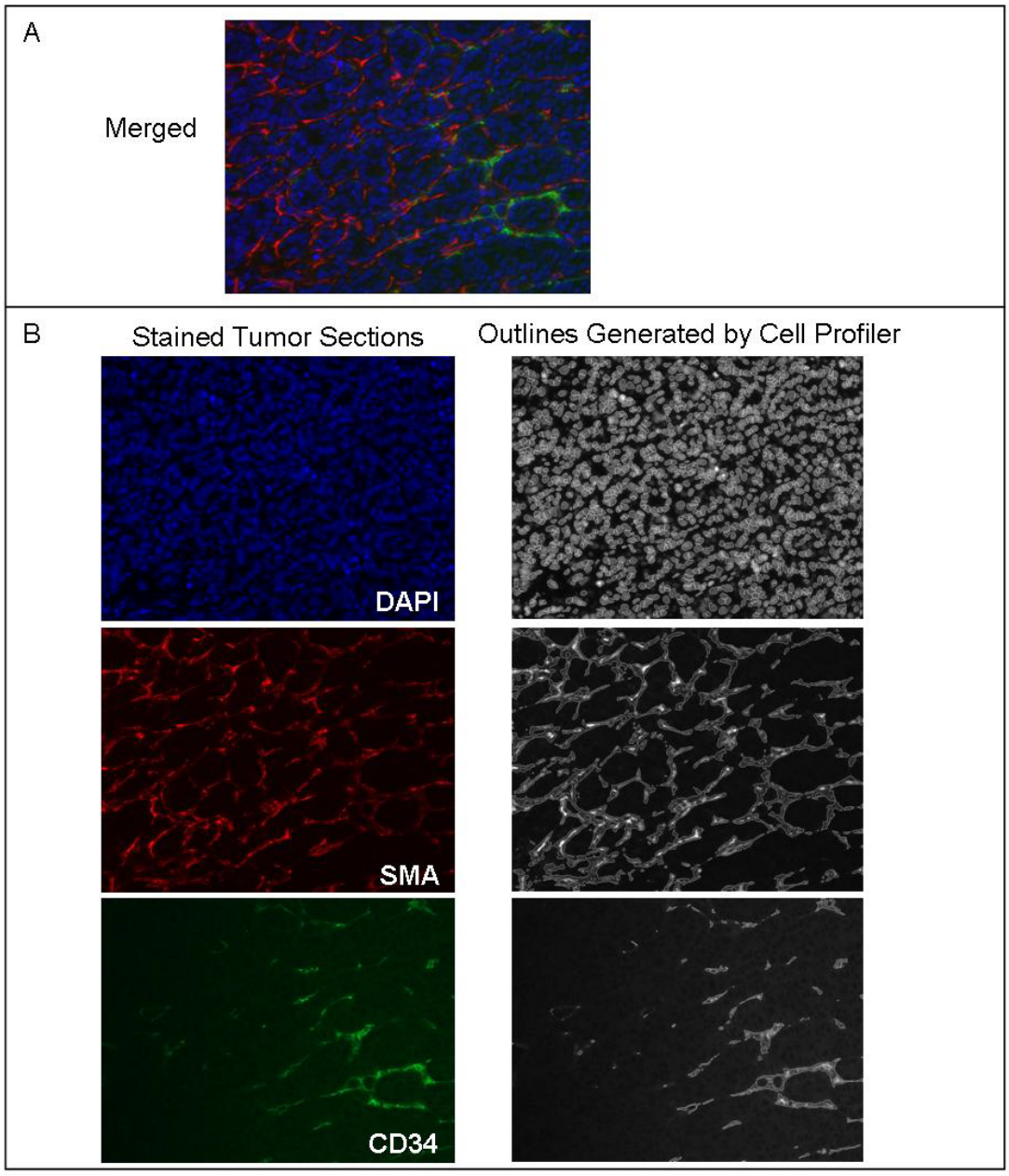

Supplementary Figure 1: Cell Profiler Outlines. Tumors sections from NOD-SCID mice bearing MCF-7 Ras-derived carcinomas expressing either $mVEGF_{164}$ (pBzeo-mVEGF), mCXCL1 (pBzeo-mCXCL1), hCCL5 (pLZR-hCCL5), or ΔhCCL5 (pWZL-ΔhCCL5) were stained using immunofluorescence for both α-SMA (red) and CD34 (green), nuclei were counterstained with DAPI (blue). **(A)** Displays the merged image. **(B)** The area of a photomicrograph covered by α-SMA staining or CD34 staining was measured by using the program Cell Profiler. An example of each of the stains is displayed on the left. An outline of the areas considered positive for each of the stains and counted by the program is shown on the right.

A

Table 1

Comparison of mVEGF-Expressing Tumors to Control pWZL-GFP- Expressing Tumors with Respect to Percent Average Area Per Tumor Section Stained for α-SMA and CD34

	% Area Covered by α-SMA+ Cells	% Area Covered by CD34+ Cells
pWZL-GFP	15.89 ±4.02	0.42 ±0.17
pBzeo-mVEGF	19.75 ±3.42	1.83 ±0.98

B

Table 2

Comparison of mCXCL1-, mVEGF-, hCCL5-, and ΔhCCL5-Expressing Tumors to Control Empty Vector Expressing Tumors with Respect to Average Percent Area Per Tumor Section Stained for α-SMA and CD34

	% Area Covered by α-SMA+ Cells	% Area Covered by CD34+ Cells
pBzeo	12.50 ±3.18	0.18±0.11
pBzeo-mCXCL1	12.05 ±3.07	0.19±0.09
pBzeo-mVEGF	18.64 ±2.50	0.94±0.60
pLZR	15.45 ±3.63	0.27±0.19
pLZR-hCCL5	16.85 ±3.38	0.15±0.09
pWZL-GFP	15.14 ±3.46	0.28±0.10
pWZL-ΔhCCL5	12.72 ±4.02	0.26±0.13

Supplementary Figure 2: mVEGF$_{164}$-Expressing MCF-7 Ras Cells Display Increased Incorporation of α-SMA-Positive Cells and CD34-Positive Cells Relative to the pWZL-GFP-Expressing Control Tumors. **(A)** Average percent area per tumor section stained for α-SMA (% Area Covered by α-SMA+ Cells) and CD34 (% Area Covered by CD34+ Cells) for the pBzeo-mVEGF$_{164}$- and pWZL-GFP-expressing tumors. **(B)** Displays the data from Figure 5A and B in table form: average percent area per tumor section stained for α-SMA (% Area Covered by α-SMA+ Cells) and CD34 (% Area Covered by CD34+ Cells) for the mCXCL1-, mVEGF-, hCCL5-, ΔhCCL5-, and control empty vector-expressing tumors.

References

Abe R, Donnelly SC, Peng T, Bucala R, Metz CN. (2001) Peripheral blood fibrocytes: differentiation pathway and migration to wound sites. *J Immunol*, **166**, 7556-62.

Anderberg C, Li H, Fredriksson L, Andrae J, Betsholtz C, Li X, Eriksson U, Pietras K. (2009) Paracrine signaling by platelet-derived growth factor-CC promotes tumor growth by recruitment of cancer-associated fibroblasts. *Cancer Res*, **69**(1), 369-78.

Barth PJ, Ebrahimsade S, Ramaswamy A, Moll R. (2002) CD34+ fibrocytes in invasive ductal carcinoma, ductal carcinoma in situ, and benign breast lesions. *Virchows Arch*, **440**(3), 298-303.

Chauhan H, Abraham A, Phillips JR, Pringle JH, Walker RA, Jones JL. (2003) There is more than one kind of myofibroblast: analysis of CD34 expression in benign, in situ, and invasive breast lesions. *J Clin Pathol*, **56**(4):271-6.

Cross MJ, Dixelius J, Matsumoto T, Claesson-Welsh L. (2003) VEGF-receptor signal transduction. *Trends Biochem Sci*, **28**(9), 488-94.

Desmoulière A, Geinoz A, Gabbiani F, Gabbiani G. (1993) Transforming growth factor-beta 1 induces alpha-smooth muscle actin expression in granulation tissue myofibroblasts and in quiescent and growing cultured fibroblasts. *J Cell Biol*, **122**(1), 103-11.

Direkze NC, Hodivala-Dilke K, Jeffery R, Hunt T, Poulsom R, Oukrif D, Alison MR, Wright NA. (2004) Bone marrow contribution to tumor-associated myofibroblasts and fibroblasts. *Cancer Res*, **64**(23), 8492-5

Dong J, Grunstein J, Tejada M, Peale F, Frantz G, Liang WC, Bai W, Yu L, Kowalski J, Liang X, Fuh G, Gerber HP, Ferrara N. (2004) VEGF-null cells require PDGFR alpha signaling-mediated stromal fibroblast recruitment for tumorigenesis. *EMBO J*, **23**(14), 2800-10.

Elenbaas B, Spirio L, Koerner F, Fleming MD, Zimonjic DB, Donaher JL, Popescu NC, Hahn WC, Weinberg RA. (2001) Human breast cancer cells generated by oncogenic transformation of primary mammary epithelial cells. *Genes Dev*, **15**(1), 50-65.

Folkman J. (2007) Angiogenesis: an organizing principle for drug discovery? *Nat Rev Drug Discov*, **6**(4), 273-86.

Gong JH, Uguccioni M, Dewald B, Baggiolini M, Clark-Lewis I. (1996) RANTES and MCP-3 antagonists bind multiple chemokine receptors. *J Biol Chem*, **271**(18), 10521-7.

Guo X, Oshima H, Kitmura T, Taketo MM, Oshima M. (2008) Stromal fibroblasts activated by tumor cells promote angiogenesis in mouse gastric cancer. *J Biol Chem*, **283**(28), 19864-71.

Hinz B, Phan SH, Thannickal VJ, Galli A, Bochaton-Piallat ML, Gabbiani G. (2007) The myofibroblast: one function, multiple origins. *Am J Pathol*, **170**(6):1807-16.

Ince TA, Richardson AL, Bell GW, Saitoh M, Godar S, Karnoub AE, Iglehart JD, Weinberg RA. (2007) Transformation of different human breast epithelial cell types leads to distinct tumor phenotypes. *Cancer Cell*, **12**(2), 160-70.

Ishii G, Sangai T, Oda T, Aoyagi Y, Hasebe T, Kanomata N, Endoh Y, Okumura C, Okuhara Y, Magae J, Emura M, Ochiya T, Ochiai A. (2003) Bone-marrow-derived myofibroblasts contribute to the cancer-induced stromal reaction. *Biochem Biophys Res Comm*, **309**, 232-240.

Kalluri R, Zeisberg M. (2006) Fibroblasts in cancer. *Nat Rev Cancer*, **6**(5), 392-401.

Karnoub AE, Dash AB, Vo AP, Sullivan A, Brooks MW, Bell GW, Richardson AL, Polyak K, Tubo R, Weinberg RA. (2007) Mesenchymal stem cells within tumour stroma promote breast cancer metastasis. *Nature*, **449**(7162), 557-63.

Lazard D, Sastre X, Frid MG, Glukhova MA, Thiery JP, Koteliansky VE. (1993) Expression of smooth muscle-specific proteins in myoepithelium and stromal myofibroblasts of normal and malignant human breast tissue. *Proc Natl Acad Sci U S A*, **90**(3), 999-1003.

Löhr M, Schmidt C, Ringel J, Kluth M, Müller P, Nizze H, Jesnowski R. (2001) Transforming growth factor-beta1 induces desmoplasia in an experimental model of human pancreatic carcinoma. *Cancer Res*, **61**(2):550-5.

Morimoto M, Irimura T. (2001) Fibroblast migratory factor derived from mouse colon carcinoma cells: potential roles of fibronectin in tumor stroma formation. *J Cell Biochem*, **80**(4), 635-46.

Rocks N, Paulissen G, Quesada-Calvo F, Munaut C, Gonzalez ML, Gueders M, Hacha J, Gilles C, Foidart JM, Noel A, Cataldo DD. (2008) ADAMTS-1 metalloproteinase promotes tumor development through the induction of a stromal reaction in vivo. *Cancer Res*, **68**(22), 9541-50.

Rønnov-Jessen L, Petersen OW. (1993) Induction of alpha-smooth muscle actin by transforming growth factor-beta 1 in quiescent human breast gland fibroblasts. Implications for myofibroblast generation in breast neoplasia. *Lab Invest*, **68**(6), 696-707.

Rønnov-Jessen L, Petersen OW, Koteliansky VE, Bissell MJ. (1995) The origin of the myofibroblasts in breast cancer. Recapitulation of tumor environment in culture unravels diversity and implicates converted fibroblasts and recruited smooth muscle cells. *J Clin Invest*, **95**(2), 859-73.

Sangai T, Ishii G, Kodama K, Miyamoto S, Aoyagi Y, Ito T, Magae J, Sasaki H, Nagashima T, Miyazaki M, Ochiai A. (2005) Effect of differences in cancer cells and tumor growth sites on recruiting bone marrow-derived endothelial cells and myofibroblasts in cancer-induced stroma. *Int J Cancer*, **115**(6), 885-92.

Schmidt M, Sun G, Stacey MA, Mori L, Mattoli S. (2003) Identification of circulating fibrocytes as precursors of bronchial myofibroblasts in asthma. *J Immunol*, **171**, 380-9.

Serini G, Gabbiani G. (1999) Mechanisms of myofibroblast activity and phenotypic modulation. *Exp Cell Res*, **250**(2), 273-83.

Shao ZM, Nguyen M, Barsky SH. (2000) Human breast carcinoma desmoplasia is PDGF initiated. *Oncogene*, **19**(38), 4337-45.

Skalli O, Ropraz P, Trzeciak A, Benzonana G, Gillessen D, Gabbiani G. (1986) A monoclonal antibody against alpha-smooth muscle actin: a new probe for smooth muscle differentiation. *J Cell Biol*, **103**(6 Pt 2), 2787-96.

Stewart SA, Dykxhoorn DM, Palliser D, Mizuno H, Yu EY, An DS, Sabatini DM, Chen IS, Hahn WC, Sharp PA, Weinberg RA, Novina CD. (2003) Lentivirus-delivered stable gene silencing by RNAi in primary cells. *RNA*, **9**(4), 493-501.

Tejada ML, Yu L, Dong J, Jung K, Meng G, Peale FV, Frantz GD, Hall L, Liang X, Gerber HP, Ferrara N. (2006) Tumor-driven paracrine platelet-derived growth factor receptor alpha signaling is a key determinant of stromal cell recruitment in a model of human lung carcinoma. *Clin Cancer Res*, **12**(9), 2676-88.

Yazhou C, Wenlv S, Weidong Z, Licun W. (2004) Clinicopathological significance of stromal myofibroblasts in invasive ductal carcinoma of the breast. *Tumour Biol*, **25**(5-6), 290-5.

Zeisberg EM, Potenta S, Xie L, Zeisberg M, Kalluri R. (2007) Discovery of endothelial to mesenchymal transition as a source for carcinoma-associated fibroblasts. *Cancer Res*, **67**(21), 10123-8.

Chapter 3: The Recruitment of Bone Marrow-Derived Cells to the Site of Tumor Formation

Matthew P. Saelzler[1,2], Sandra S. McAllister[1], Ferenc Reinhardt[1], Tan A. Ince[1,3], and Robert A. Weinberg[1,2]

(1) Whithead Institute for Biomedical Research, Cambridge, MA 02142
(2) Department of Biology, Massachusetts Institute of Technology, Cambridge, MA 02139
(3) Department of Pathology, Division of Women's and Perinatal Pathology, Brigham and Women's Hospital, Harvard Medical School, Boston, MA 02115

The bone marrow transplant experiment involving the BPHER-3 kinetics was done in collaboration with Sandra S. McAllister. Ferenc Reinhardt performed all the mouse procedures up to and including the injection of tumor cells into the mice. All other experiments carried out by the thesis author, Matthew Saelzler.

Introduction

Carcinomas arise from the uncontrolled proliferation of cancer cells, but they also contain numerous non-cancer cells that are collectively identified as stromal cells. Stromal cells affect multiple steps of tumor progression, including initiation, angiogenesis, invasion, and metastasis. Consequently, it is important to investigate the origins of these stromal cells in order to understand how they are recruited to sites of tumor formation and how this process may be potentially blocked. Cell types in the stroma can be recruited from the adjacent microenvironment, but they can also be recruited systemically from blood/bone marrow. In our studies, we have been interested in examining the recruitment of bone marrow-derived (BMD) cells to the sites of mammary carcinoma formation.

Several studies have demonstrated the ability of tumors to recruit BMD cells. In bone marrow transplantation studies, it has been shown that 58% of the F4/F80-positive macrophages and some of the myeloid cells (not quantitated) present in a gastric hyperplasia model and colorectal cancer model, respectively, are derived from the bone marrow (Guo X et al. 2008, Kitamura T et al. 2007). In the later case it was reported that the myeloid cells localized to the invasive fronts of the tumors. Additionally, some groups have also shown to various degrees that BMD cells are incorporated into tumor blood vessels (Lyden D et al. 2001, Ruzinova MB et al. 2003, Aghi M and Chiocca EA 2005).

The critical impact on cancer progression of recruiting BMD cells has been brought to light by a series of bone marrow transplantation studies. In a mouse model of

squamous carcinoma, the incidence of low grade tumors is decreased in a matrix metalloproteinase-9 (MMP-9) deficient background, and normal tumor progression is restored by the transplantation of wild-type bone marrow into the MMP-9 knock-out mice (Coussens LM et al. 2000). In this particular model, MMP-9 appears to be expressed by a group of myeloid lineage cells (macrophages, neutrophils, and mast cells) within the tumors of wild type animals. In another study, the impaired growth of xenografts in Id1+/-Id3+/- mice was attributed to a failure to induce angiogenesis, which was restored through the transplantation of wild type bone marrow into Id1+/-Id3+/- (Lyden D et al. 2001). In this model, the recruitment of bone marrow-derived endothelial cells into the tumors is believed to be responsible for restoring tumor growth to wild type levels. Recently, the recruitment of BMD cells has been implicated in tumor drug resistance to anti-vascular endothelial growth factor (VEGF) treatment (Shojaei F et al. 2007). In this case, the data suggest that CD11b+Gr-1+ myeloid cells are responsible for this activity.

These studies collectively demonstrate that various BMD cell types are involved in certain aspects of tumorigenesis, such as local remodeling and angiogenesis. However these studies likely only skim the surface of the full effects of BMD stromal cells, given the heterogeneity of the stromal compartment and how robustly these cells seem to influence tumor progression. These studies further suggest that targeting BMD stromal cells may be an important strategy to explore for cancer therapy and it will be critical to identify additional BMD cell types and their unique functions in cancer.

The cell type we wanted to focus on in these studies is the myofibroblast, which is an attractive candidate due to the fact that myofibroblasts are present in breast carcinomas, but not in the normal mammary gland (Skalli O et al. 1986, Barth PJ et al. 2002, Chauhan H et al. 2003, Yazhou C et al. 2004). Furthermore, myofibroblasts are thought to influence tumor progression in multiple ways (Kalluri R and Zeisberg M 2006, De Wever O et al. 2008). Thus, myofibroblasts would represent an optimal therapeutic target that can be inhibited without affecting the normal physiology of the breast.

It was originally thought that myofibroblasts were derived from cell types present in the adjacent tissue. This is supported by evidence that fibroblasts isolated from the mammary gland can be induced to express α-smooth muscle actin (α-SMA), a marker of myofibroblasts, upon treatment with transforming growth factor-β (TGF-β) (Rønnov-Jessen and Petersen, 1993). Additionally, mammary fibroblasts can also be induced to express α-SMA when they are co-cultured with breast cancer cells (Rønnov-Jessen L et al. 1995). It is also possible that other resident stromal cell types could be precursors to myofibroblasts present in carcinomas, including vascular smooth muscle cells, endothelial cells and even the carcinoma cells themselves (Rønnov-Jessen L et al. 1995, Hinz B et al. 2007, Zeisberg EM et al. 2007, Kalluri R and Zeisberg M 2006).

More recently it has been proposed that myofibroblasts are also recruited systemically from the blood or bone marrow. There is evidence of a circulating cell population present in the blood, termed fibrocytes, which are capable of giving rise to α-SMA-positive myofibroblast-like cells. Fibrocytes are thought to be recruited into sites of wounding where they play a role in wound repair (Bucala R et al. 1994, Abe R et al.

2001, Schmidt M et al. 2003). More importantly however, BMD-myofibroblasts have also been detected in various models of cancer (Ishii G et al. 2003, Sangai T et al. 2005, LaRue AC et al. 2006, Ishii S et al. 2008). BMD-myofibroblasts were shown to be incorporated into a human pancreatic cancer model, Capan-1, growing subcutaneously in immune-compromised mice (Ishii G et al. 2003). The authors demonstrate that at an early time point about 13% of the myofibroblasts are derived from the bone marrow, while at later time points approximately 40% are of bone marrow origin (Ishii G et al. 2003). It was also demonstrated that myofibroblasts present in other xenograft tumor models, including the MDA-MB-231 and MDA-MB-468 breast cancer models, originate from the bone marrow (Sangai T et al. 2005). In the study by Sangai T et al., they examined a panel of human tumor xenograft models and reported that the degree of BMD-myofibroblast incorporation varied from zero to about 30%.

The presence of BMD-myofibroblasts was also demonstrated in two autochthonous tumor models of pancreatic and gastric mouse model of cancer, where 25% and 12%, respectively, of myofibroblasts were derived from the bone marrow (Direkze NC et al. 2004, Guo X et al. 2008). Finally, BMD-myofibroblasts were identified, but not quantified, in two cases of human cancer; one was a gastric cancer and the other a rectal adenoma (Worthley DL et al. 2009). In these two cases the female patients had undergone a bone marrow transplant procedure from a male donor, allowing BMD cells to be identified by the presence of a Y chromosome.

The presence of bone marrow-derived cell types in tumors, including α-SMA-positive myofibroblasts, has been demonstrated for several cancer models. However, the

number of α-SMA-positive BMD-myofibroblasts recruited to the site of tumor formation varies significantly, which is important to understand so that these cells can be studied in the appropriate tumor models and tissue-specific functions might also be revealed. We sought to determine if our BPHER-3 tumor model recruits cell types from the bone marrow, more specifically, we wanted to investigate whether our model recruits α-SMA-positive stromal cells from the bone marrow. Our results demonstrate that the BPHER-3 tumor model is able to recruit BMD-cells. However, the data suggest that very few of the α-SMA-positive cells present in the BPHER-3 tumors are bone marrow-derived. Rather, we hypothesize that the majority of the α-SMA-positive cells are recruited from the local tissue microenvironment.

Results

The Recruitment of Bone Marrow-Derived Cells to BPHER-3 Tumors at Different Time Points During Tumor Growth

We generated chimeric mice by transplanting bone marrow from green fluorescent protein (GFP) transgenic mice into GFP non-expressing mice. The chimeric mice were injected subcutaneously with tumor cells, and recruitment of GFP-positive cells to the site of tumor growth was assessed by fluorescence microscopy. Due to the fact that the BPLER cells described earlier in this thesis were already GFP-positive, BPHER-3 cells were used instead for injection. BPHER-3 cells were derived in the same way as BPLER cells but originated from a different patient and do not express GFP. We assumed that the BPHER-3 tumors would recruit myofibroblasts in a similar way as BPLER tumors. However, it is likely that there are differences between them.

To test if stromal cells in the BPHER-3 xenografts were derived from the bone marrow, BPHER-3 cells were injected into NOD-SCID mice previously engrafted with Rag1-/- GFP transgenic bone marrow. In these mice, blood and certain bone marrow cells are GFP-positive, while the cells of the recipient mice do not express GFP. The production of these mice is outlined in Figure 1A. Tumor cells were injected bilaterally at subcutaneous sites in NOD-SCID mice so that each mouse had two subcutaneously growing tumors. In this experiment, we also examined the recruitment of BMD cells at different times during tumor growth.

Figure 1:

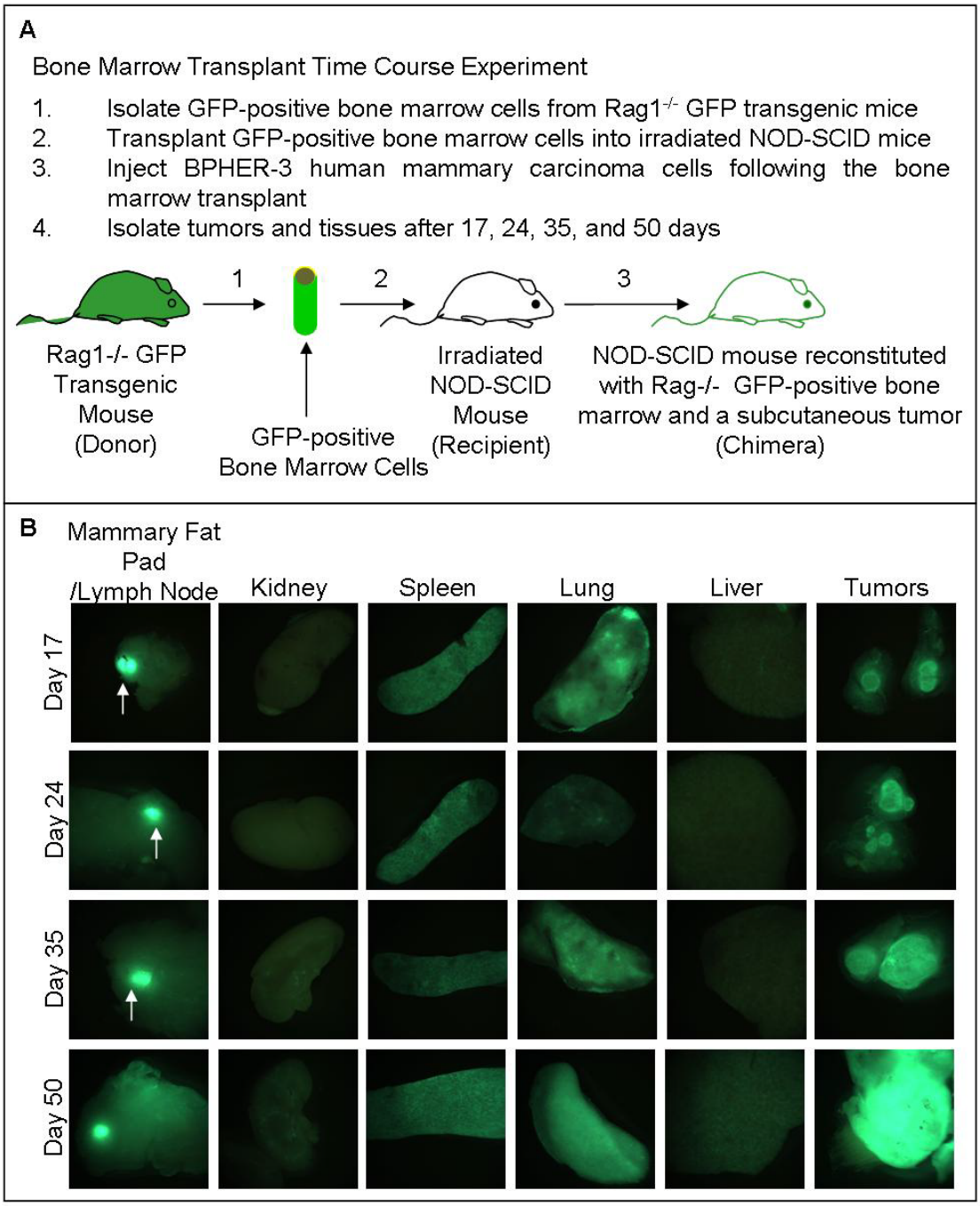
A
Bone Marrow Transplant Time Course Experiment
1. Isolate GFP-positive bone marrow cells from Rag1-/- GFP transgenic mice
2. Transplant GFP-positive bone marrow cells into irradiated NOD-SCID mice
3. Inject BPHER-3 human mammary carcinoma cells following the bone marrow transplant
4. Isolate tumors and tissues after 17, 24, 35, and 50 days
1
2
3
Rag1-/- GFP Transgenic Mouse (Donor)
GFP-positive Bone Marrow Cells
Irradiated NOD-SCID Mouse (Recipient)
NOD-SCID mouse reconstituted with Rag-/- GFP-positive bone marrow and a subcutaneous tumor (Chimera)
B
Mammary Fat Pad /Lymph Node
Kidney
Spleen
Lung
Liver
Tumors
Day 17
Day 24
Day 35
Day 50

Figure 1 (continued):

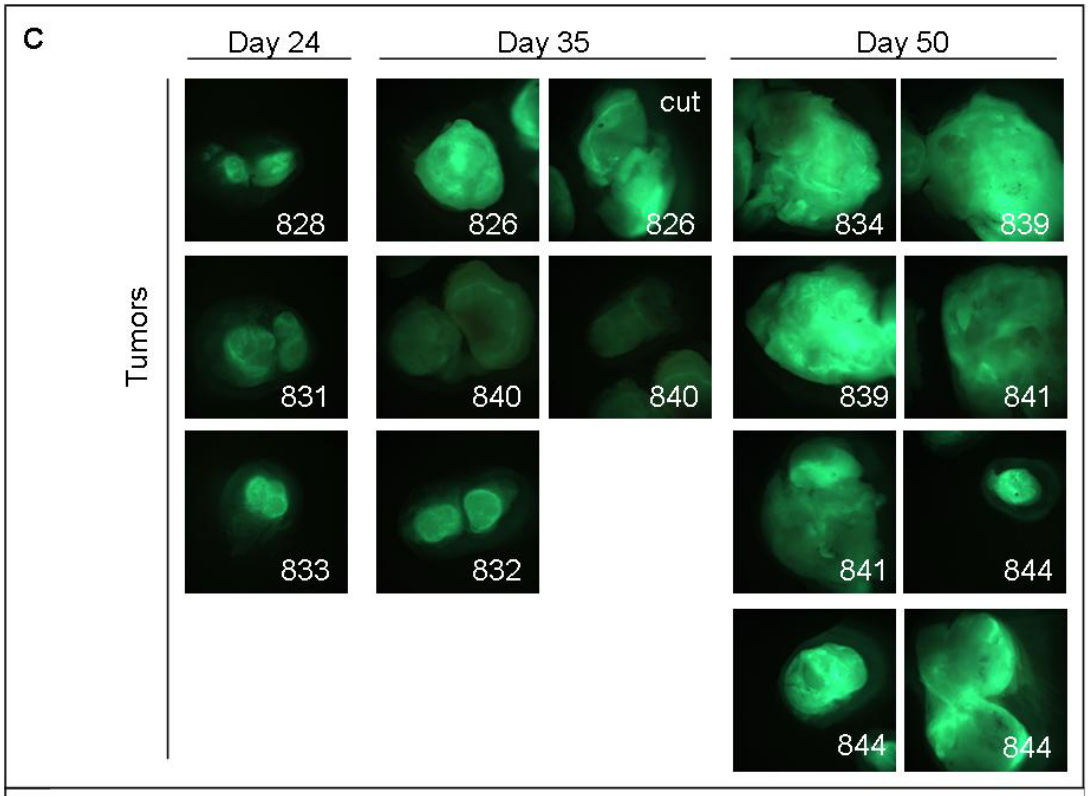

D

Day 0	%GFP	Day 17	%GFP	Day 24	%GFP	Day 35	%GFP	Day 50	%GFP
842 NT	18.62	830	34.79	828	33.49	826	23.59	839/34	9.43
		837	13.35	831	10.3	840	7.64	839/34	50.75
		835	25.86	833	49.99	827	44.41	841	22.52
		836	59.12	838	32.87	832	34.99	844	37.2
		843 NT	6.3					829 NT	30.86

Figure 1: **Bone Marrow-Derived Cells are Present in Several Tissues and BPHER-3 Tumors**

(A) Protocol for generation of tumor-bearing chimeric mice in the time course experiment. **(B)** Whole mount images of tissues and tumors, taken with a fluorescent dissecting microscope, to detect GFP-positive cells from BPHER-3 tumor-bearing NOD-SCID mice previously engrafted with bone marrow from Rag1-/- GFP transgenic mice. GFP-positive bone marrow-derived cells were examined in tumors and tissues at the 17, 24, 35 and 50 day timepoints. Arrows point to the lymph node in the mammary fat pad. **(C)** Whole mount photomicrographs of BPHER-3 tumors not shown in (A) from each of the time points. **(D)** The relative percentage of GFP-positive cells in the blood, measured by flow cytometry prior to tumor cell injection, for each of the mice in the experiment.

BPHER-3 tumor-bearing mice were sacrificed at several points during tumor progression, and the recruitment of BMD cells was assessed by fluorescence microscopy. We found that BMD GFP-positive cells were associated with the tumor mass at all time points analyzed (Figure 1B and C). Using a fluorescence dissecting microscope, we detected BMD cells in the tumors as early as day 17 and at all the other time points analyzed including the final day 50 time point (Figure 1B and C). Additionally, BMD GFP-positive cells were found in the lung, liver, kidney, mammary fat pad (MFP) and the lymph node located in the MFP (Figure 1B). Tumor sections from each of the time points were stained with antibodies against GFP and α-SMA and analyzed by immunofluorescence. Both GFP and α-SMA positive cells were detected, thereby confirming the ability of BPHER-3 tumors to recruit both BMD and α-SMA-positive cells into the tumor stroma (Figure 2). However, at this point we have not examined any relationship between the α-SMA-positive cells and the BMD cells.

Figure 2:

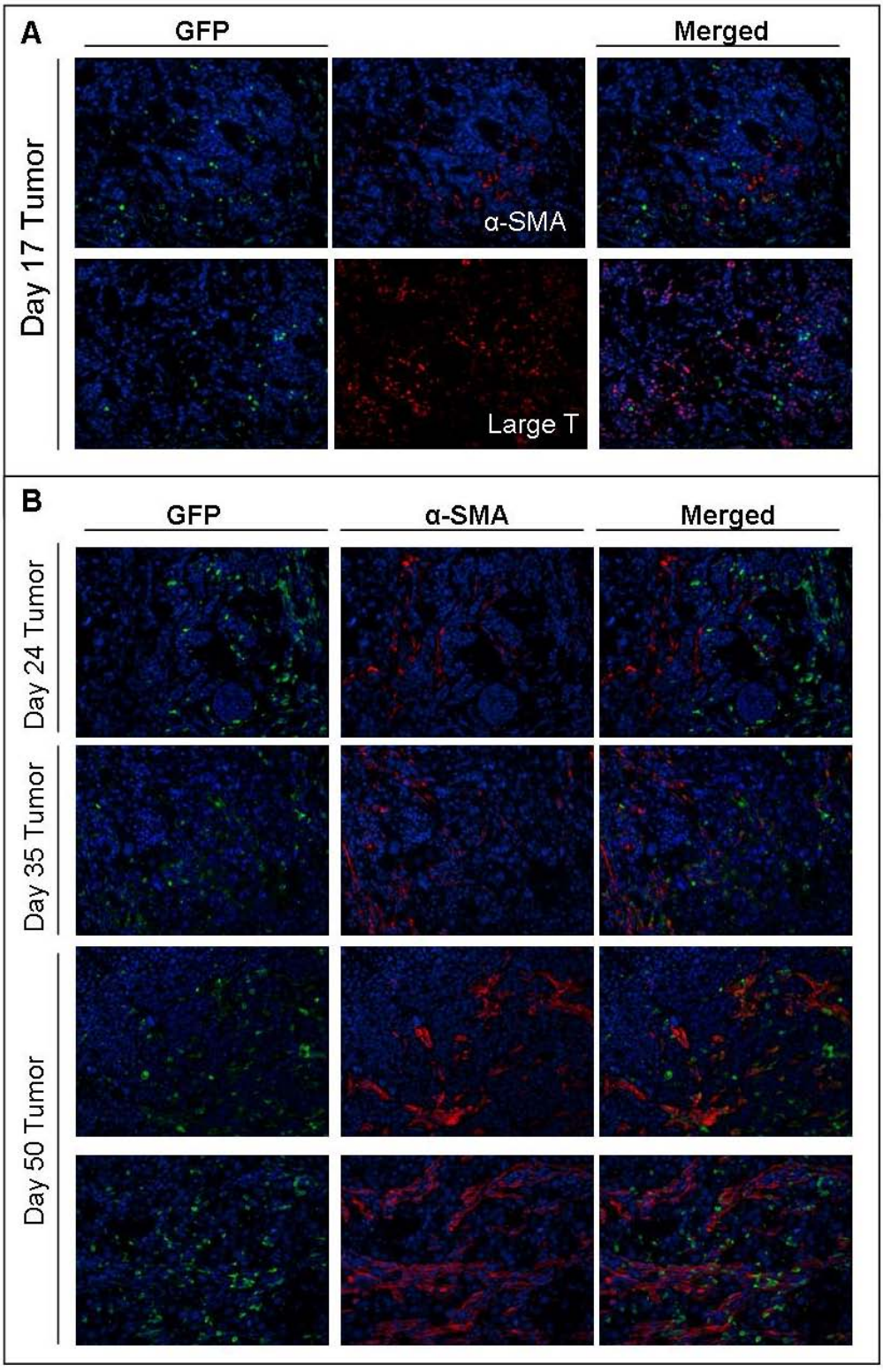
A
GFP
Merged
Day 17 Tumor
α-SMA
Large T
B
GFP
α-SMA
Merged
Day 24 Tumor
Day 35 Tumor
Day 50 Tumor

Figure 2 (continued):

Figure 2: BPHER-3 Carcinomas are Able to Recruit α-SMA-Positive Cells and Bone Marrow-Derived Cells. (A) Immunofluorescent staining of day 14 BPHER-3 tumor sections from the chimeric mice in Figure 1 for GFP (green), α-SMA (red), and Large T (red). The Large T staining was done to confirm that tumor cells were present in the excised tissue where GFP-positive cells were found. Merged pictures are displayed on the far right. **(B)** Immunofluorescent staining of day 24 (top), day 35 (middle) and day 50 (bottom) BPHER-3 tumor sections, from the chimeric mice in Figure 1, for GFP (green) and α-SMA (red). Merged pictures are displayed on the far right. All images shown were taken with a 20x objective.

The Recruitment of Bone Marrow Derived Cells to MDA-MB-231 and BPHER-3 Tumors

Due to the fact that NOD-SCID mice tolerated the bone marrow transplants poorly, we conducted the remaining experiments in NUDE mice. BHPER-3 and MDA-MB-231 cells were injected into chimeric NUDE mice previously engrafted with Rag1-/- GFP transgenic bone marrow. Similar to the previous experiment, we demonstrated that the BPHER-3 and MDA-MB-231 human mammary xenograft tumors were capable of recruiting BMD and α-SMA-positive cells in the NUDE chimeric mice (Figure 3 and 4).

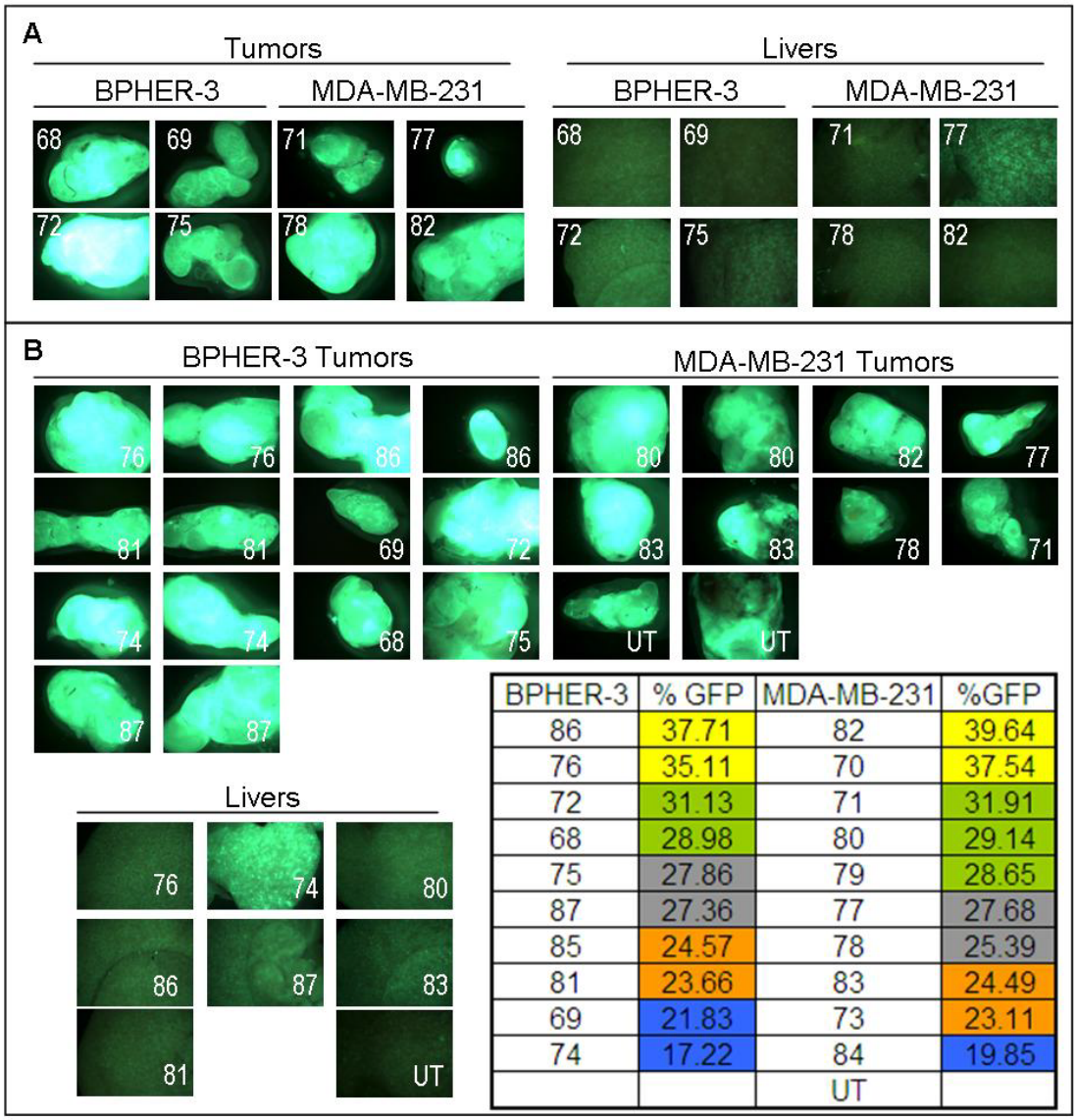

BPHER-3	% GFP	MDA-MB-231	%GFP
86	37.71	82	39.64
76	35.11	70	37.54
72	31.13	71	31.91
68	28.98	80	29.14
75	27.86	79	28.65
87	27.36	77	27.68
85	24.57	78	25.39
81	23.66	83	24.49
69	21.83	73	23.11
74	17.22	84	19.85
		UT	

Figure 3: Bone Marrow-Derived Cells are Present in BPHER-3 and MDA-MB-231 Xenografts. For (A) and (B) the white number in the corner of the picture indicates the mouse from which the tumor or liver was derived. **(A)** Whole mount images of tumors (left) and livers (right), taken with a fluorescent dissecting microscope, to depict GFP-positive bone marrow-derived cells from BPHER-3 (left) or MDA-MB-231 (right) tumor-bearing NUDE mice previously engrafted with bone marrow from Rag1-/- GFP transgenic mice. **(B)** Photomicrographs of tumors and livers not shown in (A), taken with a fluorescent dissecting microscope, from BPHER-3 (left) or MDA-MB-231 (right) tumor-bearing NUDE mice previously engrafted with bone marrow from Rag1-/- GFP transgenic mice. The table displays the relative percentage of GFP-positive cells in the blood, measured by flow cytometry prior to tumor cell injection, for each of the mice in the experiment.

Figure 4:

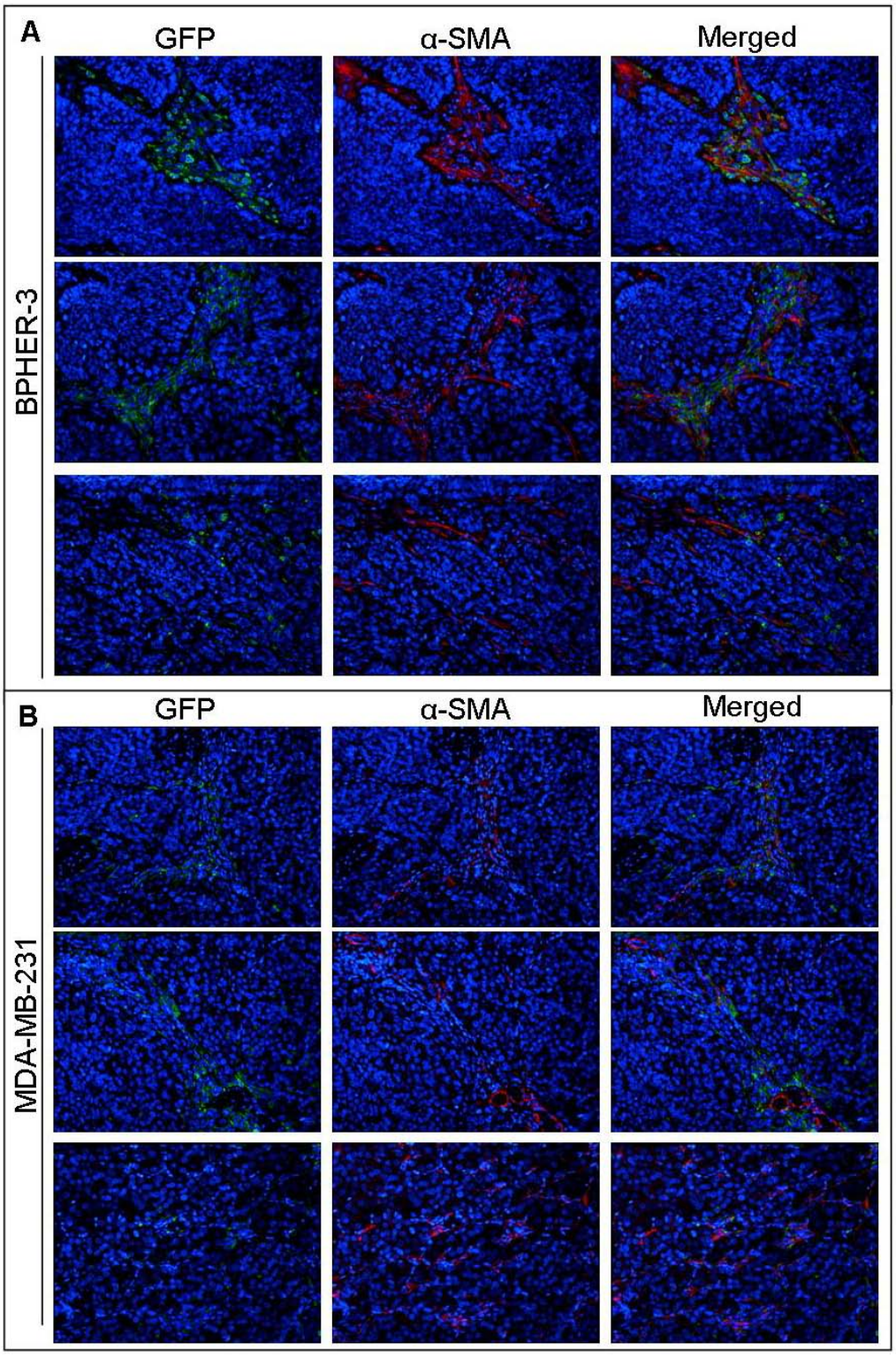

Figure 4 (continued):

Figure 4: BPHER-3 and MDA-MB-231 Carcinomas are Able to Recruit α-SMA-Positive Cells and Bone Marrow-Derived Cells. (A) Immunofluorescent staining of BPHER-3 tumor sections from BPHER-3 tumor-bearing NUDE mice previously engrafted with bone marrow from Rag1-/- GFP transgenic mice for α-SMA (red) and GFP (green). Merged pictures are shown on the right. **(B)** Immunofluorescent staining of MDA-MB-231 tumor sections from MDA-MB-231 tumor-bearing NUDE mice previously engrafted with bone marrow from Rag1-/- GFP transgenic mice for α-SMA (red) and GFP (green). Merged pictures are shown on the right.

The Source of α-SMA-Positive Cells in the BPHER-3 Tumors

We next sought to determine if the BPHER-3 tumor model recruited BMD-α-SMA-positive cells. As mentioned above, it has previously been reported that MDA-MB-231 tumors are capable of recruiting BMD-myofibroblasts (Sangai T et al. 2005). Seven BPHER-3 tumors from the experiment shown in Figure 3 were stained for α-SMA and GFP and analyzed by immunofluorescence. For each of the tumors, roughly 100 α-SMA-positive cells were identified and categorized by GFP status as positive, negative, or could not be determinined with any certainty (ND).

As the results demonstrate, an overwhelming majority, >90%, of the α-SMA-positive cells analyzed in this experiment were GFP-negative (Figure 5). In the analysis of these 7 tumors only one α-SMA-positive cell was scored as GFP-positive, which is

shown in Figure 6A. On average, only 0.15% and 3.16% of the α-SMA-positive cells were scored as GFP-positive and ND, respectively (Figure 5).

Figure 5:

A

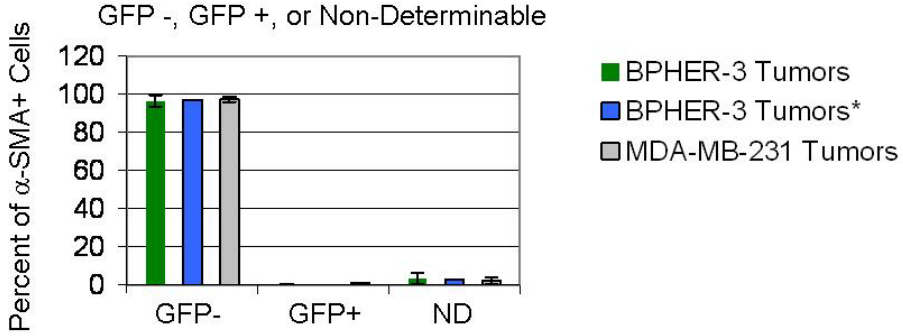

B

Table 1: Cell Counts of α-SMA+ Cells that are Either GFP -, GFP + or Undeterminable for Each Tumor Analyzed

BPHER-3 Tumors	Relative Percent Reconstition	SMA+ GFP- Cells	SMA+ GFP+ Cells	SMA+ ND	Percent of SMA+ Cells that are GFP-	Percent of SMA+ Cells that are GFP+	Percent of SMA+ Cells that are ND
H07-208-10	21.8	100	0	0	100	0	0
H07-208-22	27.4	99	0	1	99	0	1
H07-208-12	27.9	98	0	2	98	0	2
H07-208-16	29	94	0	6	94	0	6
H07-208-14	31.1	99	0	1	99	0	1
H07-208-20	35.1	93	0	7	93	0	7
H07-208-24	37.7	92	1	5	93.88	1.02	5.10
	Average Percent of SMA+ Cells				96.70	0.15	3.16
	Standard Deviation				2.95	0.39	2.81
MDA-MB-231 Tumors	Relative Percent Reconstition	SMA+ GFP- Cells	SMA+ GFP+ Cells	SMA+ ND	Percent of SMA+ Cells that are GFP-	Percent of SMA+ Cells that are GFP+	Percent of SMA+ Cells that are ND
H07-208-28	29.1	99	1	0	99	1	0
H07-208-5	31.9	34	0	1	97.14	0	2.86
H07-208-30	39.6	96	1	3	96	1	3
	Average Percent of SMA+ Cells				97.38	0.67	1.95
	Standard Deviation				1.51	0.58	1.69
BPHER-3 Tumors*	Percent Reconstition	SMA+ GFP- Cells	SMA+ GFP+ Cells	SMA+ ND	Percent of SMA+ Cells that are GFP-	Percent of SMA+ Cells that are GFP+	Percent of SMA+ Cells that are ND
H05-259-19	62.5*	82	0	1	98.80	0	1.20
H06-69-9	88*	86	0	4	95.56	0	4.44
	Average Percent of SMA+ Cells				97.18	0.00	2.82

Figure 5 (continued):

Figure 5: The Majority of α-SMA-Positive Cells Present in the Subcutaneously Injected BPHER-3 Tumors are Not Derived from the Transplanted Bone Marrow. (A) Average percent of α-SMA-positive (α-SMA+) cells that were scored as either GFP-positive (GFP +), GFP-negative (GFP -), or non-determinable (ND) in the BPHER-3 tumors, BPHER-3 tumors* obtained from S. McAllister, and MDA-MB-231 Tumors. The α-SMA-positive cells were analyzed and scored as outlined in the Material and Methods. **(B)** Table 1 displays the individual counts for each of the sections analyzed with respect to the number of α-SMA-positive cells that are GFP-negative (SMA+GFP-), GFP-positive (SMA+GFP+), and non-determinable (ND). The table also displays the individual percentage of α-SMA-positive cells that fall into each of the three categories. Table 1 also displays the relative percent reconstitution in the blood for each of the mice the tumor sections were derived from for the experiment. Reconstitution was measured before tumor cell injection. For tumors derived from S. McAllister, *indicates the percent reconstitution measured in the blood after the experiment. For one of the sections derived from S. McAllister, the percent reconstitution measured in the blood before the experiment is also displayed. Tumor section H06-69-9 was derived from a NUDE chimeric mouse and tumor section H05-259-19 was derived from a NOD-SCID chimeric mouse.

The extremely low abundance of BMD-α-SMA-positive cells could have been the result of a relatively low level, approximately 30%, of bone marrow reconstitution by the GFP-positive donor cells. To address this possibility two tumor sections derived from BPHER-3 tumor-bearing chimeric mice that had previously been engrafted with Rag1-/- GFP transgenic bone marrow were also examined. The reconstitution in these mice, as measured in the blood after the experiment, was 62.5% and 88% as shown in Table 1 of Figure 5. It must also be noted that one tumor was derived from a chimeric NUDE

mouse and one from a chimeric NOD-SCID mouse, and in both cases the BPHER-3 tumors were grown contralaterally to a weakly tumorigenic cell line HMLER-HR. After examining the α-SMA-positive cells from these tumors, once again we found that >90% of them were GFP-negative. Furthermore, between these two tumors, zero α-SMA-positive cells were scored as GFP-positive, while 2.82% were scored as ND Taken together, these experiments indicate that the bone marrow is not a major source of α-SMA-positive stromal cells recruited to BPHER-3 tumors grown subcutaneously.

It has been shown that MDA-MB-231 cells are capable of recruiting bone marrow-derived α-SMA-positive myofibroblasts (Sangai T et al. 2005). We examined three MDA-MB-231 tumors for recruitment of bone marrow derived α-SMA-positive cells. Similar to what was seen for the BPHER-3 tumors, among the α-SMA-positive cells analyzed in our MDA-MB-231 tumors, very few are derived from the GFP-positive donor bone marrow.

To qualify this interpretation, it remained formally possible that GFP expression is somehow turned off in the BMD α-SMA-positive stromal cells. This seems unlikely, given that we repeatedly observed other BMD GFP-positive cells recruited to the site of tumor formation, indicating that GFP would have to be turned off in some populations of BMD cells and not others. Additionally, α-SMA and GFP staining do appear to colocalize in tumor sections derived from tumor-bearing Rag1-/- GFP transgenic mice, suggesting that it is indeed possible to colocalize α-SMA and GFP (Figure 6). It thus seems unlikely that GFP expression is turned off specifically in α-SMA-positive cells derived from the bone marrow in the BPHER-3 tumors grown in chimeric NUDE mice.

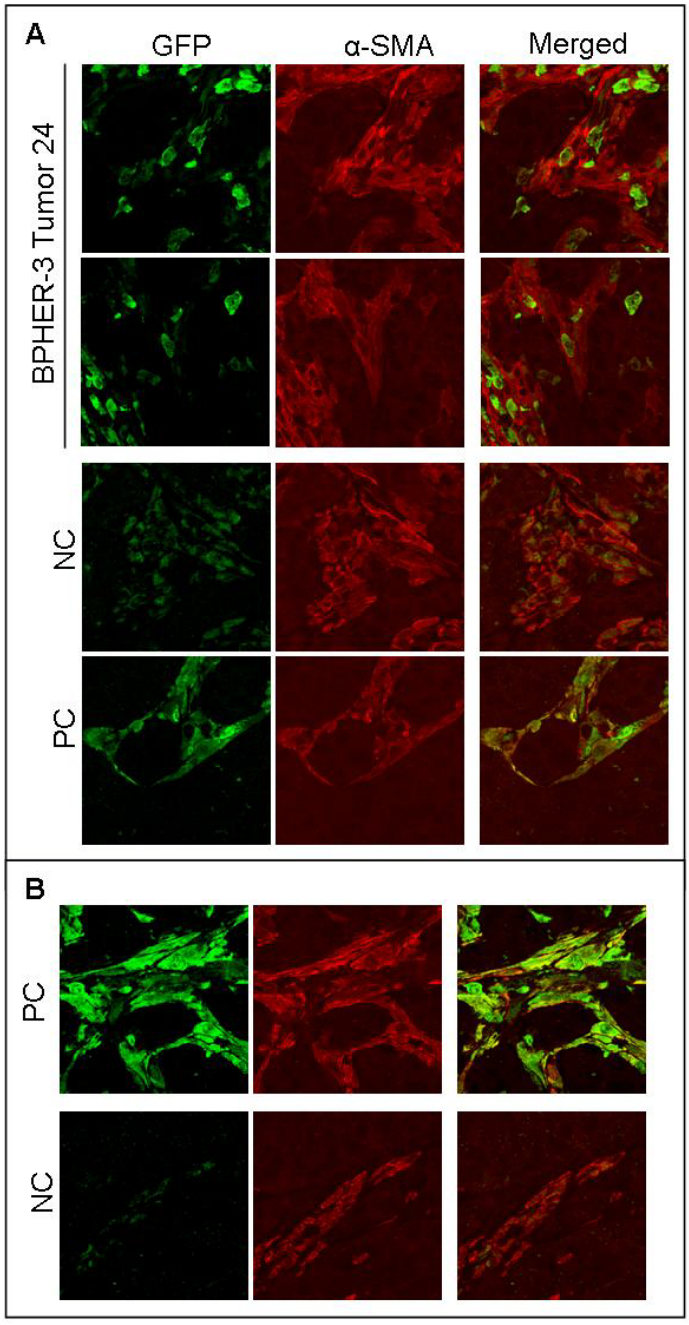

Figure 6: Confocal Images of the Tumors Analyzed for Bone Marrow-Derived α-SMA-Positive Cells. Shows images taken with a confocal microscope of tumors stained for GFP (green) and α-SMA (red) using immunofluorescence. **(A)** Displays a BPHER-3 tumor section derived from a BPHER-3 tumor-bearing NUDE mouse previously engrafted with bone marrow from Rag1-/- GFP transgenic mice for α-SMA (middle) and GFP (left). Merged pictures are shown on the right. The top set of pictures contains a α-SMA-positive cell that was scored as positive for GFP. The bottom set of pictures contains a α-SMA-positive cell that was scored as non-determinable. Also shown in (A), are tumor sections stained as negative (NC) and positive (PC) controls for GFP. The negative control is a tumor section derived from a tumor-bearing GFP-negative mouse. The positive control for GFP is a tumor section derived from a tumor-bearing Rag1-/- GFP-transgenic mouse. **(B)** Another set of images taken of the positive (PC) and negative (NC) control tumor sections stained for GFP (green) and α-SMA (red).

Discussion

In summary, we were able to demonstrate and confirm that BPHER-3 and MDA-MB-231 tumors, respectively, are capable of recruiting cell types from the blood/bone marrow. In addition to BMD cells, BPHER-3 tumors are capable of recruiting α-SMA-positive cells. However, we show that >90% of the α-SMA-positive cells analyzed were not derived from the donor GFP-positive bone marrow. These data suggest that among the α-SMA-positive cells analyzed in the BPHER-3 tumors, an overwhelming majority of them are derived from local precursors.

There is currently a debate in the field regarding the origins of myofibroblasts recruited to the site of tumor formation (Ishii G et al. 2003, Sangai T et al. 2005, Direkze NC et al. 2004, Guo X et al. 2008). This is most likely due to the fact that there is no reliable molecular marker that exclusively identifies myofibroblasts. The α-SMA-positive myofibroblasts identified by various groups may represent a heterogeneous pool of cells rather than a pure population of myofibroblasts. Some of the α-SMA-positive cells in this pool may be derived from the bone marrow while others are derived from local precursors. In our study, the data suggest that the great majority of the α-SMA-positive cells, which could include myofibroblasts and smooth muscle cells, recruited to the subcutaneously growing BPHER-3 tumors are derived from the local environment. The potential candidates in the local environment include fibroblasts and smooth muscle cells (Desmoulière A et al. 1993, Rønnov-Jessen and Petersen, 1993, Rønnov-Jessen L et al. 1995). Understandably, there would be a great benefit to the identification of BMD-myofibroblasts given the drugability of cell types in the blood as opposed to cell types

embedded in solid tissue. However, the identification of factors or pathways responsible for the recruitment or differentiation of cells in the local microenvironment might lead to potential pharmacological targets.

Acknowledgements: We would like to thank Tina Yuan for her editing and critical comments on this chapter. Also, we would like to thank Scott Valastyan for his editing on the figures presented in this chapter. We would also like to thank Sandra McAllister, Scott Valastyan, and Lynne Waldman for helpful discussions on this work. We would especially like to thank Tina Yuan for her helpful discussions on this work.

Materials and Methods

Cell Lines and Tissue Culture: The BPHER-3 cells were obtained from within the lab and were created as previously explained (Ince TA et al. et al. 2007). BPHER-3 cells were cultured as previously described except that the final concentration of glutamine may have been 1mM instead of 2mM (Ince TA et al. et al. 2007). MDA-MB-231 cells were cultured under standard conditions.

Bone Marrow Transplant Procedure: Femurs were isolated from Rag1-/- x EGFP transgenic mice and placed in Hanks' balanced salt solution (HBSS; GIBCO) containing insulin. The bone marrow cells (BMCs) were then flushed from the femurs with 3 ml of Hanks' balanced salt solution containing insulin, using a 26 gauge needle. The BMCs were then passed several times through a 19 gauge needle in order to create a single cell suspension. Next, the BMCs were washed approximately 2 times with PBS or HBSS. Then, the BMCs were counted using a hemocytometer and resuspended in PBS or HBSS. Following resuspension, approximately $2x10^6$ cells were injected retro-orbitally into either NOD-SCID or NUDE mice that had previously been irradiated with approximately 300 rads or 600 rads, respectively. Approximately, one to four weeks following the bone

marrow transplantation, the mice were tested for the engraftment of the GFP-positive cells. To test for the relative amount of engraftment, a sample of blood was taken from each of the mice, and in some experiments the red blood cells were lysed with red blood cell lysis buffer (Sigma) before flow cytometry analysis. The relative percent of GFP-positive cells in the blood was then measured by flow cytometry.

Tumor Xenografts: Nude mice were bought from Taconic (Hudson, NY). The NOD-SCID and Rag1-/- x EGFP transgenic mice were bred in the lab. The production of the chimeric mice is outlined above in the bone marrow transplant procedure. For subcutaneous injection, BPHER-3 and MDA-MB-231 cells were resuspended in BD Matrigel™ Matrix (BD Biosciences, Bedford MA) diluted in tissue culture media. The chimeric mice were injected with tumors cells approximately 1 to 2 weeks following the measurement of the percent reconstitution.

Immunofluorescence: Tumor and tissues were dissected from the mice and placed into PBS and then fixed in 4-10% formalin overnight at a minimum. The tissues were then kept in 70% ethanol until they could be processed further. Next, the tissues were embedded into paraffin wax. The embedded tumors were sectioned and placed on glass slides. In general immunofluorescence was performed as follows: The tumors sections on the slides were deparaffinized by incubating them in xylenes for at least 12 minutes. The sections were then rehydrated through serial dips in 100% ethanol, 95% ethanol, 70% ethanol and then placed in phospho-buffered saline (PBS). For antigen retrieval, the

slides were placed into 0.01M citrate buffer (pH 6.0) and heated in the microwave at 50% power for a minimum of 6 minutes. Then, the slides were left to cool in the citrate buffer for 1 hour. After antigen retrieval, the slides were rinsed in PBS and then placed in a blocking buffer for a minimum of 30 minutes. The slides were blocked in PBS containing 0.1% TWEEN-20 (PBS-T) and 5% horse serum. The primary antibodies were made up in PBS-T containing 2% horse serum. In general the antibody dilutions used were: the goat anti-GFP antibody (AbCam, Cambridge MA) was used at 1:400 for the detection of GFP and a mouse monoclonal SV40 T Ag (Pab 101) Antibody (Santa Cruz Biotechnology, Santa Cruz CA) was used at approximately 1:100 for the detection of Large T Antigen. The sections were placed in primary antibody overnight. The next day the primary antibody was removed and the slides were washed with ImmunoStain Wash Buffer and/or PBS (Gene Tex Inc., Irvine, CA). Following the washes, the slides were placed in secondary antibody for approximately 1 hour. The secondary antibodies were diluted in PBS containing 2% horse serum.

Next, fluorescent conjugated secondary antibodies were used to detect the primary antibody. A donkey anti-mouse Alexa Fluor® 594 was used to detect the α-SMA antibody and the SV40 T Ag antibody, while a donkey anti-goat Alexa Fluor® 488 (Invitrogen:Molecular Probes, Eugene OR) was used to detect the GFP antibody. The secondary antibodies were used at a 1:200 dilution.

Following the secondary antibody incubation the slides were rinsed several times with PBS. A DAPI Nucleic Acid Stain (Invitrogen: Molecular Probes, Eugene OR) was used to detect the cell nuclei. The stock solution of DAPI was made according to the

manufacturer's protocol. The stock solution was diluted in PBS at 1:10,000 and the slides were stained with DAPI for 10 minutes. Following the nucleic acid stain, the slides were rinsed twice with water and a cover slip was mounted on the slide with SlowFade® Gold antifade reagent (Invitrogen: Molecular Probes, Eugene OR). The slides were then placed at 4^{o}C in the dark until pictures could be taken with a fluorescent microscope or examined under the fluorescent dissecting microscope.

Analysis of α-SMA-Positive Cells for Expression of GFP: Tumor sections were analyzed by eye through a 100x objective for the co-expression of GFP and α-SMA. In general cells were scored as follows: first, a α-SMA positive cell was found and then was scored positive for GFP expression if GFP extended the length of the α-SMA staining and a nuclei could be seen by examining the DAPI staining. Cells not fitting the previous criteria were scored as negative. Additionally, with some α-SMA positive cells it was hard to determine whether they were positive or negative and thus they were scored as non-determinable (ND). Pictures of some of the areas analyzed were taken using the Zeiss LSM510 Laser scanning confocal system.

References

Abe R, Donnelly SC, Peng T, Bucala R, Metz CN. (2001) Peripheral blood fibrocytes: differentiation pathway and migration to wound sites. *J Immunol*, **166**, 7556-62.

Aghi M, Chiocca EA. (2005) Contribution of bone marrow-derived cells to blood vessels in ischemic tissues and tumors. *Mol Ther*, **12**(6), 994-1005.

Barth PJ, Ramaswamy A, Moll R. (2002) CD34(+) fibrocytes in normal cervical stroma, cervical intraepithelial neoplasia III, and invasive squamous cell carcinoma of the cervix uteri. *Virchows Arch*, **441**(6), 564-8.

Bucala R, Spiegel LA, Chesney J, Hogan M, Cerami A. (1994) Circulating fibrocytes define a new leukocyte subpopulation that mediates tissue repair. *Mol Med*. **1**, 71-81.

Chauhan H, Abraham A, Phillips JR, Pringle JH, Walker RA, Jones JL. (2003) There is more than one kind of myofibroblast: analysis of CD34 expression in benign, in situ, and invasive breast lesions. *J Clin Pathol*, **56**(4), 271-6.

Coussens LM, Tinkle CL, Hanahan D, Werb Z. (2000) MMP-9 supplied by bone marrow-derived cells contributes to skin carcinogenesis. *Cell*, **103**(3), 481-90.

De Wever O, Demetter P, Mareel M, Bracke M. (2008) Stromal myofibroblasts are drivers of invasive cancer growth. *Int J Cancer*, **123**(10), 2229-38.

Desmoulière A, Geinoz A, Gabbiani F, Gabbiani G. (1993) Transforming growth factor-beta 1 induces alpha-smooth muscle actin expression in granulation tissue myofibroblasts and in quiescent and growing cultured fibroblasts. *J Cell Biol*, **122**(1), 103-11.

Direkze NC, Hodivala-Dilke K, Jeffery R, Hunt T, Poulsom R, Oukrif D, Alison MR, Wright NA. (2004) Bone marrow contribution to tumor-associated myofibroblasts and fibroblasts. *Cancer Res*, **64**(23), 8492-5.

Guo X, Oshima H, Kitmura T, Taketo MM, Oshima M. (2008) Stromal fibroblasts activated by tumor cells promote angiogenesis in mouse gastric cancer. *J Biol Chem*, **283**(28), 19864-71.

Hinz B, Phan SH, Thannickal VJ, Galli A, Bochaton-Piallat ML, Gabbiani G. (2007) The myofibroblast: one function, multiple origins. *Am J Pathol*, **170**(6), 1807-16.

Ishii G, Sangai T, Oda T, Aoyagi Y, Hasebe T, Kanomata N, Endoh Y, Okumura C, Okuhara Y, Magae J, Emura M, Ochiya T, Ochiai A. (2003) Bone-marrow-derived myofibroblasts contribute to the cancer-induced stromal reaction. *Biochem Biophys Res Comm*, **309**, 232-240.

Ishii S, Tsuji S, Tsujii M, Kanazawa Y, Nishida T, Iijima H, Yasumaru M, Irie T, Yamamoto K, Tsutsui S, Eguchi H, Kawano S, Hayashi N. (2008) Involvement of bone marrow-derived stromal cells in gastrointestinal cancer development and metastasis. *J Gastroenterol Hepatol*, **23,** Suppl 2:S242-9.

Kalluri R, Zeisberg M. (2006) Fibroblasts in cancer. *Nat Rev Cancer*, **6**(5), 392-401.

Kitamura T, Kometani K, Hashida H, Matsunaga A, Miyoshi H, Hosogi H, Aoki M, Oshima M, Hattori M, Takabayashi A, Minato N, Taketo MM. (2007) SMAD4-deficient intestinal tumors recruit CCR1+ myeloid cells that promote invasion. *Nat Genet*, **39**(4), 467-75.

LaRue AC, Masuya M, Ebihara Y, Fleming PA, Visconti RP, Minamiguchi H, Ogawa M, Drake CJ. (2006) Hematopoietic origins of fibroblasts: I. In vivo studies of fibroblasts associated with solid tumors. *Exp Hematol*, **34**(2), 208-18.

Lyden D, Hattori K, Dias S, Costa C, Blaikie P, Butros L, Chadburn A, Heissig B, Marks W, Witte L, Wu Y, Hicklin D, Zhu Z, Hackett NR, Crystal RG, Moore MA, Hajjar KA, Manova K, Benezra R, Rafii S. (2001) Impaired recruitment of bone-marrow-derived endothelial and hematopoietic precursor cells blocks tumor angiogenesis and growth. *Nat Med*, **7**(11), 1194-201.

Rønnov-Jessen L, Petersen OW. (1993) Induction of alpha-smooth muscle actin by transforming growth factor-beta 1 in quiescent human breast gland fibroblasts. Implications for myofibroblast generation in breast neoplasia. *Lab Invest*, **68**(6), 696-707.

Rønnov-Jessen L, Petersen OW, Koteliansky VE, Bissell MJ. (1995) The origin of the myofibroblasts in breast cancer. Recapitulation of tumor environment in culture unravels diversity and implicates converted fibroblasts and recruited smooth muscle cells. *J Clin Invest*, **95**(2), 859-73.

Ruzinova MB, Schoer RA, Gerald W, Egan JE, Pandolfi PP, Rafii S, Manova K, Mittal V, Benezra R. (2003) Effect of angiogenesis inhibition by Id loss and the contribution of bone-marrow-derived endothelial cells in spontaneous murine tumors. *Cancer Cell*, **4**(4), 277-89.

Sangai T, Ishii G, Kodama K, Miyamoto S, Aoyagi Y, Ito T, Magae J, Sasaki H, Nagashima T, Miyazaki M, Ochiai A. (2005) Effect of differences in cancer cells and tumor growth sites on recruiting bone marrow-derived endothelial cells and myofibroblasts in cancer-induced stroma. *Int J Cancer*, **115**(6), 885-92.

Schmidt M, Sun G, Stacey MA, Mori L, Mattoli S. (2003) Identification of circulating fibrocytes as precursors of bronchial myofibroblasts in asthma. *J Immunol*, **171**, 380-9.

Shojaei F, Wu X, Malik AK, Zhong C, Baldwin ME, Schanz S, Fuh G, Gerber HP, Ferrara N. (2007) Tumor refractoriness to anti-VEGF treatment is mediated by CD11b+Gr1+ myeloid cells. *Nat Biotechnol*, **25**(8), 911-20.

Skalli O, Ropraz P, Trzeciak A, Benzonana G, Gillessen D, Gabbiani G. (1986) A monoclonal antibody against alpha-smooth muscle actin: a new probe for smooth muscle differentiation. *J Cell Biol*, **103**(6 Pt 2), 2787-96.

Worthley DL, Ruszkiewicz A, Davies R, Moore S, Nivison-Smith I, Bik To L, Browett P, Western R, Durrant S, So J, Young GP, Mullighan CG, Bardy PG, Michael MZ. (2009) Human gastrointestinal neoplasia-associated myofibroblasts can develop from bone marrow-derived cells following allogeneic stem cell transplantation. *Stem Cells*, **27**(6), 1463-8.

Yazhou C, Wenlv S, Weidong Z, Licun W. (2004) Clinicopathological significance of stromal myofibroblasts in invasive ductal carcinoma of the breast. *Tumour Biol*, **25**(5-6), 290-5.

Zeisberg EM, Potenta S, Xie L, Zeisberg M, Kalluri R. (2007) Discovery of endothelial to mesenchymal transition as a source for carcinoma-associated fibroblasts. *Cancer Res*, **67**(21), 10123-8.

Chapter 4: Conclusions and Future Directions

The presence of stromal cells within carcinomas can have a profound impact on the pathology of the disease. This collection of non-cancerous cells surrounding and intermingled with the cancer cells within a tumor can be comprised of many cell types such as immune, endothelial, smooth muscle, and myofibroblasts. Clinical studies suggest that the presence of myofibroblasts in tumors leads to a poor prognosis for cancer patients, potentially by promoting angiogenesis and invasion (Tsujino T et al. 2007, Yazhou C et al. 2004, Kalluri R and Zeisberg M 2006, De Wever O et al. 2008, Orimo A et al. 2005, Lewis MP et al. 2004, De Wever O et al. 2004). Interestingly, myofibroblasts are present in breast carcinomas, but not present in the breast under normal circumstances (Skalli O et al. 1986, Lazard D et al. 1993, Barth PJ et al. 2002, Chauhan H et al. 2003, Yazhou C et al. 2004). These observations collectively indicate that myofibroblasts represent a prime therapeutic target because they could be inhibited with minimal collateral damage done to the normal physiology of the breast. Thus, it is important to discover the factors that recruit this cell type to the site of breast carcinomas because they will provide us with a better understanding of this tumor-promoting cell type and may prove to be important therapeutic targets. In these studies we used a newly developed breast carcinoma model, which forms tumors that contain areas with numerous myofibroblasts, in order to identify paracrine factors important in the recruitment of myofibroblasts (Ince TA et al 2007).

Factors Involved in the Recruitment of Myofibroblasts to the Site of Breast Cancer Formation

In a screen to identify factors secreted by BPLER cells that contribute to the recruitment of myofibroblasts, we identified CXCL1, VEGF, CCL5 and IL-6 as candidates. We tested the effects of mouse CXCL1 (mCXCL1), mouse $VEGF_{164}$ ($mVEGF_{164}$), and human CCL5 (hCCL5) on primary tumor formation and on their ability to recruit α-SMA-positive cells.

The Effects of VEGF, CXCL1, and CCL5 expression in Breast Carcinoma Formation

We demonstrated that when $mVEGF_{164}$, but not hCCL5 or mCXCL1, is expressed in MCF-7-Ras cells, tumor formation in mice is enhanced. The $mVEGF_{164}$ expressing tumors appear to show increased angiogenesis as assessed by staining of the tumor sections with the endothelial marker CD34. In agreement with this, it has been previously been reported that the expression of either human $VEGF_{121}$ or $VEGF_{165}$ in MCF-7 cells leads to increased tumor incidence and growth with a concomitant increase in tumor angiogenesis (Fenton BM et al. 2004).

We have also shown that MCF-7-Ras cells ectopically expressing $mVEGF_{164}$, but not hCCL5 or mCXCL1, form tumors that show increased incorporation of α-SMA-positive cells. As mentioned previously, smooth muscle cells, which express α-SMA, surround endothelial cells to form blood vessels. Because the MCF-7-Ras tumors expressing $mVEGF_{164}$ show an increase in the incorporation of cells expressing CD34, a marker of endothelial cells, the increased presence of α-SMA-positive cells in these

tumors could be the result of an increase in blood vessels lined by smooth muscle cells. However, we found no correlation between the CD34-positive areas and the α-SMA-positive areas of the tumors. Furthermore, it was noted that within a tumor section, there were numerous α-SMA-positive cells that were clearly not proximal to CD34-positive cells. These observations led to the hypothesis that the increase in the average area stained for α-SMA in the $mVEGF_{164}$ tumors is primarily the result of an increase in the number of α-SMA-positive myofibroblasts. It is unclear how this increased incorporation occurs; however we propose several possible mechanisms below.

The inability of mCXCL1 to increase the recruitment α-SMA-positive cells to MCF-7-Ras tumors could be a consequence of expression level. As shown in Chapter II, while human CCL5 was ectopically expressed at higher levels in the MCF-7-Ras cells compared to BPLER cells, mouse CXCL1 was expressed at much lower levels when compared to endogenous expression in BPLER cells. Therefore, the level of mouse CXCL1 expression in the MCF-7-Ras cells may have been insufficient to elicit the recruitment of myofibroblasts *in vivo*.

CXCL1 remains an intriguing factor to us because it has been demonstrated that treatment of human fibroblasts with CXCL1 results in their senescence, as assessed by β-galactosidase staining (Yang G et al. 2006). Furthermore, fibroblasts stimulated by CXCL1 are able to promote tumor formation of immortalized human ovarian epithelial cells compared to untreated fibroblasts (Yang G et al. 2006). These data suggest that CXCL1 secreted by cancer cells may be particularly important in stimulating adjacent fibroblasts. One interesting possibility is that CXCL1 leads to the terminal differentiation

of fibroblasts into myofibroblasts, which may exhibit certain senescent phenotypes that promote tumorigenesis, as elegantly reported by J. Campisi and colleagues (Krtolica A et al. 2001). Future studies should investigate the ability of human CXCL1 to induce the differentiation of fibroblasts into myofibroblasts.

Mechanisms of VEGF-A Action

There are multiple mechanisms that VEGF-A could utilize to induce the incorporation of myofibroblasts into the tumor stroma, and our understanding is obscured by several aspects. First, there are several potential precursors to the myofibroblasts that VEGF-A could directly stimulate, including fibroblasts, smooth muscle cells, bone marrow-derived cells, endothelial cells, and the carcinoma cells themselves (Rønnov-Jessen L et al. 1995, Sangai T et al. 2005, Hinz B et al. 2007, Zeisberg EM et al. 2007, Kalluri R and Zeisberg M 2006). Secondly, it is unclear whether VEGF-A acts alone or in combination with other factors secreted by the MCF-7 Ras cells. Finally, there could be indirect, multi-step mechanisms involving VEGF-A stimulation of intermediate cell types, which lead, in turn, to the incorporation of myofibroblasts.

VEGF-A is a ligand for two receptor tyrosine kinases (RTKs), VEGFR-1 and VEGFR-2. While initially identified as a key activator of vasculogenesis and angiogenesis, these receptors are expressed by a surprisingly wide variety of cells types as shown in Figure 1A and 1B (Olsson AK et al. 2006, Cross MJ et al. 2003). While less well characterized, there is also data that suggests VEGF-A receptors are expressed by some fibroblast and myofibroblast populations (Orimo A et al. 2001, Decaussin M et al. 1999). Finally, VEGF receptors are also expressed by some breast carcinoma cells (Lee

TH et al. 2007, Wu Y et al. 2006). These important findings suggest that VEGF likely plays a much broader role in cellular signaling beyond its well-known role in the vascular compartment. Our results are in accord with this idea, implicating VEGF in the induction of myofibroblast incorporation in the tumor stroma that may only be tangentially related to its role in inducing tumor angiogenesis. I propose that VEGF interacts with one or several of these cell types to induce the incorporation of α-SMA-positive myofibroblasts.

VEGF-A can induce several biological responses that are important for the recruitment of stromal cells. For example, the binding of VEGF-A to VEGFR-2 expressed on endothelial cells results in the activation of several downstream effector pathways that are able to induce proliferation, migration, and cell survival as shown in Figure 1A (Olsson AK et al. 2006, Cross MJ et al. 2003). It is possible that these pathways are also activated downstream of VEGFR-2 activation in other cell types. Additionally, VEGFR-2 activation of endothelial cells leads to an increase in vascular permeability, which may be important in the recruitment of stromal cells, as discussed in detail below (Olsson AK et al. 2006, Cross MJ et al. 2003). Endothelial cells express VEGFR-1 and VEGFR-2, but it is thought that the effects of VEGF-A mentioned above are, by and large, mediated through VEGFR-2 (Cross MJ et al. 2003, Nagy JA et al. 2007). VEGFR-1, instead, mediates the migration of monocytes, macrophages, and hematopoietic stem cells in response to VEGF-A. However, the downstream effector pathways of VEGFR-1 are less clear (Olsson AK et al. 2006, Cross MJ et al. 2003). Some of the signaling molecules thought to interact with VEGFR-1 are shown in Figure 1B. Given that VEGFR-1 is expressed by a wide variety of cell types, we would be very

interested in exploring the possibility that VEGF acts in novel pathways downstream of VEGFR-1 activation to induce non-canonical cellular functions, including myofibroblast induction.

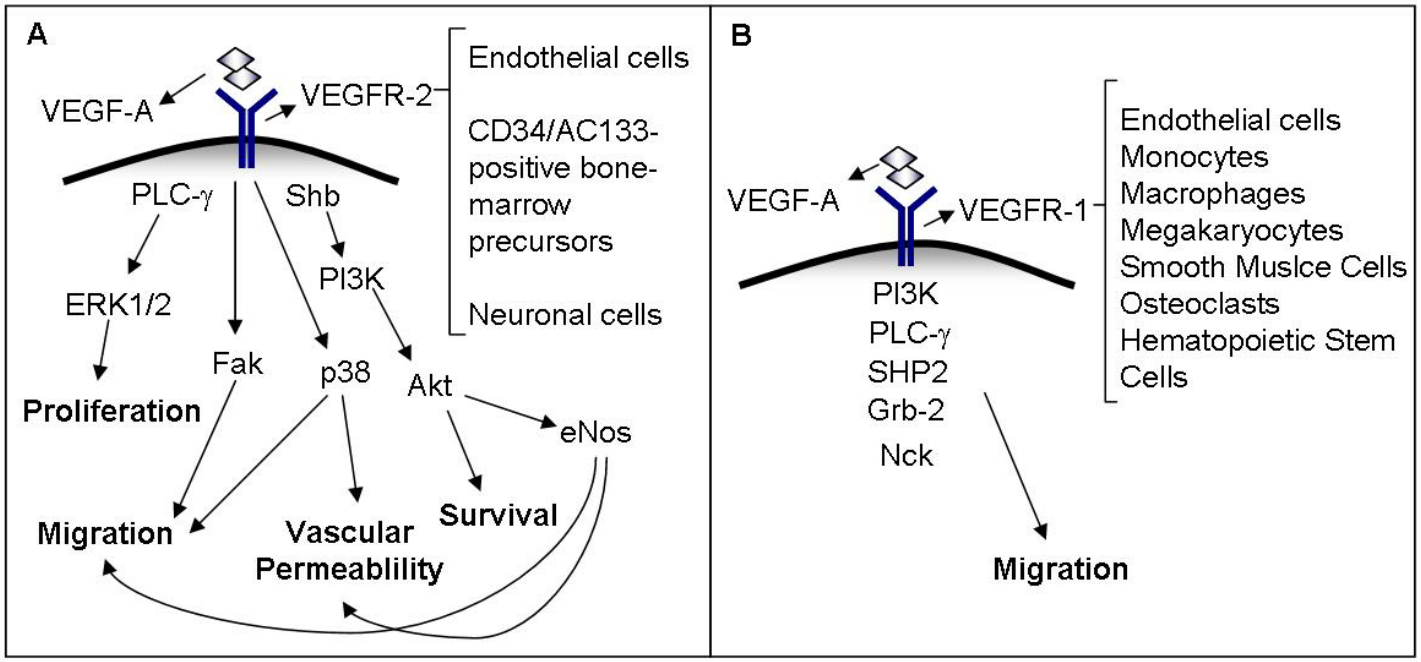

Figure 1: Downstream Effector Pathways of VEGFR-1 and VEGFR-2. (A) The binding of VEGF-A to VEGFR-2 on endothelial cells leads to the activation of several downstream signaling pathways that cause endothelial cell proliferation, migration, and survival. Additionally, activation of VEGFR-2 leads to vascular permeability. Some of the other cell types known to express VEGFR-2 are shown to the right of the receptor. (B) The dowstream signaling pathways of VEGFR-1 are less clear. Some of the signaling molecules that have been implicated are displayed. VEGFR-1 mediates the migration of monocytes and macrophages in response to VEGF-A. Some of the cells known to express VEGFR-1 are shown to the right of the receptor. Abbreviations: phospholipase C-γ (PLC-γ), SH2 and β-cells (Shb), p38 mitogen-activated protein kinase (p38), phosphatidylinositol-3 kinase (PI3K), focal adhesion kinase (Fak), extacellular regulated kinase 1 and 2 (ERK1/2), endothelial nitric oxide synthase (eNos), growth factor receptor-bound-2 (Grb2), protein tyrosine phosphatase-2 (SHP2), NCK tyrosine kinase (Nck). (Olsson AK et al. 2006 and Cross MJ et al. 2003)

Direct Mechanisms of VEGF-A Action

There are several direct mechanisms that may be used by VEGF-A to increase the incorporation of myofibroblasts as shown in Figure 2. We define direct mechanism as the ability of VEGF to directly stimulate a myofibroblast precursor or the myofibroblast itself. Two likely candidates for myofibroblast precursor cells are smooth muscle cells and fibroblasts. VEGF-A has been shown to affect both of these cell types in various biological contexts. It was demonstrated that MCF-7 tumors ectopically expressing VEGF-A and treated with tamoxifen display increased desmoplasia, as assessed by increased stromal area (Qu Z et al. 2008). Strikingly, the study concluded that the majority of the stroma consisted of fibroblasts based on their morphology; however the mechanism underlying the increase in desmoplasia in these tumors remains unknown VEGF-A has also been shown to increase the *in vitro* migration and proliferation of dermal fibroblasts and keloid fibroblasts, respectively (Wu WS et al. 2006, Ball SG et al. 2007). Interestingly, the data suggest that the migration of human dermal fibroblasts in response to VEGF-A is mediated through activation of the platelet-derived growth factor receptor (PDGFR) (Ball SG et al. 2007). As shown in Figure 1B, VEGFR-1 expression has been documented in smooth muscle cells. It has also been shown that expression of VEGF in the intestinal epithelium leads to the formation of cysts surrounded by α-SMA-positive cells (Boquoi A et al. 2009). In the normal intestine, α-SMA expression is confined for the most part to smooth muscle cells surrounding blood vessels and to mesenchymal cells present in the crypts (Boquoi A et al. 2009). However, it has also been demonstrated that VEGF-A can inhibit pericyte functions; these have many

attributes of smooth muscle cells (Greenberg JI et al. 2008). Collectively, these studies demonstrate the ability of VEGF-A to affect both fibroblasts and smooth muscle cells, suggesting that in our experiments, $mVEGF_{164}$ may contribute to the incorporation of myofibroblasts through its effects on these myofibroblast precursors.

It has also been postulated that myofibroblasts can be derived from endothelial cells and carcinoma cells themselves through the processes of endothelial-to-mesenchymal transition (EndMT) and epithelial-to-mesenchymal transition (EMT), respectively (Hinz B et al. 2007, Zeisberg EM et al. 2007, Kalluri R and Zeisberg M 2006). It is well known that endothelial cells express VEGF receptors and VEGF receptor expression has also been demonstrated in breast carcinoma cells (Olsson AK et al 2006, Lee TH et al. 2007, Wu Y et al. 2006). $mVEGF_{164}$, either alone or in combination with other factors secreted by the MCF-7 Ras cells, could thus facilitate these processes in endothelial cells or in MCF-7 Ras cells themselves.

Other factors have already been implicated in the recruitment of myofibroblasts to the sites of breast carcinoma formation, including TGF-β and PDGF. Our data leads me to include VEGF in this important family of secreted factors that induces myofibroblast incorporation into the tumor stroma. One interesting possibility is that VEGF-A acts directly on the local pool of myofibroblast precursors to induce their proliferation or recruitment, and another factor subsequently induces their differentiation into myofibroblasts. This model is especially plausible, given the known ability of TGF-β to induce the differentiation of fibroblasts into myofibroblasts and its ability to induce EndMT and EMT (Gabbiani G 2003, Hinz B et al. 2007, Zeisberg EM et al. 2007, Thiery

JP 2002). It will thus be important to see if VEGF-A and TGF-β, or other combinations of factors, can act synergistically to induce myofibroblast incorporation in the tumor stroma.

One can address these possibilities in future studies by examining the effects of conditioned media from MCF-7-Ras cells expressing $mVEGF_{164}$ on the proliferation, migration, and transdifferention of fibroblasts, smooth muscle cells, endothelial cells and breast carcinoma cells relative to control cell conditioned media , $mVEGF_{164}$ alone, or $mVEGF_{164}$ with TGF-β.

Figure 2:

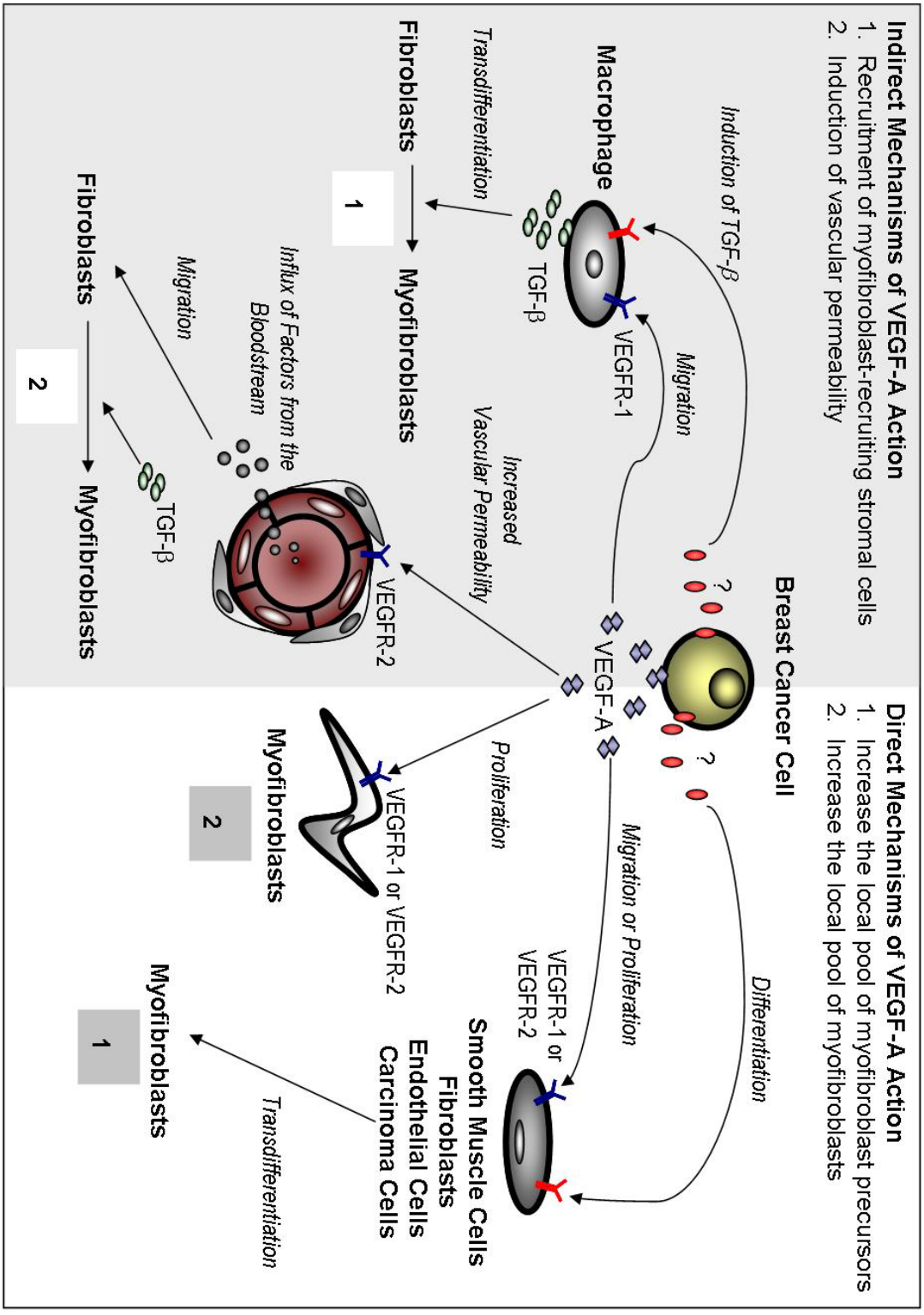
Indirect Mechanisms of VEGF-A Action
1. Recruitment of myofibroblast-recruiting stromal cells
2. Induction of vascular permeability
Direct Mechanisms of VEGF-A Action
1. Increase the local pool of myofibroblast precursors
2. Increase the local pool of myofibroblasts
Breast Cancer Cell
Induction of TGF-β
Migration
Macrophage
VEGFR-1
TGF-β
Transdifferentiation
Increased Vascular Permeability
Fibroblasts
1
Myofibroblasts
VEGF-A
Differentiation
Migration or Proliferation
VEGFR-1 or VEGFR-2
Smooth Muscle Cells
Fibroblasts
Endothelial Cells
Carcinoma Cells
Proliferation
VEGFR-1 or VEGFR-2
Myofibroblasts
2
Transdifferentiation
Myofibroblasts
1
Influx of Factors from the Bloodstream
VEGFR-2
Migration
TGF-β
Fibroblasts
2
Myofibroblasts

Figure 2 (continued):

Figure 2: VEGF-A Could Increase the Incorporation of Myofibroblasts Through Several Direct and Indirect Mechanisms. The direct mechanisms are shown on the right and the indirect mechanisms on the left. The first direct mechanism begins with the stimulation of proliferation or migration of VEGFR-expressing myofibroblast precursors (smooth muscle cells, fibroblasts, endothelial cells, and carcinoma cells), followed by their differentiation into myofibroblasts by a second factor. The second direct mechanism involves VEGF-A directly stimulating the proliferation of recruited myofibroblasts. The first indirect mechanism is initiated by the recruitment of VEGFR-1-expressing macrophages and monocytes followed by their release of TGF-β. The induction of TGF-β expression may involve a second factor. The TGF-β could then cause the differentiation of fibroblasts into myofibroblasts. The second indirect mechanism begins with the binding of VEGF to VEGFR-2-expressing endothelial cells resulting in the stimulation of vascular permeability. The increased vascular permeability causes the efflux of factors from the bloodstream that then induce the influx of fibroblasts into the tumor. These invasive fibroblasts could then differentiate into myofibroblasts.

Indirect Mechanisms of VEGF-A Action

As discussed above, VEGF-A's ability to induce the incorporation of myofibroblasts in the stroma may not be through direct stimulation of myofibroblasts or its precursors, but rather through indirect action on another stromal cell type (Figure 2). A precedent for this model is the ability of GM-CSF to induce the presence of myofibroblasts potentially by recruiting myeloid cells, such as macrophages, which secrete TGF-β. The TGF-β secreted by the recruited macrophages is then thought to recruit and/or differentiate myofibroblasts (Serini G and Gabbiani G 1999). In this vein, VEGFR-1 is known to be expressed by monocytes and macrophages, which migrate in response to VEGF-A (Olsson AK et al 2006). We thus envision a model where VEGF-A is secreted by carcinoma cells, resulting in recruitment of these TGF-β–secreting monoctyes and macrophages (Figure 2). The secreted TGF-β could then cause fibroblasts to differentiate into myofibroblasts at the site of tumor growth. In addition to VEGF-A, there may be additional signals secreted by tumor cells that induce the expression of TGF-β in monocytes or macrophages.

In future studies, it will be interesting to analyze the MCF-7 Ras tumors expressing $mVEGF_{164}$ for the presence of monocytes and macrophages relative to control tumors. An increase in monocytes and macrophages would justify experiments that examine the ability of conditioned media from the MCF-7 Ras cells expressing $mVEGF_{164}$ to induce the *in vitro* migration and proliferation of monocytes and macrophages, as well as its ability to induce the secretion of TGF-β. If $mVEGF_{164}$ is not

acting alone, it will be important to identify collaborating factors through a screen using the *in vitro* experiments established above.

In addition to acting on immune cells, VEGF-A's ability to induce the presence of myofibroblasts in the stroma may be operating through other indirect mechanisms (Figure 2). VEGF-A not only induces angiogenesis but it also induces vascular permeability (Nagy JA et al. 2007). Increased permeability can subsequently lead to an efflux of proteins from the blood stream to the tumor, leading not only a release of growth factors but the deposition of extracellular matrix (ECM) (Nagy JA et al. 2007). One possible scenario is that local resident fibroblasts may be stimulated by or recruited to the deposited ECM and proteins, where they undergo terminal differentiation into myofibroblasts.

We noted earlier that some of the $mVEGF_{164}$-expressing tumors contained what appeared to be to be extensive areas of necrosis. In another interesting scenario, it is possible that a major immune response to necrosis leads to an influx of immune cells that subsequently secrete signals that induce the influx of myofibroblasts as discussed above. To address this possibility, one can analyze smaller tumors that have not yet become necrotic for the absence of α-SMA positive cells compared to tumors with large necrotic regions.

One of the most promising aspects of our identification of VEGF in the induction of myofibroblast incorporation is the fact that numerous inhibitors of the VEGF signaling pathway already exist and are in use in the clinic. It would be interesting to treat our mice with Avastin and other anti-angiogenic drugs to see if they affect

myofibroblast recruitment. If recruitment were inhibited, this would suggest, surprisingly, that these drugs may act on multiple stromal cell types to inhibit tumor growth.

The Recruitment of Bone Marrow-Derived Cells to the Site of Tumor Formation

Until now we have focused on the prospect of inhibiting myofibroblast incorporation into tumors by targeting the factors that either recruit them or differentiate their precursors. I now switch my focus to understanding precisely where these cells reside and if this physiological niche can be therapeutically targeted. Several studies have shown that bone marrow-derived (BMD) cells that home to primary tumor sites can enhance tumor progression (Coussens LM et al. 2000, Lyden D et al. 2001, Shojaei F et al. 2007). Of particular interest to us was the fact that some of these BMD cell types are known to express α-SMA and that up to 80% of stromal cells present in breast carcinomas can express α-SMA (Ishii G et al. 2003, Sangai T et al. 2005, Direkze NC et al. 2004, Guo X et al. 2008, LaRue AC et al. 2006, Ishii S et al. 2008, Worthley DL et al. 2009, and Sappino AP et al. 1988). This led me to hypothesize that in breast carcinomas, myofibroblasts or their precursors originate from the bone marrow.

In our studies we therefore examined whether the α-SMA-positive cells incorporated into our BPHER-3 tumors are bone marrow-derived (BMD). Surprisingly, we demonstrated that nearly 100% of all α-SMA-positive cells analyzed in our tumor model are *not* derived from the bone marrow, which strongly suggests that they are in fact derived from cells present in the adjacent tissue.

This result was surprising to us, given that the recruitment of α-SMA-positive bone marrow-derived myofibroblasts (BMD-MFs) has previously been described in human xenograft tumor models, autochthonous mouse tumor models, and 2 cases of human cancer (Ishii G et al. 2003, Sangai T et al. 2005, Direkze NC et al. 2004, and Guo X et al. 2008, LaRue AC et al. 2006, Ishii S et al. 2008, Worthley DL et al. 2009). Sangai and colleagues demonstrated that of all myofibroblasts recruited to MDA-MB-468 and MDA-MB-231 human breast xenograft tumors, 14% and 20.6%, respectively, were bone marrow-derived. In contrast, our studies using another human breast carcinoma model demonstrated that essentially none of the α-SMA-positive stromal cells appear to be recruited from the bone marrow. These conflicting results raise important questions regarding the identification of BMD-MFs, as discussed below.

In both ours and previously cited studies, the recruitment of BMD-MFs was assessed by the co-localization of a bone marrow-specific marker, such as GFP, and α-SMA. Unfortunately, α-SMA has been the only molecular marker used to identify cells as myofibroblasts. In addition to the expression of α-SMA, cellular morphology has also been used for the identification of these cells. Using these criteria, several studies have shown that in certain tumor models, α-SMA-myofibroblasts incorporated into the tumors can indeed be bone marrow-derived.

The discrepancy between these other studies and our own, which show no derivation from the bone marrow, may be explained by the fact that the α-SMA-positive cells represent a heterogeneous population of cells. Under these circumstances, there are two possible scenarios that may explain our data. First, it is possible that there are two

lineages of myofibroblasts—one originating from the bone marrow and another originating from the adjacent tissue. In this case, our BPHER-3 model may represent a unique system to study myofibroblast recruitment exclusively from the adjacent tissue.

A second possible scenario is that the α-SMA-positive population contains not only myofibroblasts and smooth muscle cells, but a variety of other fibroblast-like cell types. In this case, it is possible that the absence of BMD-MF in our studies can be explained simply by the fact that our BPHER-3 tumor cells preferentially recruited these other cell types rather than myofibroblasts from the bone marrow. In this case, it will be critical to further stratify the heterogeneous α-SMA-positive population in order to identify and target other critical cell types in the tumor stroma.

Cellular heterogeneity in the fibroblast compartment of the tumor stroma has indeed been previously reported (Sugimoto H et al. 2006). These other authors analyzed the fibroblasts incorporated into both a 4T1 breast tumor model and a Rip1-Tag2 pancreatic cancer model. In their study, heterogeneity within the fibroblast population was established by showing differential expression of several molecular markers of fibroblasts and smooth muscle cells, including fibroblast specific protein-1 (S100A4/FSP1), α-SMA, neuronal-glial antigen-2 (NG2), and the platelet-derived growth factor receptor-β (PDGFR-β) (Sugimoto H et al. 2006). As Sugimoto *et al* showed in the fibroblast population, we hypothesize that the α-SMA positive population is also heterogeneous. Defining other molecular markers of myofibroblasts will be a critical step in subdividing the α-SMA population into subtypes to better understand their functions and their origins.

One clear result from our studies is that the α-SMA-positive cells recruited to the BPHER-3 model are not bone marrow-derived, and thus are likely to have been derived locally from cells in the adjacent tissue. Two candidate precursor cell types present in the adjacent tissue are smooth muscle cells and fibroblasts. Smooth muscle cells already express α-SMA, and fibroblasts recruited to the site of tumor formation could give rise to α-SMA-expressing myofibroblasts. In order to further define the α-SMA-positive cell population recruited to the site of BPHER-3 tumor growth, tumor sections should be co-stained with α-SMA and other markers of both fibroblasts and smooth muscle cells. This characterization will allow one to differentiate the respective contributions of myofibroblasts and smooth muscle cells to the α-SMA-positive stromal cells in our model.

Given that a majority of our α-SMA-positive stromal cells are derived from the local environment, it will be important to study the recruitment of these cells when the BPHER-3 cells are injected orthopically. In fact, other avenues of cancer research have shown that tumors progress differently depending on their site of implantation. Specifically, some cancer models metastasize more frequently when injected orthotopically than subcutaneously (Lacroix M et al. 2004). The anatomical location of tumor xenografts may have a profound impact on the types of cells recruited to the site of tumor formation, simply because the cellular environment surrounding the cells differs. Hence, orthotopic injection of cancer cells is more likely to recapitulate the natural tissue environment in which these types of tumors would arise in human patients.

Beyond these additional *in vivo* studies, I would also be interested in looking at the interactions of smooth muscle cells and fibroblasts isolated from the human mammary gland with our BPHER-3 cells in an *in vitro* setting. This will allow one to evaluate the ability of the BPHER-3 cells to recruit smooth muscle cells and fibroblasts in a much more controlled setting. Additionally, one could temporally monitor the transdifferentiation of fibroblasts and smooth muscle cells by immunofluorescence and potentially develop a screen to identify the relevant secreted factors involved in their differentiation and recruitment.

The stromal response elicited during tumor formation can have a profound impact on the pathology of the disease and can, in certain cases, be a critical rate-limiting determinant of tumor growth. Importantly, this is likely to be true for both primary tumor growth and the growth of secondary metastases. For this reason, it is essential to understand the mechanisms that various carcinomas utilize to foster a tumor-promoting stroma and the sources of the recruited stromal cells. Identification of secreted factors will allow one to better understand and inhibit this process. Furthermore, knowing the origins of specific cell types in the tumor stroma would allow us to develop better therapeutic strategies to inhibit their recruitment.

References

Ball SG, Shuttleworth CA, Kielty CM. (2007) Vascular endothelial growth factor can signal through platelet-derived growth factor receptors. *J Cell Biol*, **177**(3), 489-500.

Barth PJ, Ebrahimsade S, Ramaswamy A, Moll R. (2002) CD34+ fibrocytes in invasive ductal carcinoma, ductal carcinoma in situ, and benign breast lesions. *Virchows Arch*, **440**(3), 298-303.

Boquoi A, Jover R, Chen T, Pennings M, Enders GH. (2009) Transgenic expression of VEGF in intestinal epithelium drives mesenchymal cell interactions and epithelial neoplasia. *Gastroenterology*, **136**(2), 596-606.

Chauhan H, Abraham A, Phillips JR, Pringle JH, Walker RA, Jones JL. (2003) There is more than one kind of myofibroblast: analysis of CD34 expression in benign, in situ, and invasive breast lesions. *J Clin Pathol*, **56**(4), 271-6.

Coussens LM, Tinkle CL, Hanahan D, Werb Z. (2000) MMP-9 supplied by bone marrow-derived cells contributes to skin carcinogenesis. *Cell*, **103**(3), 481-90.

Cross MJ, Dixelius J, Matsumoto T, Claesson-Welsh L. (2003) VEGF-receptor signal transduction. *Trends Biochem Sci*, **28**(9), 488-94.

De Wever O, Demetter P, Mareel M, Bracke M. (2008) Stromal myofibroblasts are drivers of invasive cancer growth. *Int J Cancer*, **123**(10), 2229-38.

De Wever O, Nguyen QD, Van Hoorde L, Bracke M, Bruyneel E, Gespach C, Mareel M. (2004) Tenascin-C and SF/HGF produced by myofibroblasts in vitro provide convergent pro-invasive signals to human colon cancer cells through RhoA and Rac. *FASEB J*, **18**(9), 1016-8.

Decaussin M, Sartelet H, Robert C, Moro D, Claraz C, Brambilla C, Brambilla E. (1999) Expression of vascular endothelial growth factor (VEGF) and its two receptors (VEGF-R1-Flt1 and VEGF-R2-Flk1/KDR) in non-small cell lung carcinomas (NSCLCs): correlation with angiogenesis and survival. *J Pathol*, **188**(4), 369-77.

Desmoulière A, Geinoz A, Gabbiani F, Gabbiani G. (1993) Transforming growth factor-beta 1 induces alpha-smooth muscle actin expression in granulation tissue myofibroblasts and in quiescent and growing cultured fibroblasts. *J Cell Biol*, **122**(1), 103-11.

Direkze NC, Hodivala-Dilke K, Jeffery R, Hunt T, Poulsom R, Oukrif D, Alison MR, Wright NA. (2004) Bone marrow contribution to tumor-associated myofibroblasts and fibroblasts. *Cancer Res*, **64**(23), 8492-5.

Dong J, Grunstein J, Tejada M, Peale F, Frantz G, Liang WC, Bai W, Yu L, Kowalski J, Liang X, Fuh G, Gerber HP, Ferrara N. (2004) VEGF-null cells require PDGFR alpha signaling-mediated stromal fibroblast recruitment for tumorigenesis. *EMBO J*, **23**(14), 2800-10.

Fenton BM, Paoni SF, Liu W, Cheng SY, Hu B, Ding I. (2004) Overexpression of VEGF121, but not VEGF165 or FGF-1, improves oxygenation in MCF-7 breast tumours. *Br J Cancer*, **90**(2), 430-5.

Gabbiani G. (2003) The myofibroblast in wound healing and fibrocontractive diseases. *J Pathol*, **200**(4), 500-3.

Gallucci RM, Lee EG, Tomasek JJ. (2006) IL-6 modulates alpha-smooth muscle actin expression in dermal fibroblasts from IL-6-deficient mice. *J Invest Dermatol*, **126**(3), 561-8.

Greenberg JI, Shields DJ, Barillas SG, Acevedo LM, Murphy E, Huang J, Scheppke L, Stockmann C, Johnson RS, Angle N, Cheresh DA. (2008) A role for VEGF as a negative regulator of pericyte function and vessel maturation. *Nature*, **456**(7223), 809-13.

Guo X, Oshima H, Kitmura T, Taketo MM, Oshima M. (2008) Stromal fibroblasts activated by tumor cells promote angiogenesis in mouse gastric cancer. *J Biol Chem*, **283**(28), 19864-71.

Hinz B, Phan SH, Thannickal VJ, Galli A, Bochaton-Piallat ML, Gabbiani G. (2007) The myofibroblast: one function, multiple origins. *Am J Pathol*, **170**(6), 1807-16.

Ince TA, Richardson AL, Bell GW, Saitoh M, Godar S, Karnoub AE, Iglehart JD, Weinberg RA. (2007) Transformation of different human breast epithelial cell types leads to distinct tumor phenotypes. *Cancer Cell*, **12**(2), 160-70.

Ishii G, Sangai T, Oda T, Aoyagi Y, Hasebe T, Kanomata N, Endoh Y, Okumura C, Okuhara Y, Magae J, Emura M, Ochiya T, Ochiai A. (2003) Bone-marrow-derived myofibroblasts contribute to the cancer-induced stromal reaction. *Biochem Biophys Res Comm*, **309**, 232-240.

Ishii S, Tsuji S, Tsujii M, Kanazawa Y, Nishida T, Iijima H, Yasumaru M, Irie T, Yamamoto K, Tsutsui S, Eguchi H, Kawano S, Hayashi N. (2008) Involvement of bone marrow-derived stromal cells in gastrointestinal cancer development and metastasis. *J Gastroenterol Hepatol*, **23** Suppl 2, S242-9.

Kalluri R, Zeisberg M. (2006) Fibroblasts in cancer. *Nat Rev Cancer*, **6**(5), 392-401.

Kitamura T, Kometani K, Hashida H, Matsunaga A, Miyoshi H, Hosogi H, Aoki M, Oshima M, Hattori M, Takabayashi A, Minato N, Taketo MM. (2007) SMAD4-deficient intestinal tumors recruit CCR1+ myeloid cells that promote invasion. *Nat Genet*, **39**(4), 467-75.

Krtolica A, Parrinello S, Lockett S, Desprez PY, Campisi J. (2001) Senescent fibroblasts promote epithelial cell growth and tumorigenesis: a link between cancer and aging. *Proc Natl Acad Sci U S A*, **98**(21), 12072-7.

Lacroix M, Leclercq G. (2004) Relevance of breast cancer cell lines as models for breast tumours: an update. *Breast Cancer Res Treat*, **83**(3), 249-89.

LaRue AC, Masuya M, Ebihara Y, Fleming PA, Visconti RP, Minamiguchi H, Ogawa M, Drake CJ. (2006) Hematopoietic origins of fibroblasts: I. In vivo studies of fibroblasts associated with solid tumors. *Exp Hematol*, **34**(2), 208-18.

Lazard D, Sastre X, Frid MG, Glukhova MA, Thiery JP, Koteliansky VE. (1993) Expression of smooth muscle-specific proteins in myoepithelium and stromal myofibroblasts of normal and malignant human breast tissue. *Proc Natl Acad Sci U S A*, **90**(3), 999-1003.

Lee TH, Seng S, Sekine M, Hinton C, Fu Y, Avraham HK, Avraham S. (2007) Vascular endothelial growth factor mediates intracrine survival in human breast carcinoma cells through internally expressed VEGFR1/FLT1. *PLoS Med*, **4**(6), e186.

Lewis MP, Lygoe KA, Nystrom ML, Anderson WP, Speight PM, Marshall JF, Thomas GJ. (2004) Tumour-derived TGF-beta1 modulates myofibroblast differentiation and promotes HGF/SF-dependent invasion of squamous carcinoma cells. *Br J Cancer*, **90**(4), 822-32.

Lyden D, Hattori K, Dias S, Costa C, Blaikie P, Butros L, Chadburn A, Heissig B, Marks W, Witte L, Wu Y, Hicklin D, Zhu Z, Hackett NR, Crystal RG, Moore MA, Hajjar KA, Manova K, Benezra R, Rafii S. (2001) Impaired recruitment of bone-marrow-derived endothelial and hematopoietic precursor cells blocks tumor angiogenesis and growth. *Nat Med*, **7**(11), 1194-201.

Nagy JA, Dvorak AM, Dvorak HF. (2007) VEGF-A and the induction of pathological angiogenesis. *Annu Rev Pathol*, **2**, 251-75.

Olsson AK, Dimberg A, Kreuger J, Claesson-Welsh L. (2006) VEGF receptor signalling - in control of vascular function. *Nat Rev Mol Cell Biol*, **7**(5), 359-71.

Orimo A, Gupta PB, Sgroi DC, Arenzana-Seisdedos F, Delaunay T, Naeem R, Carey VJ, Richardson AL, Weinberg RA. (2005) Stromal fibroblasts present in invasive human breast carcinomas promote tumor growth and angiogenesis through elevated SDF-1/CXCL12 secretion. *Cell*, **121**(3), 335-48.

Orimo A, Tomioka Y, Shimizu Y, Sato M, Oigawa S, Kamata K, Nogi Y, Inoue S, Takahashi M, Hata T, Muramatsu M. (2001) Cancer-associated myofibroblasts possess various factors to promote endometrial tumor progression. *Clin Cancer Res*, **7**(10), 3097-105.

Qu Z, Van Ginkel S, Roy AM, Westbrook L, Nasrin M, Maxuitenko Y, Frost AR, Carey D, Wang W, Li R, Grizzle WE, Thottassery JV, Kern FG. (2008) Vascular endothelial growth factor reduces tamoxifen efficacy and promotes metastatic colonization and desmoplasia in breast tumors. *Cancer Res*, **68**(15), 6232-40.

Rønnov-Jessen L, Petersen OW, Koteliansky VE, Bissell MJ. (1995) The origin of the myofibroblasts in breast cancer. Recapitulation of tumor environment in culture unravels diversity and implicates converted fibroblasts and recruited smooth muscle cells. *J Clin Invest*, **95**(2), 859-73.

Sangai T, Ishii G, Kodama K, Miyamoto S, Aoyagi Y, Ito T, Magae J, Sasaki H, Nagashima T, Miyazaki M, Ochiai A. (2005) Effect of differences in cancer cells and tumor growth sites on recruiting bone marrow-derived endothelial cells and myofibroblasts in cancer-induced stroma. *Int J Cancer*, **115**(6), 885-92.

Sappino AP, Skalli O, Jackson B, Schürch W, Gabbiani G. (1988) Smooth-muscle differentiation in stromal cells of malignant and non-malignant breast tissues. *Int J Cancer*, **41**(5), 707-12.

Serini G, Gabbiani G. (1999) Mechanisms of myofibroblast activity and phenotypic modulation. *Exp Cell Res*, **250**(2), 273-83.

Shojaei F, Wu X, Malik AK, Zhong C, Baldwin ME, Schanz S, Fuh G, Gerber HP, Ferrara N. (2007) Tumor refractoriness to anti-VEGF treatment is mediated by CD11b+Gr1+ myeloid cells. *Nat Biotechnol*, **25**(8), 911-20.

Skalli O, Ropraz P, Trzeciak A, Benzonana G, Gillessen D, Gabbiani G. (1986) A monoclonal antibody against alpha-smooth muscle actin: a new probe for smooth muscle differentiation. *J Cell Biol*, **103**(6 Pt 2), 2787-96.

Sugimoto H, Mundel TM, Kieran MW, Kalluri R. (2006) Identification of fibroblast heterogeneity in the tumor microenvironment. *Cancer Biol Ther*, **5**(12), 1640-6.

Tejada ML, Yu L, Dong J, Jung K, Meng G, Peale FV, Frantz GD, Hall L, Liang X, Gerber HP, Ferrara N. (2006) Tumor-driven paracrine platelet-derived growth factor receptor alpha signaling is a key determinant of stromal cell recruitment in a model of human lung carcinoma. *Clin Cancer Res*, **12**(9), 2676-88.

Thiery JP. Epithelial-mesenchymal transitions in tumour progression. (2002) *Nat Rev Cancer*, **2**(6), 442-54.

Tsujino T, Seshimo I, Yamamoto H, Ngan CY, Ezumi K, Takemasa I, Ikeda M, Sekimoto M, Matsuura N, Monden M. (2007) Stromal myofibroblasts predict disease recurrence for colorectal cancer. *Clin Cancer Res*, **13**(7), 2082-90.

Worthley DL, Ruszkiewicz A, Davies R, Moore S, Nivison-Smith I, Bik To L, Browett P, Western R, Durrant S, So J, Young GP, Mullighan CG, Bardy PG, Michael MZ. (2009) Human gastrointestinal neoplasia-associated myofibroblasts can develop from bone marrow-derived cells following allogeneic stem cell transplantation. *Stem Cells*, **27**(6), 1463-8.

Wu WS, Wang FS, Yang KD, Huang CC, Kuo YR. (2006) Dexamethasone induction of keloid regression through effective suppression of VEGF expression and keloid fibroblast proliferation. *J Invest Dermatol*, **126**(6), 1264-71.

Wu Y, Hooper AT, Zhong Z, Witte L, Bohlen P, Rafii S, Hicklin DJ. (2006) The vascular endothelial growth factor receptor (VEGFR-1) supports growth and survival of human breast carcinoma. *Int J Cancer*, **119**(7), 1519-29.

Yang G, Rosen DG, Zhang Z, Bast RC Jr, Mills GB, Colacino JA, Mercado-Uribe I, Liu J. (2006) The chemokine growth-regulated oncogene 1 (Gro-1) links RAS signaling to the senescence of stromal fibroblasts and ovarian tumorigenesis. *Proc Natl Acad Sci U S A*, **103**(44), 16472-7.

Yazhou C, Wenlv S, Weidong Z, Licun W. (2004) Clinicopathological significance of stromal myofibroblasts in invasive ductal carcinoma of the breast. *Tumour Biol*, 25(5-6), 290-5.

Zeisberg EM, Potenta S, Xie L, Zeisberg M, Kalluri R. (2007) Discovery of endothelial to mesenchymal transition as a source for carcinoma-associated fibroblasts. *Cancer Res*, **67**(21), 10123-8.

Appendix 1: Perturbations of Cells in the Blood by Subcutaneously Growing Human Breast Cancer Xenografts

Matthew P. Saelzler[1,2], Ferenc Reinhardt[1], Tan A. Ince[1,3], and Robert A. Weinberg[1,2]

(1) Whithead Institute for Biomedical Research, Cambridge, MA 02142
(2) Department of Biology, Massachusetts Institute of Technology, Cambridge, MA 02139
(3) Department of Pathology, Division of Women's and Perinatal Pathology, Brigham and Women's Hospital, Harvard Medical School, Boston, MA 02115

Ferenc Reinhardt performed all the mouse procedures up to and including the injection of tumor cells into the mice. Blood analysis was submitted to and performed by the Division of Comparative Medicine at MIT. All other parts of the experiment were carried out by the thesis author, Matthew Saelzler.

Introduction

It is well known that tumor cells are capable of perturbing the local environment that they colonize. However, it is becoming increasingly evident that primary tumors can also induce changes in the environment of distant organs. For example, it was reported that there is an increase in myeloid cells in both the spleens and peripheral blood of tumor-bearing mice (Melani C et al. 2003, Yang L et al. 2004). Work from our own lab has demonstrated that primary tumors can affect the distribution of certain cell types in the bone marrow (McAllister SS et al 2008). McAllister et al. have shown that MDA-MB-231 or BPLER tumor-bearing mice display a decrease in Lin-/Sca1+/cKit+ cells in the bone marrow when compared to non-tumor bearing mice or mice bearing a PC-3 tumor. This work not only illustrates the ability of primary tumors to perturb the systemic environment, but also that these effects can be tumor type specific (McAllister SS et al 2008). Work from other laboratories has further shown that a primary tumor is able to induce changes in the distal environment of the lung, including induction of matrix metalloproteinase-9 (MMP-9), S100A8, S100A9 and fibronectin expression (Hiratsuka S et al. 2002, Kaplan RN 2005, Hiratsuka S et al. 2006). Additionally, primary tumors can also affect the cellular composition of the lung as shown by an increase in Mac 1+ cells in the lung of tumor-bearing animals (Hiratsuka S et al. 2006).

Not only are tumors able to perturb distant sites in the body, but it is also clear that these changes can affect the pathology of the disease. Work form our own lab by McAllister et al. has demonstrated that bone marrow cells (BMCs) prepared from a tumor-bearing animal are capable of stimulating the growth of weakly tumorigenic cells

in vivo, while BMCs from a non-tumor-bearing host fail to do so (McAllister SS et al 2008). It was also shown that certain aggressive tumor cell lines have the capacity to promote the outgrowth of a weakly tumorigenic cell line growing on the opposite side of the mouse. Furthermore, they demonstrated that an aggressive tumor cell line was capable of inducing the outgrowth of weakly metastatic cells in the lung (McAllister SS et al 2008). Additionally, the changes induced by primary tumors in the lung microenvironment mentioned above are also thought to play a role in the establishment of lung metastatic growth (Hiratsuka S et al. 2002, Kaplan RN 2005, Hiratsuka S et al. 2006). These data suggest that the ability of primary tumors to perturb the systemic environment has important ramifications for the successful establishment of distant metastases.

Perturbation of the bone marrow compartment by primary tumors may be of particular therapeutic importance in light of recent data that implicate bone marrow-derived cells in conferring tumor resistance to anti-vascular endothelial growth factor (VEGF) therapy (Shojaei F et al. 2007). In this study, Shojaei et al. demonstrated that co-injection of BMCs, isolated from mice bearing tumors that are more resistant to anti-VEGF treatment, with B16F1 melanoma cells, which are more sensitive to anti-VEGF treatment, results in the promotion of tumor growth and increased resistance to anti-VEGF treatment. Thus, a tumor's ability to affect the systemic environment may also have consequences for disease treatment.

In this section we focus on the ability of subcutaneous human mammary xenografts to perturb the cellular composition of the blood. The results presented in this section are considered preliminary.

Results

Creation of Tumor Bearing and Control Mice for Blood Analysis

BPHER-3, BPLER-1, HMLER-1, MCF-7 Ras and MDA-MB-231 cells were injected bilaterally and subcutaneously into NOD-SCID mice, and control mice were similarly injected with Matrigel. Each group contained 5 mice except the MDA-MB-231 and Matrigel groups which consisted of 8 and 10 mice, respectively. Given that these cell lines form tumors at various rates, groups of mice were euthanized at different time points in order to obtain the same average tumor weight between the different xenograft models. Two to three control mice were euthanized at each of the different time points. The BPHER-3, BPLER-1, MDA-MB-231, HMLER-1 and MCF-7 Ras tumors were allowed to progress for 19, 27, 19, 18, and 20 days, respectively. The average tumor weights are shown in Figure 1A. It is important to note that the HMLER-1 tumor weights were highly variable as will be addressed below.

Description of Blood Analysis

Following carcinoma formation, samples of blood were taken from both the tumor-bearing and control Matrigel-injected mice. In order to look at the effects the tumors might have on various cell types in the blood, each sample of blood was subjected to a complete blood count (CBC), which includes a white blood cell count (WBC), red blood cell count (RBC) and a platelet count (Plat Ct). Additionally, the hematocrit (HCT), mean corpuscular volume (RBC MCV), mean corpuscular hemoglobin (MCH), mean corpuscular hemoglobin concentration (MCHC), and the amount of hemoglobin in

the blood (Hgb) were measured in this analysis. Finally, a differential count was performed on the blood samples, which specifically examines the composition of the white blood cell population and determines the percent of white blood cells that are of a specific cell type. The individual cell types enumerated in the differential count include neutrophils (Neutr), immature neutrophils (Bands), lymphocytes (Lymphs), monocytes (Monos), and eosinophils (Eosins). The numbers for each of these parameters among the different groups is displayed in Supplementary Figure 1.

The results of the WBC, RBC, Neutrophil Differential and Lymphocyte Differential are shown in Figure 1B and C. In this experiment there were a total of 10 control mice. It was observed that if the 10 control mice were split into two groups of 5 based on their date of birth, the WBC count was the only parameter that displayed a statistically significant difference, $p=0.01$ (Supplementary Figure 1). Therefore, when possible, control mice ($n=5$) and tumor-bearing mice with the same date of birth were compared for the analysis of the WBC. For the remaining measurements, tumor-bearing mice were compared to all 10 matrigel-injected control mice (all matrigel-injected control mice). The numbers for each of the measurements along with the p-values for each of the comparisons between the different groups is displayed in Supplementary Figure 1.

Figure 1:

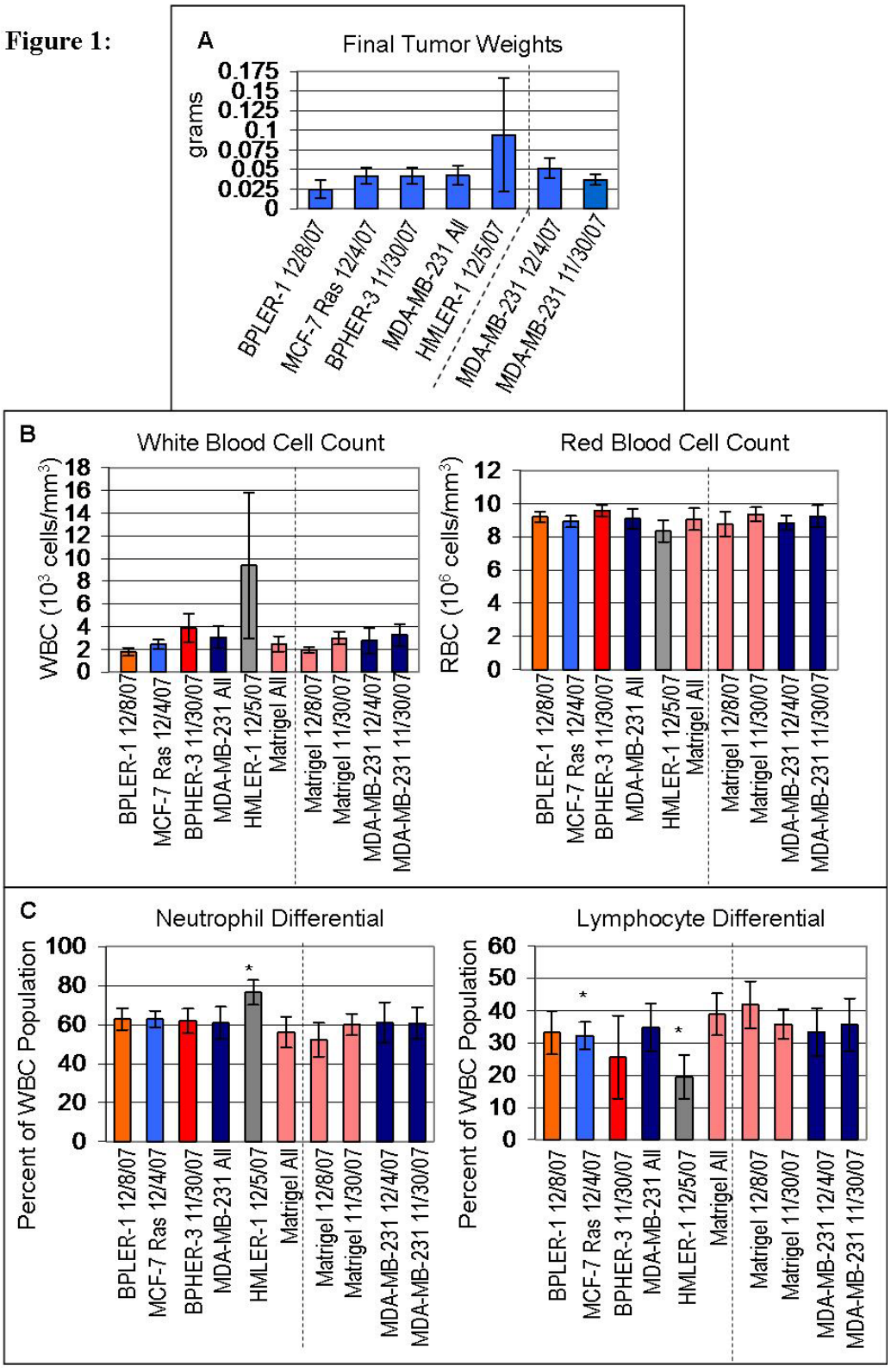
A
Final Tumor Weights
grams
0.175
0.15
0.125
0.1
0.075
0.05
0.025
0
BPLER-1 12/8/07
MCF-7 Ras 12/4/07
BPHER-3 11/30/07
MDA-MB-231 All
HMLER-1 12/5/07
MDA-MB-231 12/4/07
MDA-MB-231 11/30/07
B
White Blood Cell Count
WBC (10^3 cells/mm^3)
Matrigel 12/8/07
Matrigel 11/30/07
Matrigel All
Red Blood Cell Count
RBC (10^6 cells/mm^3)
C
Neutrophil Differential
Percent of WBC Population
Lymphocyte Differential

Figure 1 (continued):

Figure 1: Analysis of Blood Cells in Tumor-Bearing NOD-SCID Mice. **(A)** Mice were injected with BPLER-1, MCF-7 Ras, BPHER-3, MDA-MB-231 and HMLER-1 tumor cells and the tumor-bearing mice were compared to matrigel-injected control mice. The graph shows the average tumor weight at the end of the experiment. Each group of mice was euthanized at different timepoints in an attempt to obtain the same average tumor weight between the different xenograft models. Additionally, 2-3 control matrigel-injected mice were euthanized at each of the different timepoints. The legnth of time allowed for tumor growth is noted in the text. **(B)** Displays the average white blood cell count (WBC), on the left, and the average red blood cell count (RBC), on the right, of mice bearing either BPLER-1, MCF-7 Ras, BPHER-3, MDA-MB-231 or HMLER-1 tumors, along with the average WBC and RBC count of the control matrigel-injected mice. **(C)** Average neutrophil, on the left, and lymphocyte, on the right, differentials (the percent of white blood cells that are either neutrophils or lymphocytes, respectively) of the mice analyzed in (B). In (C), * indicates $p<0.05$ when compared to all matrigel-injected control mice (Matrigel All). In (A), (B) and (C) the date of birth (DOB) is shown for each of the mice. The MDA-MB-231 bearing and matrigel control mice had two groups of mice with different DOBs. The average of all the mice in either the matrigel or MDA-MB-231 groups is shown and the label on the graph is not followed by the DOB, but by All. The graphs also show the averages if these groups, to the right of the dashed line, are separated by the DOB.

Analysis of Blood in Tumor-Bearing Mice

The HMLER-1 tumor-bearing mice displayed the most dramatic blood cell perturbations, but it should be noted that this group also had the largest tumor burden (Figure 2). The HMLER-1 tumor-bearing mice had a 3.8 fold increase in their WBC relative to all Matrigel-injected control mice; however this was not statistically significant ($p=0.07$). The standard deviation of the WBC in the HMLER-1 tumor bearing mice was much greater than control values (Figure 2A). This variability is likely due to the differences in tumor weights, given that among the 5 mice injected with HMLER-1 cells, there appeared to be a correlation between the total tumor burden and the WBC (Figure 3A). This result suggests that tumor burden alone can have an effect on perturbations in the blood.

The HMLER-1 tumor-bearing mice did exhibit statistically significant changes in their neutrophil and lymphocyte differential, platelet count, HCT, MCH, and MCHC (Figure 2A, B and C). Relative to all matrigel-injected control mice, HMLER-1 tumor-bearing mice displayed an increase in their neutrophil differential, MCH, and MCHC, while they showed a decrease in their lymphocyte differential, HCT, and platelet count. These parameters did not show a strong correlation with tumor burden (Figure 3B-E).

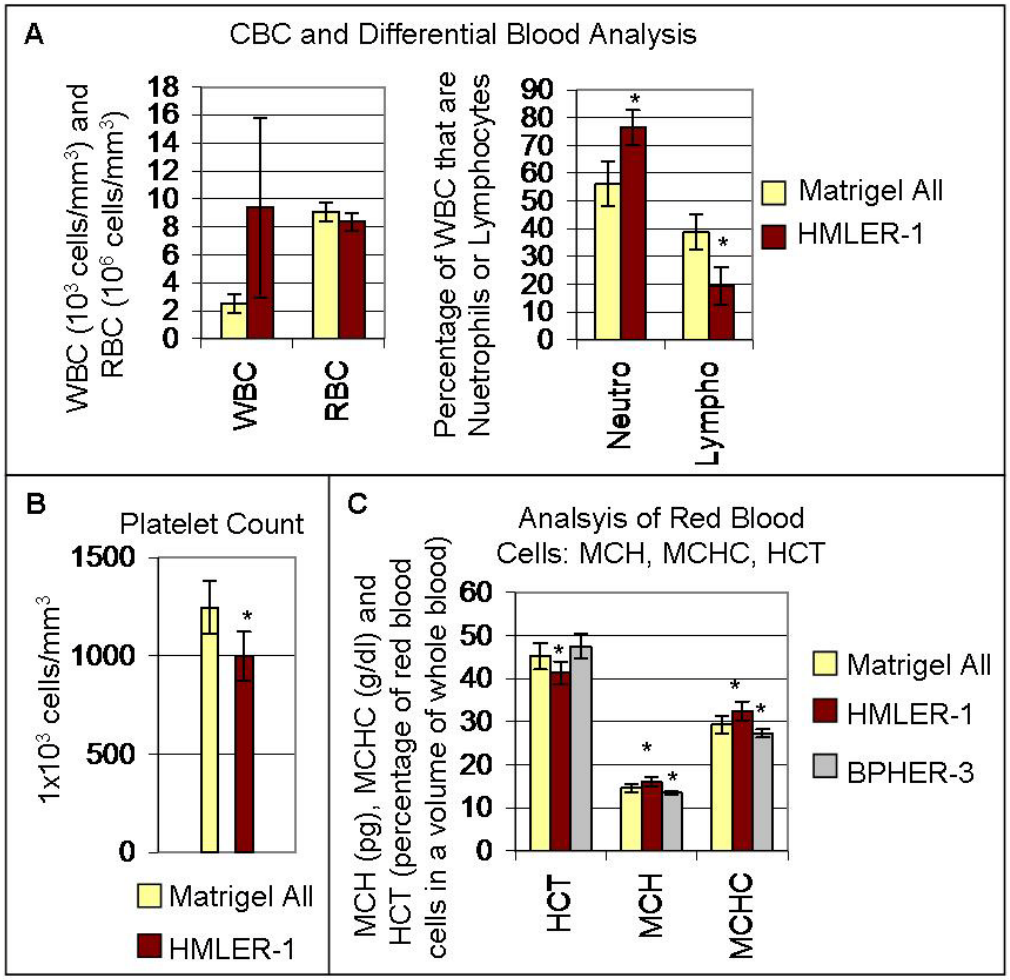

Figure 2: Analysis of Blood Cells in HMLER-1 Tumor-Bearing NOD-SCID Mice. (A) A complete blood count with a differential was performed on HMLER-1 tumor-bearing mice and matrigel-injected control mice. The graph on the left displays the average white blood cell count (WBC) and red blood cell count (RBC) of HMLER-1 tumor-bearing mice (HMLER-1) compared to all matrigel-injected control mice (Matrigel All). The graph on the right compares the neutrophil (Neutro) and lymphocyte (Lympho) differential (the percent of white blood cells that are either neutrophils or lymphocytes, respectively) between the HMLER-1 and Matrigel All groups. **(B)** The graph compares the platelet count between HMLER-1 tumor-bearing (HMLER-1) and all matrigel-injected control mice (Matrigel All). **(C)** The graph compares the hematocrit (HCT, percent), mean corpuscular hemoglobin (MCH, pg) and mean corpuscular hemoglobin concentration (MCHC, g/dl) between HMLER-1 tumor-bearing (HMLER-1), BPHER-3 tumor-bearing (BHPER-3), and all matrigel-injected control mice (Matrigel All). In (A), (B), and (C) * indicates that $p<0.05$ when compared to all matrigel-injected control mice. Calculated p-values are shown in Supplementary Figure 1B.

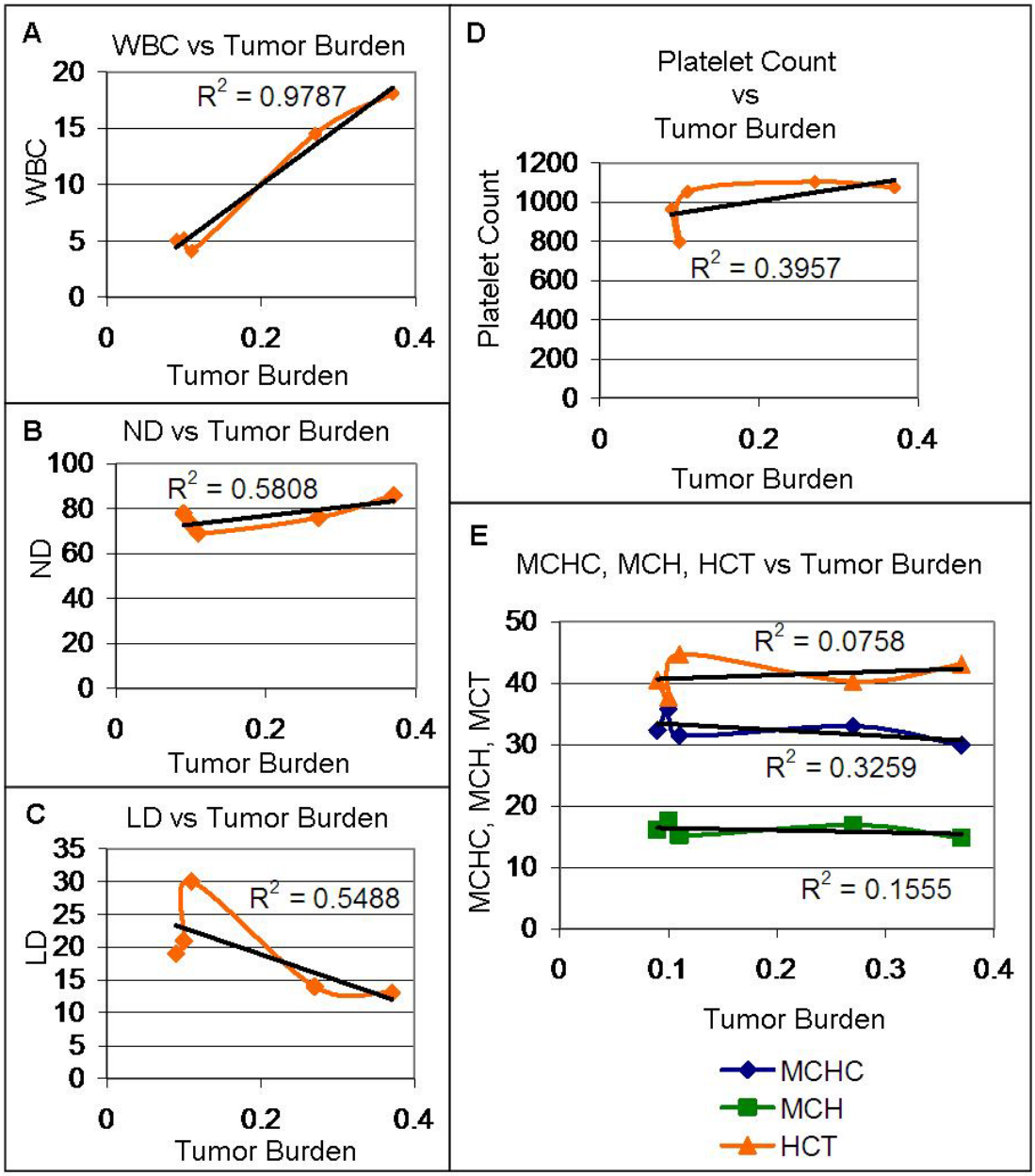

Figure 3: Correlation Between Blood Measurements and Total Tumor Burden in the HMLER-1 Tumor-Bearing Mice. For the statistically significant changes in the HMLER-1 tumor-bearing mice shown in Figure 3, graphs were made of each measurement as a function of increasing HMLER-1 tumor burden. Then, for each of the lines a linear trend line was created using Excel and the R^2 value is displayed on the graph. The WBC (A), Neutrophil Differential (ND) (B), Lymphocyte Differential (LD) (C), Platelet Count (D), the MCH (E), MCHC (E), and HCT (E) are displayed as a function of increasing tumor burden in the HMLER-1 tumor-bearing mice.

The BPHER-3 tumor-bearing mice displayed the same trends as the HMLER-1 tumor-bearing mice in terms of their WBC, neutrophil differential, and lymphocyte differential, however, the differences seen in the BPHER-3 mice were not statistically significant (Figure 1B and C). Interestingly, in contrast to the HMLER-1 tumor-bearing mice, the BPHER-3 tumor-bearing mice showed statistically significant decreases in their MCH and MCHC relative to all Matrigel-injected control mice (Figure 2C).

For the remaining tumor-bearing mice, including those injected with BPLER-1, MCF-7 Ras, and MDA-MB-231, there were no significant differences in the various blood cell measurements with the exception of the MCF-7 Ras tumor-bearing mice, which displayed a decrease in the lymphocyte differential relative to all Matrigel-injected control mice. However, while some differences are very small, all the tumor-bearing groups displayed the trend of increased neutrophil differential and decreased lymphocyte differential relative to all matrigel-injected control mice (Figure 1B and C).

Discussion

While these results need to be repeated, there are some interesting observations and implications for future studies on systemic perturbations in the blood. In summary, the HMLER-1 tumors were capable of perturbing certain cell types in the blood; however they also had the largest tumors relative to the other tumor models. The tumor burden in the HMLER-1 group appears to correlate with the WBC, suggesting that tumor burden alone may have some effect on perturbing the systemic environment. In a similar manner, it has been demonstrated in an autochthonous mouse mammary carcinoma model that Gr-1+Mac-1+ myeloid cells are increased in the blood during tumor

progression (Melani C et al. 2003). The authors also demonstrated that the increase in the number of GR-1+/Mac-1+/ER-MP12+ cells during tumor progression appeared to be correlated with the number of tumors present in the mouse. This is important to keep in mind when trying to discern systemic perturbations caused directly by the actions of a tumor versus being caused indirectly as a consequence of the increased tumor weight.

The HMLER-1 tumor-bearing mice displayed statistically significant changes in the neutrophil differential count and lymphocyte differential count. The HMLER-1 tumor-bearing mice displayed an increase in the neutrophil differential and a decrease in the lymphocyte differential. As mentioned earlier, the differential is calculated as a percentage of the white blood cell population. If the absolute number of neutrophils and lymphocytes are calculated using the WBC in HMLER-1 tumor-bearing mice, then there is roughly a 5.2 fold increase in neutrophils, but also a 1.6 fold increase in lymphocytes relative to all Matrigel-injected control mice. Future experiments may want to look at the absolute numbers of these cell types in a given volume of blood, this will help to elucidate which cell type(s) in the blood are perturbed the most in the tumor-bearing mice. Furthermore, it is unknown at this point whether the ratio of neutrophils to lymphocytes or the absolute number of lymphocytes and neutrophils in the blood of tumor-bearing animals is important for tumor progression.

These results also suggest that perturbations in the blood may be tumor cell type specific. For example, the different effects on the MCH and MCHC caused by HMLER-1 tumors compared to BPHER-3 tumors may suggest that these two tumor models have

some differences in their systemic perturbations. These differences may shed light on how different tumor cell lines utilize blood cells during tumor progression.

Acknowledgements: We would like to thank Tina Yuan for her editing and critical comments on this chapter. Also, we would like to thank Scott Valastyan for his editing on the figures presented in this chapter. We would also like to thank Sandra McAllister, Scott Valastyan, and Lynne Waldman for helpful discussions on this work. We would especially like to thank Tina Yuan for her helpful discussions on this work.

Materials and Methods

Cell Lines and Tissue Culture: The BPLER-1, BPHER-3, HMLER-1, and HMLER-HR cells were obtained from within the lab and were created as previously explained (Elenbaas B et al. 2001, Ince TA et al. et al. 2007). The BPLER-1 and BPHER-3 cells were cultured as previously described except that the final concentration of glutamine was 1mM instead of 2mM (Ince TA et al. et al. 2007). In general, the HMLER-HR cells were cultured in a 1:1 mix of Dulbecco's Modified Eagle's (DME) Medium and F12 Medium. The DME/F12 mix was supplemented with 5% calf serum, 10 ng/mL of EGF, 1-2 ug/mL of hydrocortisone, 10 ug/ul of insulin, penicillin and streptomycin. The HMLER-1 cells were cultured in a 1:1 mix of MEGM or MEMB (LONZA, Walkersville MD) and DME/F12 Media supplemented as described above but without the calf serum. MCF-7 Ras and MDA-MB-231 cells were cultured under standard conditions.

Tumor Xenografts: For subcutaneous injection, all cancer cell lines were resuspended in BD Matrigel™ Matrix (BD Biosciences, Bedford MA) diluted in tissue culture media. For the blood analysis experiments comparing xenografts, the following number of cells

was used per injection: 1 x10^6 BPLER-1, HLMER-1 and BPHER-3 cells, 2 x10^6 MCF-7 Ras and MDA-MB-231 cells.

Complete Blood Count and Differential: A sample of blood was taken intra-cardially and placed into a BD Microtainer® Tubes with EDTA (Becton, Dickinson and Company, Franklin Lakes NJ). During this procedure, there is a possibility that the blood will clot and this could affect the subsequent analysis. Additionally, the amount of blood sent to DCM may have been different between individual mice. The blood samples were submitted to the Division of Comparative Medicine at MIT for a complete blood count and differential.

Statistical Analysis: T-tests were performed using excel. A two-tailed T-test with unequal variance was performed to calculate the p-values for all comparisons.

Supplementary Material

Figure 1:

A

		WBC	RBC	HCT	Hgb	Plat Ct	RBC MCV	Neutr	Bands	Lymphs	Monos	Eosins	MCH	MCHC
BPLER-1	AVG	1.788	9.2	46.32	13.22	1324.8	50.36	62.8	2.2	33.2	1.4	0.4	14.36	28.54
12/8/2007 n=5	Std. Dev.	0.358	0.33	1.618	0.672	154.64	0.357771	5.586	1.3038	6.72309	0.8944	0.54772	0.555	1.26807
MCF-7 Ras	AVG	2.44	8.92	43.9	12.94	1264.8	49.2	62.8	2.2	32.2	1.8	1	14.52	29.48
12/4/2007 n=5	Std. Dev.	0.419	0.33	1.867	0.445	97.125	0.761577	4.147	1.4832	4.20714	1.7889	0.70711	0.179	0.28636
BPHER-3	AVG	3.876	9.59	47.46	12.94	1329.4	49.46	61.8	2.6	25.6	2.2	0.6	13.48	27.3
11/30/2007 n=5	Std. Dev.	1.267	0.35	2.862	0.594	169.75	1.301153	6.301	1.6733	12.818	1.7889	0.89443	0.476	0.92736
HMLER-1	AVG	9.384	8.34	41.26	13.38	998.6	49.5	76.4	2.6	19.4	1.2	0.4	16.1	32.5
12/5/2007 n=5	Std. Dev.	6.427	0.65	2.711	0.46	124.58	1.122497	6.348	2.881	6.80441	0.8367	0.54772	1.129	2.17601
MDA-MB-231	AVG	3.09	9.08	44.96	13.15	1236.4	49.525	60.88	1.625	34.75	2	0.625	14.48	29.25
All n=8	Std. Dev.	0.973	0.59	2.58	0.795	56.798	0.751665	8.236	2.7742	7.42101	1.6903	0.74402	0.282	0.7746
MDA-MB-231	AVG	2.773	8.84	43.4	12.93	1258.7	49.1	61	2.6667	33.3333	1.3333	1.33333	14.6	29.8333
12/4/2007 n=3	Std. Dev.	1.118	0.45	2.1	0.551	90.007	0.1	10.39	4.6188	7.37111	1.5275	0.57735	0.436	0.85049
MDA-MB-231	AVG	3.28	9.23	45.9	13.28	1223	49.78	60.8	1	35.6	2.4	0.2	14.4	28.9
11/30/2007 n=5	Std. Dev.	0.955	0.66	2.552	0.947	31.599	0.875785	8.044	1.2247	8.17313	1.8166	0.44721	0.158	0.52915
Matrigel	AVG	2.49	9.06	45.17	13.19	1246.8	49.86	56.1	2.6	38.8	1.75	1.83333	14.6	29.31
All n=10	Std. Dev.	0.679	0.65	3.047	0.431	132.35	0.846168	7.978	2.2706	6.52857	0.8864	1.60208	0.987	2.0207
Matrigel	AVG	1.976	8.76	44.02	13.12	1202.4	50.22	52.2	2.6	41.8	2	1.4	15.02	29.98
12/8/2007 n=5	Std. Dev.	0.26	0.74	3.704	0.249	170.04	0.85557	8.672	1.5166	7.25948	1.2247	2.07364	1.268	2.68459
Matrigel	AVG	2.147	9.13	45.87	13.07	1298	50.23333	55.67	3	39	2	0.33333	14.3	28.5
12/8/07-27 Days n=3	Std. Dev.	0.14	0.51	2.021	0.321	122.85	1.101514	10.21	1.7321	8.7178	1.7321	0.57735	0.52	0.95394
Matrigel	AVG	3.004	9.36	46.32	13.26	1291.2	49.5	60	2.6	35.8	0.8	0.8	14.18	28.64
11/30/2007 n=5	Std. Dev.	0.557	0.41	1.968	0.586	74.624	0.744983	5.477	3.0496	4.54973	0.4472	0.83666	0.377	0.92628
Matrigel	AVG	3.093	9.37	46.6	13.33	1294.3	49.76667	59.67	1.3333	37.3333	1	0.66667	14.23	28.6333
11/30/07-19 Days n=3	Std. Dev.	0.574	0.58	2.722	0.814	95.028	0.450925	4.163	0.5774	5.1316	0	0.57735	0.513	1.28582

Supplementary Material: Figure 1 (continued)

B

	WBC	RBC	HCT	Hgb	Plat Ct	RBC MCV	Neutr	Bands	Lym-phs	Monos	Eosins	MCH	MCHC
Group Comparisons	p-value	p-value	p-value	p-value	p-value	p-value	p-value	p-value	p-value	p-value	p-value	p-value	p-value
BPLER-1 12/8/07 v. Matrigel 12/8/07	0.37295	0.2812	0.2546	0.7675	0.2682	0.7485	0.0561	0.6668	0.0881	0.4045	0.3493	0.3309	0.3219
BPLER-1 12/8/07 v. Matrigel	0.02139	0.601	0.3575	0.9307	0.3665	0.133	0.0854	0.6728	0.1638	0.5092	0.0834	0.5578	0.3852
MCF-7 Ras 12/4/07 v. Matrigel	0.86362	0.5798	0.3386	0.3307	0.7711	0.1621	0.0521	0.6898	0.0362	0.9557	0.2884	0.8088	0.7997
MCF-7 Ras 12/4/07 v. Matrigel 11/30/07	0.11069	0.1024	0.0812	0.3611	0.6436	0.5465	0.3907	0.8011	0.2303	0.2851	0.6941	0.1206	0.1134
BPHER-3 11/30/07 v. Matrigel 11/30/07	0.21288	0.378	0.4866	0.416	0.6627	0.9543	0.6429	1	0.1545	0.1568	0.7245	0.0342	0.0516
BPHER-3 11/30/07 v. Matrigel	0.06901	0.0625	0.1883	0.4336	0.3746	0.5562	0.1624	1	0.0818	0.6218	0.1462	0.011	0.0205
BPHER-3 11/30/07 v. Matrigel 11/30/07 Sac'd on Same Day	0.27935	0.5983	0.6907	0.5146	0.721	0.6496	0.5863	0.1792	0.1222	0.208	0.9024	0.1069	0.2071
MDA-MB-231 v. Matrigel	0.16465	0.945	0.8777	0.9005	0.8259	0.3877	0.2344	0.4364	0.245	0.7183	0.1327	0.7101	0.9326
MDA-MB-231 11/30/07 v. Matrigel 11/30/07	0.59553	0.7175	0.7786	0.9691	0.1144	0.6013	0.8593	0.3237	0.9634	0.1207	0.2062	0.2791	0.6043
MDA-MB-231 11/30/07 v. MDA-MB-231 12/4/07	0.55045	0.363	0.1924	0.5371	0.568	0.158	0.9788	0.5984	0.7037	0.4142	0.0516	0.5144	0.1867
HMLER-1 12/5/07 v. Matrigel	0.07431	0.0765	0.0324	0.4647	0.0066	0.5489	0.0003	1	0.0008	0.2888	0.0834	0.0386	0.0268
HMLER-1 12/5/07 v. Matrigel 12/8/07	0.06145	0.3664	0.2189	0.3082	0.0657	0.2892	0.0013	1	0.001	0.2666	0.3493	0.1932	0.1432
HMLER-1 12/5/07 v. Matrigel 11/30/07	0.09049	0.0218	0.0111	0.7285	0.0033	1	0.0025	1	0.0029	0.3815	0.4012	0.0161	0.0129
Matrigel 12/8/07 v. Matrigel 11/30/07	0.01067	0.1656	0.2654	0.6421	0.3297	0.1943	0.1344	1	0.1631	0.0941	0.5734	0.2183	0.3402
Matrigel 12/8/07-27 Days v. Matrigel 11/30/07-19 Days	0.09637	0.6233	0.7284	0.6394	0.9695	0.5516	0.5799	0.2322	0.7927	0.4226	0.5185	0.882	0.8928

Supplementary Figure 1: Complete Blood Count with Differential Analysis of Tumor-Bearing and Matrigel Control Mice. For (A) and (B) the measurements in the table include a WBC (10^3 cells/mm^3), RBC (10^6 cells/mm^3), hematocrit (HCT, percent), Hemoglobin (Hgb, g/dl), platelet count (Plat Ct, 10^3 cells/mm^3), mean corpuscular volume (RBC MCV, fl), neutrophil differential (Neutr, percent), band differential (Bands, percent), lymphocyte differential (Lymphs, percent), monocyte differential (Monos, percent), eosinophil differential (Eosins, percent), mean corpuscular hemoglobin (MCH, pg) and mean corpuscular hemoglobin concentration (MCHC, g/dl). **(A)** Table showing the averages (AVG) and Standard Deviations (Std. Dev.) for all the blood measurements in both the tumor-bearing and control mice from the experiment shown in Figures 2, 3, and 4. The number (n) of mice in each group is displayed in the table after the name and date of birth (DOB) of the group. As in Figure 2, the MDA-MB-231-bearing and matrigel control mice had two groups of mice with different birth dates. For (A) and (B) the numbers for all the mice in either the matrigel or MDA-MB-231 groups is shown and the label in the tables is not followed by the DOB. The tables also show the averages and p-values if these groups are separated by the DOB. **(B)** The table displays the p-values when two groups are compared, and the groups being compared are shown in the first column. T-tests were performed using Excel. A two-tailed t-test with unequal variance was performed to calculate the p-values for all comparisons. Comparisons with a significant p-value are highlighted in yellow. For (A) and (B) the names of the mouse groups are followed by their DOB except where noted above.

References

Melani C, Chiodoni C, Forni G, Colombo MP. (2003) Myeloid cell expansion elicited by the progression of spontaneous mammary carcinomas in c-erbB-2 transgenic BALB/c mice suppresses immune reactivity. *Blood*, **102**(6), 2138-45.

Hiratsuka S, Nakamura K, Iwai S, Murakami M, Itoh T, Kijima H, Shipley JM, Senior RM, Shibuya M. (2002) MMP9 induction by vascular endothelial growth factor receptor-1 is involved in lung-specific metastasis. *Cancer Cell*, **2**(4), 289-300.

Hiratsuka S, Watanabe A, Aburatani H, Maru Y. (2006) Tumour-mediated upregulation of chemoattractants and recruitment of myeloid cells predetermines lung metastasis. *Nat Cell Biol*, **8**(12), 1369-75.

Kaplan RN, Riba RD, Zacharoulis S, Bramley AH, Vincent L, Costa C, MacDonald DD, Jin DK, Shido K, Kerns SA, Zhu Z, Hicklin D, Wu Y, Port JL, Altorki N, Port ER, Ruggero D, Shmelkov SV, Jensen KK, Rafii S, Lyden D. (2005) VEGFR1-positive haematopoietic bone marrow progenitors initiate the pre-metastatic niche. *Nature*, **438**(7069), 820-7.

McAllister SS, Gifford AM, Greiner AL, Kelleher SP, Saelzler MP, Ince TA, Reinhardt F, Harris LN, Hylander BL, Repasky EA, Weinberg RA. (2008) Systemic endocrine instigation of indolent tumor growth requires osteopontin. *Cell*, **133**(6), 994-1005.

Shojaei F, Wu X, Malik AK, Zhong C, Baldwin ME, Schanz S, Fuh G, Gerber HP, Ferrara N. (2007) Tumor refractoriness to anti-VEGF treatment is mediated by CD11b+Gr1+ myeloid cells. *Nat Biotechnol*, **25**(8), 911-20.

Yang L, DeBusk LM, Fukuda K, Fingleton B, Green-Jarvis B, Shyr Y, Matrisian LM, Carbone DP, Lin PC. (2004) Expansion of myeloid immune suppressor Gr+CD11b+ cells in tumor-bearing host directly promotes tumor angiogenesis. *Cancer Cell*, **6**(4), 409-21.